Benefits of using remotely sensed time series data in optimizing water management decisions

TU Delft | Deltares

Saket Keshav

Benefits of using remotely sensed times series data in optimizing water management decisions

by

Saket Keshav

to obtain the degree of Master of Science
at the Delft University of Technology,
to be defended publicly on Tuesday October 27, 2020 at 14:00 hrs.

Student number:	4834577	
Project duration:	November, 2019 – October, 2020	
Thesis committee:	Dr. ir. Hessel Winsemius,	TU Delft, supervisor
	Mark Hegnauer,	Deltares
	Dr. ir. Jan Kwakkel,	TU Delft
	Dr. ir. Rolf Hut,	TU Delft

An electronic version of this thesis is available at http://repository.tudelft.nl/

TU Delft

Deltares

Contents

List of Figures

List of Tables

Acknowledgements

This thesis wouldn't have been possible without the constant guidance and supervision of some very important individuals. I take this opportunity to thank Dr. Ir. Hessel Winsemius, for his guidance and assistance throughout the project, and also for encouraging me to pursue this thesis at Deltares. I am grateful to the support of Mark Hegnauer for constantly addressing my doubts through weekly meetings that were necessary to keep this thesis at pace.

The optimization was an important part of this thesis and without the expertise of Dr. Ir. Jan Kwakkel and Bramka Jafino it would have been impossible for me to set up the running python code and getting the thesis done on time. I would also like to thank Dr. Ir. Rolf Hut for helping me understand the intricacies of the problem and how it can help the scientific community as a whole. Without his suggestions, I wouldn't have been able to get something relevant out of this project.

Additionally, I would like to thank Dr. Gennaddi Donchyts for introducing me to the amazing set of remotely sensed time-series data that forms the very basis of this thesis, Wil van der Krogt for helping me get the water allocation decision model and important data from the Moroccan authorities and Marnix van der Vat for helping me with scripts to execute the water allocation decision model with Python.

Finally, and most importantly I would like to thank my family and friends for their constant support and belief throughout my Thesis.

Saket Keshav
Delft, October 2020

Abstract

Big data sources can play an important role in revolutionizing the field of water resources research. Time series data with high temporal and spatial dimensions encapsulates with itself numerous factors essential for coming up with robust decisions. In this thesis, we assess one such big data source for efficient water management in the Oum Er Rbia basin, Morocco. The surface water detection technique furnished by Dr. Donchyts [15] is found to be accurate in detecting the surface water sources and its temporal and spatial dynamics.

The remotely sensed time-series data of reservoir area was used to come up with Level-Area-Storage(LAS) relationships for the five main reservoirs in the Oum Er Rbia basin. These curves were able to approximate the present set of LAS curves well. Hence, were used in place of the local LAS curves in a water allocation decision model called RIBASIM. Thus, we had two scenarios one where the local LAS curves were used to optimize reservoir operations and the other where remotely sensed LAS curves were used instead of the local LAS curves.

The operating rule curves in the water allocation decision model were then optimized for the two scenarios. The optimization was done to maximize the performance of the system across three objectives: a)public water supply, b)irrigation and c)hydroelectricity generation. A trade-off between the three objective functions was then shown using parallel and scatter plots. It was observed that for the same set of LAS curves the performance across all three objectives improved post-optimization of the operating rule curves. This showed that there were rooms for improvement in the existing reservoir operating rule curves. The operating rule curves for the water allocation decision model with remotely sensed LAS curves were then optimized. The best set of operating rule curves that we got from the second optimization were then used with the local LAS curves to see how the system would perform with these operating rule curves. This gave us an idea of the feasibility of using remotely sensed data to come up with water management decisions and also to assess the benefits of using remotely sensed time-series data. Though the performance over the three objectives was not as good as the results we got by optimizing the system with local LAS curves, it was better than the system performance across the three objectives with the existing set of operating rules and local LAS curves. Thus, it can be used when there is a dearth of proper LAS curves.

Besides, optimizing operating rule curves, the remotely sensed time-series data of reservoir surface area was used to assess the effects of sedimentation in the reservoir storage. It was observed that for larger reservoirs the percentage change is not much as compared to the smaller reservoirs. Apart from the size of the reservoir, more study is required to make a detailed analysis of how factors like topography and soil texture influence the rate of sedimentation. Despite its limitations, the remotely sensed time-series data of reservoir surface area can be used to perform a qualitative analysis of the rate of sedimentation and can give reservoir authorities an idea of the need for bathymetry. This can help in avoiding unnecessary bathymetries which are infeasible both economically and physically.

1

Introduction

Water allocation decisions in a basin are taken based on the hydrological pieces of information on water availability and its demand in the region. However, it is often noticed that this information is mostly uncertain. In the field of water resources management, the credibility of the data sources and its availability plays a key role in carrying out any type of research or activities. It has often been observed that the use of extensive hydrological information is beneficial in reducing the rate of occurrence of sub-optimal water allocation decisions, ultimately contributing to the overall functioning of the basin[32]. Efforts have been made on technical fronts to have an easy, accurate, and easily accessible data source for the use of water managers across the globe. With the technological advancements and development in the field of remote sensing and earth observatory, researchers have witnessed success in these fields. The development of remote sensing-based datasets and modeling can be a key to a better understanding of numerous hydrological aspects in data-scarce areas. Big data sources can play a very important role in scientific research. Using these data for water management research can attenuate the economic and physical costs associated with such research [26][38] [40].

Reservoirs are constructed on a river for numerous reasons. They have been used across economic, social, ecological, and environmental dimensions [50]. These include power generation, flood control, drought mitigation, and water supply. These multi-objective systems are self competing and require extensive analysis to optimize reservoir operations. When it comes to reservoir operations, it is very vital to have a balanced operating policy to ensure water availability for all the activities prevalent in the region. An accurate and detailed hydrological information can help water managers to come up with robust operating rules for the reservoir which can further attenuate the effects of extreme droughts and floods, ensuring optimum water resources management in the basin.

1.1. Scope and Relevance

Remote sensing (RS) and Earth observation (EO) in particular are rapidly growing fields. The spatially continuous global coverage that remote sensing provides facilitates comparability across basins and scales. This contributes to better information for water managers and decision-makers[20]. In the last decade, these fields have produced an enormous amount of data. However, one of the biggest challenges is to extract valuable information from multiple satellite data, resulting in a higher temporal resolution. The advent of parallel satellite data processing platforms like google earth engine proved to be an answer to many such technical

limitations. The advancements and outreach efforts undertaken by large companies resulted in the development of parallel processing platforms like Google Earth Engine and the growing volumes of data further the need for automated methods for surface water detection from satellite images.

Dr. Gennaddi Donchyts[15] came up with a new method for accurate surface water detection based on a local threshold of spectral indices computed from multi-spectral satellite data sets. He came up with a set of fully automated algorithms and software tools to enable the processing of multi-spectral satellite imagery for surface water detection with high spatial and temporal resolutions. As a part of his research, he created a global dataset of reservoir surface area time series with the help of Google Earth Engine.

This thesis involves utilizing remotely sensed sources of data in water management decisions. Different water allocation decision models were set up using local and remotely accessible data sources, finally, an extensive comparison of the trade-offs amongst different water objectives in a basin was analyzed for both the models with different data sources to categorically assess the benefits of using remotely sensed data for water resources management in a basin. The remotely sensed data can provide a whole new set of alternative data and can bridge the gap in water management research owing to lack of accurate and extensive datasets. Assessing the use of such data in optimizing water management decisions can give us an alternative in the form of big data sources and can improve the quality and intricacies of water management research.

1.2. Objectives and research questions

The main research objective of this project is to assess the benefits of utilizing remotely sensed time-series data of reservoir surface areas along with other open-source data in optimizing water management decisions.

Water is a scarce resource and this calls for continuous improvement in the field of water resources management. Lack of accurate, easily available data is one of the main obstructions in the field of water resources research. Local data are usually hard to get, tedious to process and are expensive. Even if we get access to the local data sources it is usually accompanied by sporadic errors and gaps in data leading to sub-optimal water allocations.

The time-series data of the reservoir surface area over a long period can help us include the effects of climatic variability in decision-making processes. This data when compared to the local data of the reservoirs in the river basin can help us identify the rate of sedimentation and involve adaptive optimization of reservoir operations. Here, we attempt to compare different datasets to furnish different objectives and assess its implications on the water resources decisions in the basin.

Keeping all these factors in mind we finally narrowed down to three research questions as a part of this thesis. Assessing the benefits of remotely sensed time-series data of reservoir area along these lines will help in robust analysis and comparison of different sources of data.

1.2.1. Research Question

Can a remotely sensed time series data-set of the reservoir areas in combination with the already existing other open sources of data be used as an alternative to local data in optimizing water allocation decisions?

Sub-Questions

- How do Level-Area-Storage relationships constructed using remotely sensed time series data compares to local Level-Area-Storage relationships?
- How does the surface water flow alters due to change in data source from local to remotely sensed time series data?
- How do decision trade-offs compare to each other when using remotely sensed time series data of reservoir area or local data?

Addressing these research questions will further the cause of open-source data in the field of water resources research. The performance of the remotely sensed time-series data over the Oum Er Rbia(OER) basin can open doors to extensive research over a larger scale. This will have many implications and can play an important role in addressing issues of the global water crisis, Interstate conflicts, etc. This is particularly important as surface water sources are interdependent. Knowledge of the upstream availability of water can help water managers upstream to tap the available water resources without affecting the water resources downstream.

2

Literature Review

Numerous literature has stressed over the fact of how the dearth of data can lead to sub-optimal water resources management. World Meteorological Organization [57] stresses on the fact that the data are important for efficient decision making and inferior data can eventually lead to inferior decisions.

Data with high volume, velocity, and variety are known as big data. The big data sources require the latest technologies and techniques and can enhance decision making in a basin[7]. The advent of big data in the field of water resources management has a huge potential in better water resources management and can be an alternative to tedious and financially exhaustive data sources.

Adamala et al[7] emphasizes that big data sources are showing huge promise to water managers to plan water systems optimally, to analyze climate change impact, changes in the ecosystem through remote sensing, predict natural changes, man-made calamities, irrigation planning, etc.

The utilization of big data in the field of water management was however pretty much non-existent till 2013. Wang et al[55] took the first step towards introducing the water resources and hydropower cloud GIS platform. The developed platform managed various and massive data efficiently and, in a way, opened doors to the use of big data in water resources management. Satellites have been used for decades to accumulate large amounts of information, resulting in multi-petabyte archives of image collected. Despite the great progress in the harmonization of freely available satellite data, the progress of higher-level products remained non-automatable. The recent developments in cloud computing have enabled the transformation of these massive amounts of data into something valuable[15].

Parallel processing platforms like Google Earth Engine and the growing volumes of data can be harnessed to come up with an automated way to do that. The existing methods for surface water detection from multi-spectral satellites use the trait of water to absorb most radiation in the near-infrared region. This trait makes it relatively easier to detect clear water with the help of spectral indices such as the Normalized Difference Water Index (NDWI) [43]. The Modified Normalized Difference Water Index (MNDWI)[58], appears to be more sensitive, due to the use of the short wave infrared band rather than the near-infrared band as in the case for NDWI. The NDWI and MNDWI are among the most widely used spectral indices available for water detection. However, there have been other efforts to come up with efficient and accurate sur-

face water detection methods, based on a simple linear band combination automated water extraction index (AWEI) [22] WI2015 [23], and based on hue saturation value (HSV) transformation [46]. Despite so many indices all of them are highly dependent on the composition of the validation pixels, and none of them performs best across all water and non-water pixels[23].

Reservoir operating rules primarily depends on these data sources and are based on local climatology and surface water resources. The long time series of satellite data can help identify the general trend in water availability which helps decision-makers in the basin to come-up with robust operating rules. While it is relatively simple to operate single-purpose reservoirs, operating rules for multi-purpose reservoirs are complex. There are several rules of thumbs that provide guidelines for the operation of multi-reservoir systems.

Bower et al[11] suggested two rules for determining releases over time. The target rule specifies that whenever there is an excess of water and releases beyond specified targets have some benefits, water available in excess should be released to realize those benefits. These releases free the reservoir space, thus reducing the likelihood of future spills. The hedging rule specifies that whenever there is a shortage of water, it is advantageous to accept a small current deficit to decrease the probability of acute water shortage and energy deficit. For single-purpose water supply systems with reservoirs in series, the water in the downstream reservoirs should be used before using water stored in upstream reservoirs. This method minimizes unnecessary spilling at the most downstream reservoir in the event of high lateral flows. For Parallel reservoirs supplying joint demands, two rules are used. The space rule [11] which aims to equalize available space in each of the parallel reservoirs.The NYC rule [13] which attempts to equalize the probability of filling of each reservoir. In systems with side demands, where each demand can be satisfied by only one reservoir, one must balance the likelihood of spills in each reservoir while keeping in mind the likelihood of shortages at the demand site.

For systems concerned with hydropower generation, Johnson et al [30] defined an energy production space rule, similar to the water supply space rule. As per the rule if potential energy stored in each reservoir has a constant head. Then water supply space rule is equivalent to the energy production space rule. In that case, the combination of the water supply space rule with the appropriate energy and water constraints yields a policy that minimizes water and energy spills. Similarly, many authors came up with different rules keeping in mind different states of the reservoir and demands. The rules discussed above are only valid for single-purpose reservoirs. When the reservoir system serves several purposes and its operation is heavily constrained, these rules cannot be applied directly. In such cases, the optimization algorithms are used to come up with an optimum set of rule curves to serve the multiple objectives in the region. This has been a part of water system analysis studies from the very beginning of operation research in the field of water management.

The field of operation research in water system analysis started during world war 2 [10][52][34]. This field expanded greatly to its military roots during this period, and the greatest advancements came in the field of water resources system analysis (WRSA) [47]. Harvard Water Program, which was an interdisciplinary effort by political scientists, economists, and engineers recognized the multi-objective nature of designing the water resources systems to address the social and environmental needs of the society. Optimization of water resources has been a primary focus over the last half-century. The field of WRSA has continually pushed the field of water resources research to come up with novel ways of optimizing reservoir operations. However, there has been low adoption of these methods among water managers [12][60][36].

The earlier discussions of reservoir operation for planning and analysis of water resources were done by Loucks et al [39] in Water Resource System Planning and Analysis Textbook in the year 1981. Diwekar et al[14] presents more advanced techniques of optimization. Yeh et al[60] wrote a state of the art review list of mathematical models for planning and management for optimal reservoir operation. He suggested that the reservoir operators must be involved in the development of the model. Labadie et al[36] made a comprehensive study on the optimal operation of multi-reservoir systems. He concluded that to successfully implement the reservoir optimization model to the real world it is important to increase the confidence of the decision-makers by carrying out interactive involvement during the development of the system. The link to the simulation model can address the issue of the relatively opaque nature of the optimization algorithm and thus increase the acceptability of different optimization methods.

Ferreira et al[21] found the trade-off between power generation and the environmental constraints to assure optimal operation of the reservoir. The reservoir needs to provide enough water for conservation flow to meet downstream water quality goals. This results in less water allocation for power generation and reduces the production of electricity. Yang et al[59] had the same argument when they optimized the operation of the Danjiangkau reservoir while maximizing ecological requirement. their study shows that the power generation output is lower because of the exorbitant abandonment of water during high flow which cannot be used for power generation.

Optimization and economic aspects in the field of water resources management is essential to analyze the investment in the reservoirs and operate the reservoirs to assure maximum return on investment. Economic-engineering optimization for water supply in California was assessed using California Value Integrated Network by Draper et al [16] in the year 2003. Harou et al[25] further discussed the importance of hydro-economic concepts in the design and application of future projects. They suggested that the modeler, managers, and operators should work together to embrace the hydro-economic component in their existing operating model.

3

Study Area

The Oum Er Rbia river (OER) basin, located in the mid-west of Morocco between El Jadida and Safi is the largest river basin in Morocco. It spreads over an area of 35,000 Sq.km and covers 194 provinces. The OER basin originates in the Middle Atlas at 1,800m above sea level, crosses the Middle Atlas chain, the Tadla plain, and the coastal Meseta, to finally flow into the Atlantic Ocean about 16 km north of the city of El Jadida.

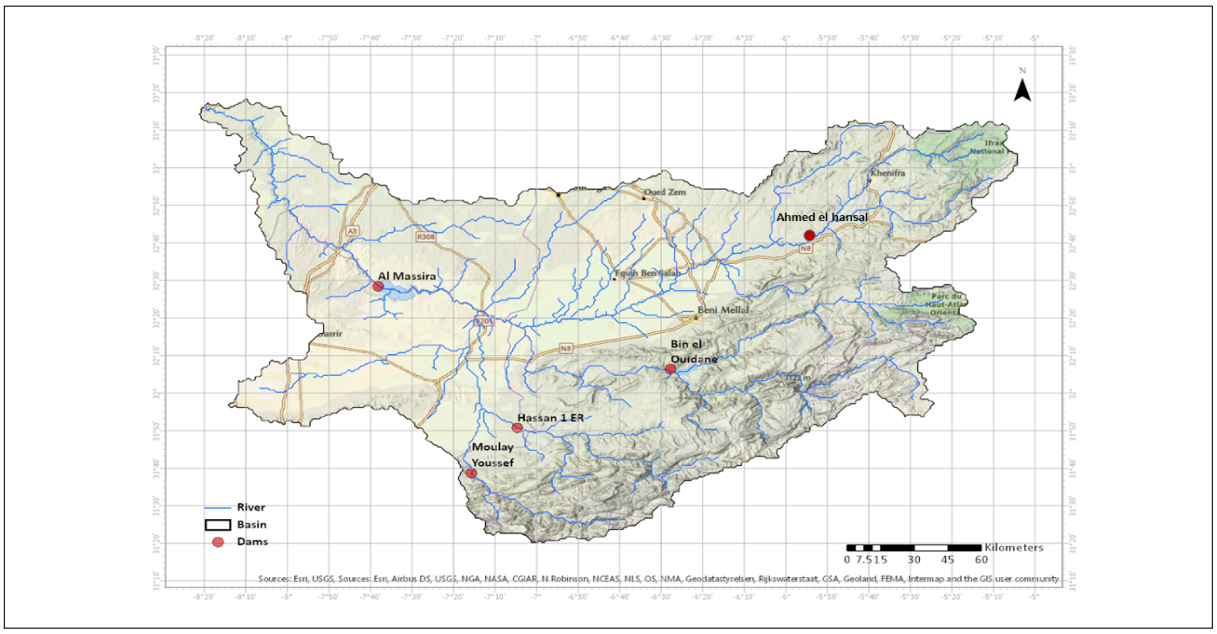

Figure 3.1: Oum Er Rbia Basin

The hydrographic network of the basin is formed by the OER river and its tributaries: Tassaout, El Abid, Lakhdar, Derna, Melloul, Ouamana, Srou, Chbouka, Quirine, Gzef, El Touim, and Faragh. With the inputs in this zone ranging from 1,300 Mm^3/year to 3,730 Mm^3/year, there is a large variability in the meteorological and hydrological regime of the region [62]. Despite the highly variable nature of the input to the basin, water managers here have been able to utilize available sources of water pretty well, with 3,365 Mm3 of the 4,000 Mm3 of mobilizable water potential already under use [17]. However, climate change forecasts for this region point to an increase in global warming by 2030 with an increase in losses due to evaporation

and transpiration. According to these forecasts, precipitation levels will stagnate or decline in the region [17], this along with increasing demography makes optimization of available water resources important.

There is a strong temporal and spatial irregularity in surface water between north and south. This results in the construction of major dams to store inputs from the wet year and also furnish the needs of the basins by planning pipelines for the transfer of water. The OER basin has various hydraulic infrastructures which include a system of 15 reservoirs. These structures mobilize approximately 3550 Mm^3 of water that are used to furnish numerous water demands in the basin [28].

For this project, we optimize the operation of the system of reservoirs.

There are two types of structures in the OER basin:

1. Regulation works which are reservoir dams:
   (a) Ahmed El Hansal dam
   (b) Bin El Ouidane dam
   (c) Hassan 1er dam
   (d) Moulay Youssef dam
   (e) Al Massira dam

   Two large dams are also planned in the OER basin. 1) Taghzirt dam on Oued Derna and 2) Tiyoughza dam on Oued Tessaout above Moulay Youssef and Sidi Driss dam
2. Intake and compensation works
   (a) Ait Ouarda dam
   (b) Sidi Driss dam
   (c) Ait Messaoud dam
   (d) Kasba Tadla dam
   (e) Timinoutine dam
   (f) Prise d'Agadir Bou□Achiba
   (g) Sidi Said Mâachou dam
   (h) Imfout dam
   (i) Daourat dam
   (j) Safi dam
   (k) Sidi Daoudi dam

Figure 3.2 shows the connection of the reservoir. It is interesting to note that Al Massira is the only downstream reservoir in this network and is dependent on the outflow from the other four reservoirs. For optimum utilization of these structures, the water managers shall ensure the coordinated operation of the reservoirs.

This thesis addresses the trade-offs between different water demands in the basin. With the limited source of water, we optimized reservoir operation using area-capacity curves generated from different data sources to address water requirements across the following sectors:

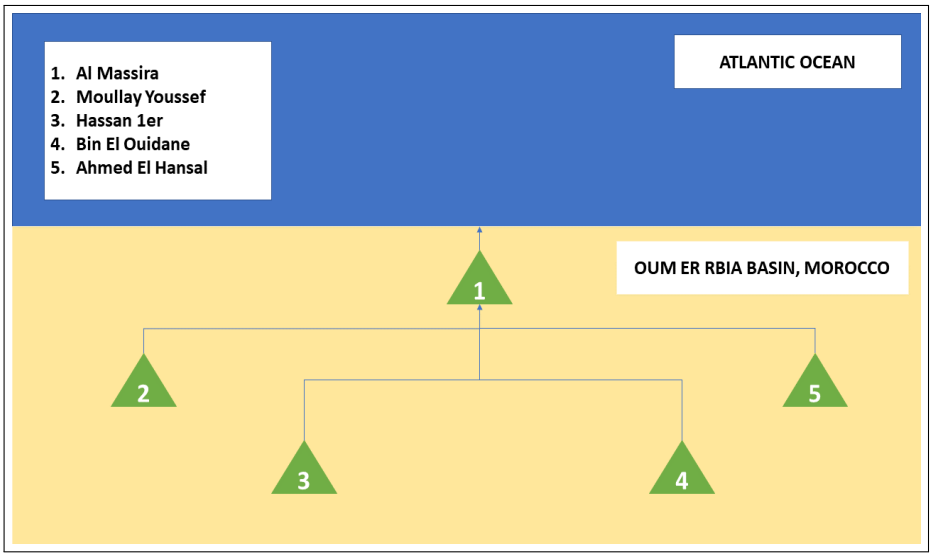

Figure 3.2: Reservoir system in Oum Er Rbia basin

1. Public water supply
2. Irrigation
3. Hydro-power

3.1. Public water supply

Being the most important river basin in Morocco, OER basin is bound to play a major role in furnishing drinking and industrial water demands in the region. The data was retrieved from the PDAIRE/basin update study[4]. The total domestic water demand in the basin is 418 Mm^3/year in the year 2015 which is expected to rise to 529 Mm^3/year by 2030. With the population of 4.5 million this roughly translates to 254 litres/person/day to 322 litres/person/day. These demands don't take into account the need for water for industrial activity, The industrial activity in this region usually feed on desalination and reuse of other resources. The minimum domestic water demand that the government shall furnish under extreme conditions is 164 litres/person/day [41] which is equal to 6% of 2740 litres/person/day of the water available per inhabitant in Morocco 4% of the available water is for addressing industrial water demands and rest 90% is utilized for irrigation purposes.

3.2. Irrigation

OER basin has a well-developed irrigation infrastructure. Agriculture is the largest water user in the basin and consumes over 90 % of the country's freshwater resources [31][48][41]. The irrigated lands are supplied by regulated as well as unregulated basin and groundwater. Irrigated areas are represented by the four large perimeters: The Tadla, Doukkalas, Tessaout, and Haouz. Overall irrigation accounts for approximately 45 % of the annual crop production and 75% of exports. Despite its contribution to the annual crop production only 15% of the agricultural land is irrigated and the available water resources invariably fails to meet the irrigation water demand [6]. Amendments are needed on both fronts. While the government is promoting water-efficient irrigation practices like drip irrigation [31]. There is a need to adopt available water management techniques, and the optimization of the reservoir network is a step towards that.

3.3. Hydro-power

OER river basin has a hydraulic generating park comprising of 13 hydroelectric plants that contribute to 70% of the national hydroelectric production [18]. At present the total installed capacity of Morocco is 8,262 MW. In 2020 hydropower constituted 19% of the total energy mix and the government aims to increase the renewable generation capacity to 42% of the energy mix by 2030. As the energy demand is expected to double by 2025, the government plans to accelerate the pace of reforms this will enable public and private operators to develop 10,000 MW of additional capacity by 2030. This will help Morocco reach 2000 MW of installed capacity by 2020 [3]

In the management of surface water resources, priority in the allocation of water is given to drinking water, followed by irrigation, and hydroelectric production is a by-product of these two uses. The contribution of hydro-power to a renewable source of energy is highly variable depending on the available surface water sources, which can have high intra-annual variability. The dependence of hydro-power on the climate is very much clear and hence, calls for efficient management of water resources.

4

Datasets

4.1. Remotely sensed time series data set

Water scarcity can be regarded as a perennial problem, due to the low availability of water supply and poorly managed demand[54]. To achieve water security and resilience to hydrological extremes it is very vital to understand water resources dynamics at the basin scale. This knowledge and understanding can be based on data and observations and is the foundation for managing water optimally and efficiently in economic and social terms[54]. Extensive data is needed on the state of water resources (e.g. surface water such as rivers, reservoirs, and snowpack, and subsurface water like soil moisture and groundwater). Similarly, for floods, data on riverine flows, and inundated areas are required to assess the impact and identify the flood plains. This can help in early warnings and help policymakers to come up with robust policies. Forecasts are essentials especially for hydrological variables and potential agricultural impacts to get the lead time that makes the implementation of measures and management plans efficient. These forecasts are initialized and verified with observational data[49][51][61]

Donchyts [15] automated different methods of surface water detection from satellite imagery and introduced new algorithms to get very accurate detection of surface water and surface water changes. The method applicable from local to the global level, and for detecting both low and high-frequency changes in surface water. Time series data of the reservoir surface area can be used for varied purposes, such as assessing the climatic variation over the years, interpreting the sedimentation due to the change in bathymetry, etc. This thesis focuses on using the remotely sensed time-series data of reservoir surface area to come up with Level-Area-Storage (LAS) curves for different reservoirs in the basin which shall then be assessed based on its performance across different objectives.

Figure 4.1 shows the interface of the water watch project in the Earth Engine App. It has an interactive interface, where we can click on different surface water sources to see the surface area time series in Sq.km of that water body. The upper plot shows the area time series from the surface water detection method put forth by Donchyts [15]. while the lower plot is the surface area time series from unprocessed data sources. The interface also shows streams and other water sources. Users can view as per their requirements different levels of catchments. Making it easier to carry out catchment specific research.

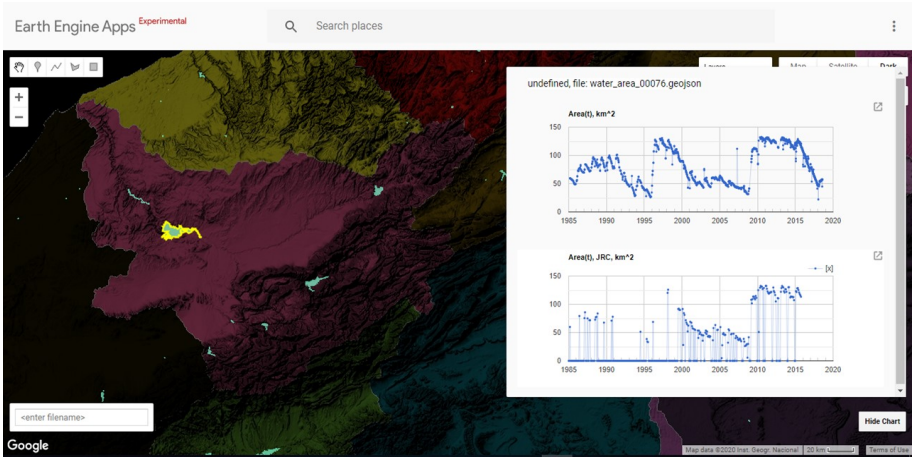

Figure 4.1: Water Watch, Remotely sensed time series data of reservoir surface area

4.2. Global reservoir and dam (GRanD) dataset

Reservoirs and dams have many environmental, social, and economic implications. From the very beginning, they have been a prime source of water distribution in a basin. Its ability to significantly alter the hydrological flow in the riverine ecosystem has always been the main reason for numerous conflicts between the relevant stakeholders. Despite its large spatial and temporal effects, there was a lack of comprehensive data set of global dams and reservoirs. The World Register of Dams, which is one of the most comprehensive databases on dams has been compiled by the International Commission on Large Dams (ICOLD) which currently lists more than 33,000 records of large dams and their attributes (ICOLD 1998-2009). However, this list is not georeferenced which limits its utility for many applications. Many researchers and organization have thus created their own global and spatial datasets of dams and reservoirs. This was done mostly by identifying the reservoirs on maps and compiling attribute information from various sources. These data are very inconsistent in the number of records, quality of attributes ranging from coarse coordinates to lumped national or regional assignments. The Global Water System Project (GWSP), a joint project of the Earth System Science Partnership (ESSP), to overcome the inconsistencies in the database of dams and reservoirs initiated an international effort to collect existing dam and reservoir data sets aiming to provide a single geographically explicit and reliable database for the scientific community: The Global Reservoir and Dam database[37]

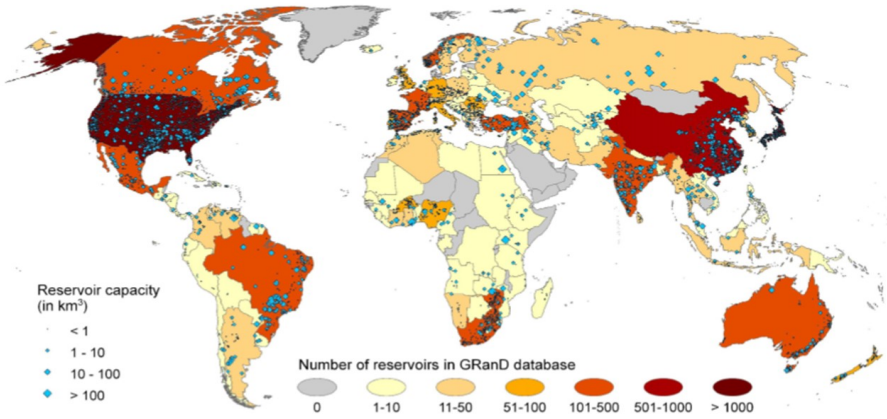

Figure 4.2: Global distribution (by country) of large reservoirs in GRanD database [37]

The development of GRanD is primarily aimed at compiling the available reservoir and dam information. It was corrected through extensive cross-validation, error checking, identifying duplicate records, and finally completing the missing information from new sources. The GRanD datasets are geospatially referenced and assigned to reservoirs (polygons) with high spatial resolution. The current version 1.1 of GRanD contains 6,862 records of reservoirs and their associated dams with a cumulative storage capacity of 6,197 km3.

Figure 4.2 shows the global distribution by countries of large reservoirs in the GRanD database. Africa has one of the least reservoir density, While North America has the most.

4.3. Local data

The local data were retrieved from the River Basin and Simulation Model (RIBASIM) model, a water allocation decision model developed by Deltares, an independent institute for applied research in the field of water and subsurface. It was used by a Moroccon water consultancy, NOVEC as a part of their project to assess the effects of climate change in the OER basin[4]. The OER basin has witnessed a significant drop in rainfall in the last four decades. This reduction has a significant impact on the water availability of the region, which eventually affects water supply for irrigation and electricity generation. Thus, aware of the issues associated with climate change and growing population, ABHOER initiated a series of studies to understand climate change in the region. The RIBASIM model used in this project was a part of one such study aimed at:**"Technical assistance for the integration and assessment of climate risks (ERC) in the planning and development of water resources at the level of the Oum Er Rbia basin, Morocco - Consultant mastering the RIBASIM tool"**[27][28]. It encapsulates extensive data on local conditions of OER basin that includes, incoming flow, public and irrigation water demands, etc. It ranges from the year 1941 to 2015 on a monthly scale.

5

Methodology

5.1. Outline of the methodology

The thesis focuses on assessing the benefits of having easily accessible satellite data like the one developed by Gennaddi Donchyts [15] for efficient water management. In regions with a dearth of extensive and accurate data sources due to the inaccessible nature of the region, extreme weather, and other logistical issues. Accurate satellite data can prove to be a great asset

For this thesis, we narrowed down the use of remotely sensed time-series data to come up with Level-Area-Storage (LAS) curves for the reservoirs. The reservoir operations are then optimized for different LAS curves from different data sources, local and satellite. The optimization results are then compared for the two sets of LAS curves enabling us to address our main research objective of assessing the benefits of using remotely sensed time-series data of reservoir surface area in optimizing water resources management.

Figure 5.1, gives a flow of the methodology followed to address the three sub-questions which in turn helped us achieve the main research objective of this thesis.

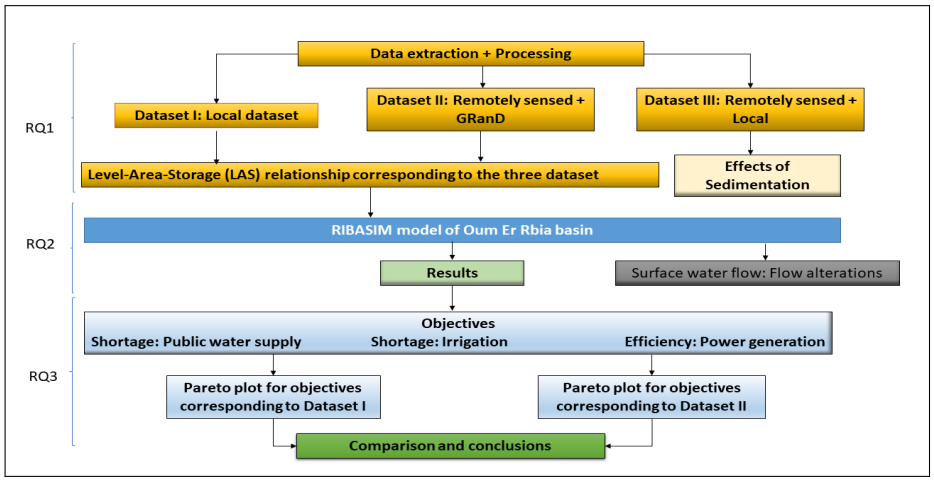

Figure 5.1: Flow of the research indicating research questions answered and steps taken

The main research objective of this thesis is to analyze the remotely sensed data and how it can be used in the field of water resources research. This thesis gives us a way to first process the data for water allocation decision tools like RIBASIM and finally utilizing it to assess and address water management limitations in a basin

To answer the main research question, each sub-questions were answered at a time. This helped in having a structured approach throughout the thesis. Given below is a gist of the methods that were followed to answer different research questions:

- **Research question 1:How do Level-Area-Storage relationships constructed using remotely sensed time series data compares to local Level-Area-Storage relationships?**

  The remotely sensed time series of the surface water area, can be used to extract and study the spatial and temporal variability of surface water sources. The time series data retrieved were then used to come up with Level-Area-Storage (LAS) curve. This curve was then compared to the local LAS curve retrieved from the water allocation decision model RIBASIM of the OER basin

- **Research question 2: How does the surface water flow alters due to change in data source from local to remotely sensed time series data?**

  The water allocation decision models depend on water availability, which is equal to the upstream flow of water at that particular location. When we use a new set of LAS curves for the reservoirs constructed using remotely accessed data, depending on the characteristics of the reservoir, and operating rules the outflow from the reservoir changes. In a system of reservoir, it plays an important role as it affects the outflow of the connecting reservoirs as well. Thus, changing the overall water availability in the basin. The water allocation decision models like RIBASIM helps simulate the surface water link. This shall help us assess the change in the outflow from the reservoir and what are its implications on the overall system operation.

- **Research question 3: How do decision trade-offs compare to each other when using remotely sensed time series data of reservoir area or local data?** This research hypothesizes that the LAS curves constructed using remotely accessed data are quite reasonable when compared to the local LAS curves and can serve as an alternative in absence of the local data. To assess the feasibility of using remotely accessed LAS curves, the water allocation decision model for the OER basin shall be assessed by first optimizing the operating rule curves for the three objectives of public water supply, irrigation, and energy generation with the local LAS curves. This is followed by optimizing the rule curves with the new set of LAS curves created using remotely accessed data. The trade-offs are then compared for the optimized set of operating rule curves. The best set of operating rule curves corresponding to the remotely sensed LAS curve is then used with the local LAS curves to see the change in trade-offs across the objectives. The performance across the three objectives with this set of operating rules and local LAS curves shall give us an idea of the feasibility of using remotely sensed time series data for water management decisions.

The following section delve deeper into the methodology to answer the research questions and gives an extensive overview of the steps followed for the completion of the project.

5.2. Research question 1: How do Level-Area-Storage relationships constructed using remotely sensed time series data compares to local Level-Area-Storage relationship?

The remotely sensed times series data gives us an idea of temporal and spatial variability of the surface water in a basin. It is quite necessary to take these variations into account to optimize water allocation decisions. The water allocation decision model used for this thesis is the River basin simulation model (RIBASIM), which is a generic model and simulates a river basin behaviors under various hydrological conditions. The flow-through different networks of rivers, streams, canals, reservoirs, and demand by different users are described using networks of nodes and links. It is capable of evaluating a large set of system modeling options and outputs. For example, measures related to infrastructure, changes in water distribution, and the consumption pattern across different sectors [53]. The reservoir in the RIBASIM model can take as one of the physical inputs the Level-Area-Storage (**LAS**) curve. These curves can be created using any data-set with periodic measurements of the level and storage. However, the time-series data required to come up with such curves are usually hard to get. Remotely sensed time-series data of the surface area of the reservoirs can then be utilized along with other open-source datasets like GRanD to come up with LAS curves.

For assessing the benefits of using remotely sensed data we have two sets of LAS curves, one has been retrieved from the RIBASIM model of the OER basin used in the PDAIRE or basin study carried out by NOVEC[4], while the other is derived by processing the data retrieved from remotely sensed time-series data of reservoir surface area in combination with the GRanD database and Google Earth Pro software. The storage values that we get from the two LAS curves are then used to get the root mean square error (rmse) values. This rmse was then divided by the capacity of the respective reservoirs to get an idea of the approximation of the storage with the new set of remotely sensed LAS curves.

To derive the LAS curve using remotely sensed data and GRanD database the formula Kaveh et al[33] derived was used. The steps to get LAS curves using remotely accessible data has been illustrated in the following sections.

The RIBASIM model encompasses water management decisions over a long period, from 1941 to 2015. The long time series has been used to implicitly include the effects of climatic variability and thus take into account different hydro-meteorological situations possible.

5.2.1. Data Processing

One of the objectives of this thesis is to have an alternate source of dependable data to address the lack and inaccessibility of data in the field of water resources management. To bridge this gap we come up with a new set of LAS curves using remotely sensed time-series data in combination with other open-access data sources like the GRanD or Google Earth Pro software. These curves are first compared to the local LAS curves to assess their performance in approximating the original local LAS curves. They are then used to optimize the operating rule curves for the reservoirs in the OER basin.

As a part of this project we have two sets of data:

1. **Dataset I: Local data**
2. **Dataset II: Remotely sensed time series data + GRanD**

Dataset I: Local data
As discussed in section 4.3 the RIBASIM model for the OER basin was developed by the NOVEC consultancy as a part of their project to assess the impacts of climate change on the OER basin and its implication on water consumption by different user groups. The model for the basin is pretty extensive with the updated LAS curves created in the year 2015. The model has extensive data with irrigation demand, firm energy demand, and public water supply-demand, etc. The RIBASIM model with the local LAS curves shall be used as a reference model. Optimization of reservoir operations shall be performed to get the best set of operating rule curves for the reservoirs.

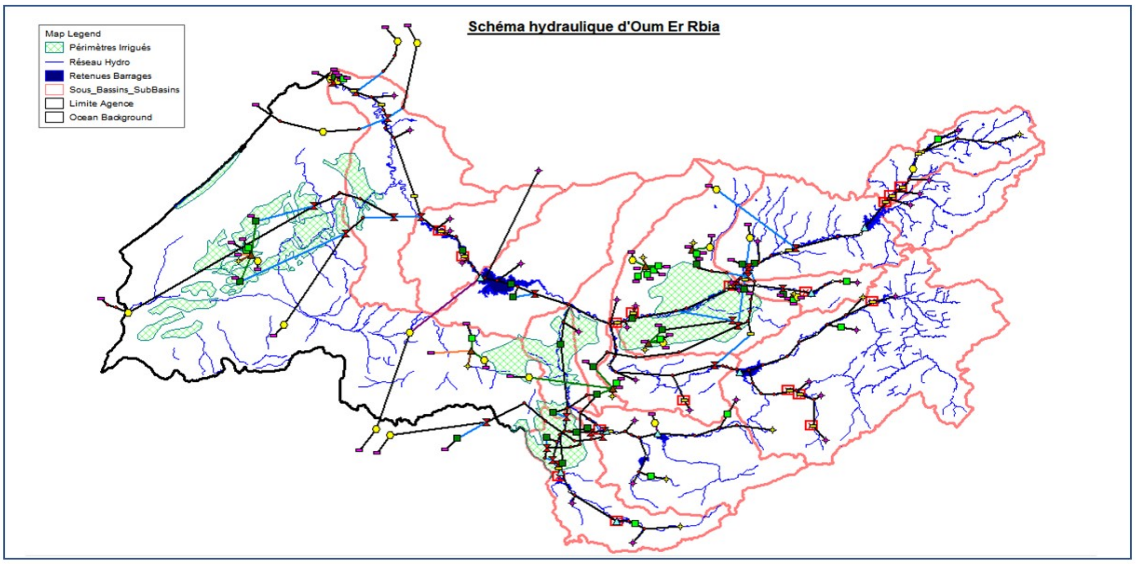

Figure 5.2: RIBASIM network Oum Er Rbia basin, Morocco

Figure 5.2 shows the RIBASIM network of the OER basin. There are eight reservoirs in the basin. Out of this, only five are active while the other three are planned to address the increasing need for water resources and declining water availability and are yet to start their operation.

Dataset II: Remotely sensed time-series data + GRanD
In absence of the LAS curve, the time series data in combination with other sources of data can prove to be handy in deriving the relation between level, area, and storage. There have been numerous researches to develop empirical and semi-empirical approaches[44][19][29][33] that can help a water manager/researchers to come up with LAS curves for their use.

Kaveh et al [33] came up with a more precise dimensionless capacity equation with fewer unknown parameters and coefficients. The LAS curve for a reservoir depends totally on the shape of the reservoir. Hence, it becomes vital to have a coefficient representative of the shape of the reservoir. In the equation suggested by Kaveh et al [33] that coefficient is referred to as the reservoir coefficient. Calculating the reservoir coefficient 'N' thus becomes the first step to get the LAS curve for a reservoir. Equation 5.1 shows the formula for calculating N, also known as the shape factor:

$$N = \frac{2V_m}{y_m A_m} \tag{5.1}$$

where:

N	Reservoir coefficient
V_m	Maximum storage of the reservoir in m^3
y_m	Full reservoir level in m
A_m	Surface area at maximum storage in m^2

N gives us an idea of the shape of the reservoir and is vital in coming up with LAS curves. The area-level relationship and storage level relationship is only feasible till the reservoir coefficient 'N' in the equation 5.1 is less than or equal to 2. When N is equal to 2 the area-capacity curve becomes a straight line with the constant area, for N>2 the trend inverts and the area decreases with increasing storage. Hence, the feasibility of using this method to come up with the LAS is limited to values of N<=2. Shape factor greater than 2 suggests the product of maximum level and maximum surface area is less than the storage which is not possible unless the surface area of the reservoir increases with decreasing depth.

Once we have the reservoir coefficient we can get the relation between level and area using the equation 5.2.

$$A_y = \frac{2V_m}{Ny}\left(\frac{y}{y_m}\right)^{\frac{2}{N}} \tag{5.2}$$

where:

N	Reservoir coefficient
A_y	Surface area of the reservoir at level y in m^2
y	Level of the reservoir in m
y_m	Full reservoir level in m

Similarly equation 5.3 shows the relation between volume and level.

$$V_y = V_m\left(\frac{y}{y_m}\right)^{\frac{2}{N}} \tag{5.3}$$

where:

N	Reservoir coefficient
V_y	Storage of the reservoir at level y in m^3
V_m	Maximum storage of the reservoir in m^3
y	Level of the reservoir in m
y_m	Full reservoir level in m

Substituting

$$y = y_m\left(\frac{V_y}{V_m}\right)^{\frac{N}{2}} \tag{5.4}$$

in the equation 5.2 we get the equation for area-capacity curve

$$A_y = \frac{2{V_m}^{\frac{N}{2}}}{Ny_m}\left(V_y^{\frac{2-N}{2}}\right) \tag{5.5}$$

where:

N	Reservoir coefficient
V_y	Storage of the reservoir at level y in m^3
V_m	Maximum storage of the reservoir in m^3
y_m	Full reservoir level in m

For the OER basin, the GRanD dataset had reservoir data for four of the five reservoirs: Al Massira, Bin El Ouidane, Moullay Youssef and Hassan 1er reservoirs. Reservoir coefficient calculated using equation 5.1 for the Hassan 1er reservoir was greater than 2. As discussed before N $>$ 2 is infeasible, therefore we used the elevation data from google earth pro software and subtracted it from the full reservoir level (FRL) of the Hassan 1er reservoir to get an approximate maximum depth of the Hassan 1er reservoir. We followed similar process for the Ahmed El Hansal reservoir, which is not there in GRanD. The maximum storage and FRL for both the reservoirs were retrieved from Fanack Water website [5] which has documented pretty much all the major reservoirs in Morocco.

The LAS curves can be used to identify sedimentation in the reservoir. The updated local LAS curves were used along with storage and level time series received by the Moroccan authorities to see how well these reservoirs approximate the remotely sensed reservoir area time series. The remotely sensed time-series data shall also be used with local LAS curves to approximate local storage. In both cases if there is an effect of sedimentation the approximation should improve with time as the LAS curves have been updated recently by the reservoir authorities and are representative of the altered shapes of the reservoirs due to prolonged sedimentation.

To identify the percentage of sedimentation in the reservoirs, the maximum surface area detected by satellites should be used with LAS curves to get the maximum storage of the reservoir. It shall then be compared to the maximum capacity furnished by the local authorities. However, there is an assumption that the reservoir reaches its FRL in the recent past and hence, encapsulates the effect of sedimentation in the reservoir.

5.3. Research question 2: How does the surface water flow alters due to change in data source from local to remotely sensed time series data?

The outflow from the reservoir depends on water demand, operating rule curves, and the state of the reservoir. The LAS curve gives a relation between the level, area, and storage in the reservoir. For a particular time step, the reservoir gets as an input a certain amount of water. Depending on the LAS curve and storage, the surface water reservoir node in the RIBASIM model determines the level in the reservoir. Finally, RIBASIM based on the operating rule curves and water demands determines the release of water from the surface water reservoir node.

Hence, alteration in the LAS curves changes the outflow from the reservoirs. The outflow from the upstream reservoirs like Ahmed El Hansal, Bin El Ouidane, Hassan 1er, and Moullay Youssef is an inflow to the downstream Al Massira reservoir. This eventually changes the outflow of the downstream reservoir in the connection, figure 3.2. Thus, affecting the water availability in the basin. Here, we see the alteration in surface water flow in the RIBASIM model of the OER basin for local and remotely sensed LAS curves. The alteration in flow reflects on the performance of the model across different objectives.

The flow at the output of the reservoir node shall be extracted from the RIBASIM model corresponding to both the sets of LAS curves. This surface water flow time series will then be assessed for the wet and dry seasons to perform a detailed study of the implication of flow alterations on the water management in the OER basin. We assess the average and 90^{th} per-

centile interval of the monthly water outflows for wet and dry seasons starting from November until April and from March to October respectively [45]. A climatology plot showing mean, and 90^{th} percentile interval shall help us analyze the change in flow for the wet and dry seasons. It will give us an insight into the performance of the reservoir in furnishing water demands.

5.4. Research question 3: How do decision trade-offs compare to each other when using remotely sensed time series data of reservoir area or local data?

If the LAS curves derived using remotely sensed time-series data of reservoir surface area are a reasonable approximation of the local LAS curves. It makes sense to assess its viability in coming up with water management decisions in the basin. In order to assess that we set up two different RIBASIM models for the OER basin. The two models have a different set of LAS curves from the two different data sources. These two models are then optimized for three primary purposes pertinent to the basin: a)Public water supply, b)Irrigation, and c)Hydropower. The local authorities are concerned with ensuring water allocation decisions to serve the three demands. However, during droughts priority is given to furnishing public water supply-demand followed by irrigation and finally hydro-power while maintaining the firm energy demand. The three objectives that have been used for the purpose are as follows:

1. Public water supply objective (pwsobjective): Sum of top 1 percentile of the monthly public water shortage from 1941-2015.

2. Variable irrigation objective (virobjective): Sum of top 1 percentile of the monthly variable irrigation demand shortage from 1941-2015.

3. Energy objective (energyobjective): Sum of top 1 percentile of the monthly energy generated from 1941-2015.

The public water supply includes domestic water supply in the region, it doesn't take into account the industrial water demands which feed on desalination and reuse of other resources in the basin. The variable irrigation objective shows the shortage in the water supply to variable irrigation nodes in the RIBASIM. These nodes explicitly take into account actual and expected rainfall along with factors like crop water requirements and irrigation efficiency to calculate water demand at that particular time-step, since these demands can vary these nodes are known as variable irrigation nodes. Finally, the energy objective aims to maximize the energy generation from these reservoirs.

The water management issues in a basin are rarely a one-dimensional issue. With varied uses of water in a basin, it is essential to have a proper trade-off between different objectives to reach a decent level of utility amongst water users. This requires optimizing water over different objectives. In contrast to single-objective optimization, a solution to a multi-objective problem is more of a concept. In multi-objective optimization, there is no single global solution, and it is often necessary to determine a set of points that all fit a predetermined definition for an optimum known as **Pareto optimal**. Pareto optimal refers to the state or solutions if and only if there are no other solutions that would improve one objective without deteriorating the other [42].

The two RIBASIM models with different LAS curves are then optimized using optimization algorithms like Particle Swarm Optimization (PSO), Non-sorting genetic algorithm II (NSGA-II), Epsilon non-sorting genetic algorithm II (ϵ-NSGA-II), multi-objective genetic algorithm (MOGA),

Strength Pareto evolutionary algorithm (SPEA), Borg multi-objective evolutionary algorithm (Borg-MOEA), etc. Here, we use ϵ-NSGA-II to optimize reservoir operations in the RIBASIM model. We used Evolutionary Modelling and Analysis (EMA) workbench as a platform to optimize the system of reservoirs in the OER basin. The EMA workbench is a platform that provides support to perform optimizations developed in different modeling packages and environments.

Reservoir operation in RIBASIM
Reservoir operation in RIBASIM is described by a set of rule curves varying across the year as presented in figure 5.3 :

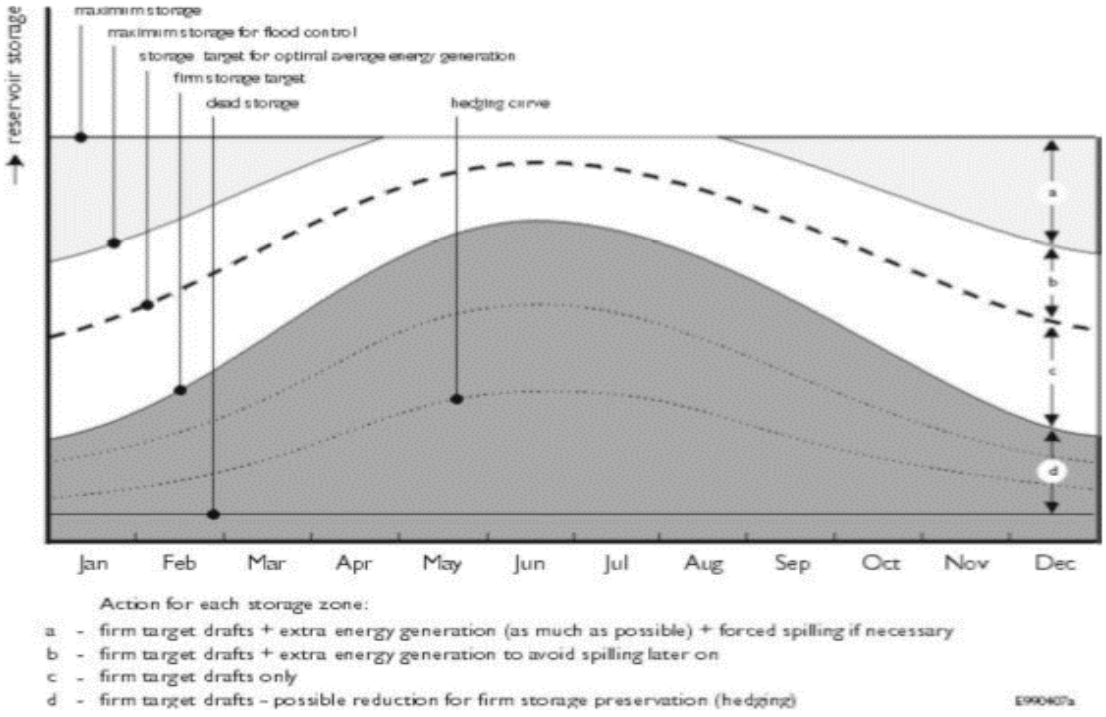

Figure 5.3: Operation rules for reservoirs in RIBASIM[35]

The reservoir operation in RIBASIM depends on a set of three operationg rule curves:

1. Flood control curve which keeps the storage space for floods.
2. Maximum hydro power production target curve balancing the maximization of head and minimization of spill.
3. Firm storage curve indicating minimum storage/level required to maintain downstream water supply and minimum acceptable (firm) hydropower generation throughout a critical dry period.

The operation of a reservoir in this way has thirty six parameters which can be manipulated in order to optimize the reservoir operations.

1. Monthly values for flood control level
2. Monthly values for target level

3. Monthly values for firm level

These parameters are later optimized using evolutionary multi-objective optimization using EMA workbench.

Evolutionary Modelling and Analysis Workbench
Evolutionary Modelling and Analysis Workbench is a research methodology that utilizes computational experiments to analyze complex and uncertain systems [9]. It provides support to perform exploratory modeling developed in various modeling packages and environments. However, one of the biggest benefits of using EMA workbench is that it supports simulations in parallel processors on both single machines as well as on clusters. Which turned out to be useful for the completion of this thesis. Besides, the workbench is flexible. It supports all the optimization algorithm that comes with the platypus-opt package, or the Generational Borg algorithm in workbench. However, for this thesis we stick to ϵ-NSGA-II algorithm and all the optimizations are done using that.

Directed Search
Exploratory modeling investigates how uncertainty and policy levers affect the outcome. The investigation of these mappings are done using sampling-based strategies (open exploration) or optimization-based strategies (directed search). For, this thesis we utilize the directed search capabilities of the workbench.

Search over levers
Directed search is very often used to perform optimization over decision levers. Here the operating rules for the reservoir are the decision levers that eventually affect the outcome over multiple objectives. This is pretty straightforward to perform using the workbench. Thus, making it one of the best candidates for the assessment of reservoir performance over the three objectives.

Tracking convergence
In multi-objective optimization one of the vital components in assessing the convergence of the algorithm. Hypervolume and epsilon progress are the two metrics that workbench supports. Hypervolume is a measure of how much of the objective space is covered by a given set of non-dominated solutions. The higher the hypervolume, the larger the space that is covered by the objectives. It grows early on and starts to stabilize once the algorithm starts to converge. Epsilon progress measures how often a solution is found in a new grid cell of the epsilon gridded output space. Initially, the solutions in new grid cells are found quite frequently. Once the algorithm starts to converge, epsilon progress becomes more difficult thus stabilizing the algorithm.

6

Results

6.1. Level-Area-Storage curves

The first research goal of this thesis was to process the data so that it can be used by different water management tools. For RIBASIM, the LAS curve in the reservoir node bridges that gap. The local LAS curves were part of the RIBASIM model furnished by the NOVEC consultancy[4]. To evaluate the benefits of having remotely sensed data especially in situations when the local data are not easily accessible or are not available, the LAS curves using a combination of remotely sensed time-series data and some other open-source database like GRanD was derived using equations 5.1, 5.2, and 5.3.

6.1.1. Remotely sensed time series data + GRanD

The area-capacity and level-capacity curve for the reservoirs in the basin derived from the remotely sensed dataset and GRanD database have been shown in Figures 6.1 and 6.2 respectively. The blue line is for the curve derived using remotely accessed data while the orange lines show the relationship from the local data. Table 6.1 shows that the storage for the large reservoirs is approximated better as compared to the small reservoirs. This makes sense as the empirical formulas have a larger volume to approximate these curves and hence, estimates the LAS curves better for the large reservoirs as compared to the smaller reservoirs. The relative root mean square error (**RMSE**) values for the storage that we get from the kaveh et al[33] for large reservoirs like Al Massira and Bin El Ouidane reservoir is less than the Moullay Youssef reservoir this is also true for the Ahmed El Hansal and Hassan 1er reservoirs. The better approximation for the large reservoirs validates this hypothesis.

Reservoir	Relative RMSE	Storage (Mcm)	Source
Al Massira	0.29	2988	Remote sensing + GRanD
Bin El Ouidane	0.21	1390	Remote sensing + GRanD
Moullay Youssef	0.39	154	Remote sensing + GRanD
Hassan 1er	0.45	531.09	Remote sensing + Google earth pro
Ahmed El Hansal	0.19	840.38	Remote sensing + Google earth pro

Table 6.1: Relative rmse of the storage we get from the remotely sensed LAS curves with respect to that we get from local LAS curves

The approximation also depends on the sources of data being used to come up with the LAS curves. For Hassan 1er and Ahmed El Hansal reservoirs, we used the google earth pro software to get the depth. The relatively better approximation of the storage for the Ahmed El Hansal reservoir as compared to the Al Massira and Bin El Ouidane reservoirs can be due to the different sources of data used to come up with the shape factor **N** discussed in section 5.2.1. This can very well be the reason for a better approximation of Moullay Youssef as compared to the Hassan 1er reservoir. To address the lack of data in the GRanD database we used google earth pro software to get the approximate depth of the Hassan 1er and Ahmed El Hansal reservoir. The images for the two reservoirs were however captured at different points of time and might not be representative of the maximum depth. For the Al Massira, Bin El Ouidane, and Moullay Youssef reservoirs, we used the average depth from the GRanD database which is again not equal to the maximum depth that we get from the local data. These approximations shall improve if we have an accurate source of maximum depth and storage.

Figure 6.1 shows that for the dry season when the storage in the reservoir is less, the remotely sensed area-capacity curve for Al Massira, Bin El Ouidane, and Moullay Youssef tends to overestimate the reservoir surface area. The Hassan 1er overestimates the surface area throughout the plot for both low and high storages. Finally, Ahmed El Hansal underestimates the area of reservoir surface for both high and low storage values i.e. for both dry and wet seasons. For the wet seasons when the storage in the reservoir is more Al Massira, Bin El Ouidane and Moullay Youssef underestimate the reservoir surface area.

When we delve deeper into the LAS curves. We observe that in figure 6.2 the level-capacity curve derived using remotely accessed data overestimates the level in dry seasons with less storage for the Al Massira, Bin El Ouidane, Hassan 1er, and Ahmed El Hansal reservoirs. This shall reflect on the energy generated from these reservoirs. Hence, there shall be an increase in the energy generation from these reservoirs in dry periods. For the Moullay Youssef reservoir, the level is underestimated for the same storage as per the remotely sensed level-capacity curve compared to the local level-capacity curve. This is true for both wet and dry periods.

For wet periods when the storage is high in the reservoirs, Al Massira and Bin El Ouidane will have less level for the same storage when we use the remotely sensed level-capacity curve instead of the local level-capacity curve. The remotely sensed level-capacity curves for the Hassan 1er and Ahmed El Hansal reservoirs overestimate the level for both dry and wet seasons. Owing to its large energy capacity a decrease in level during the wet seasons for the Al Massira, Bin El Ouidane there shall be a decline in the amount of top one percentile of the energy generated from the reservoir system. This has been discussed in detail later in this report.

6.2. Local LAS curve and sedimentation

Apart from coming up with the new set of LAS curves, we can also utilize the remotely sensed time-series data for the detailed analysis of the effects of sedimentation in the reservoir. The remotely sensed reservoir surface area time series has been proved to be quite accurate in surface water detection[15] and can be used to identify the effects of sedimentation in the reservoirs.

Figure 6.3 shows the surface area time series for the four reservoirs: Al Massira, Bin El

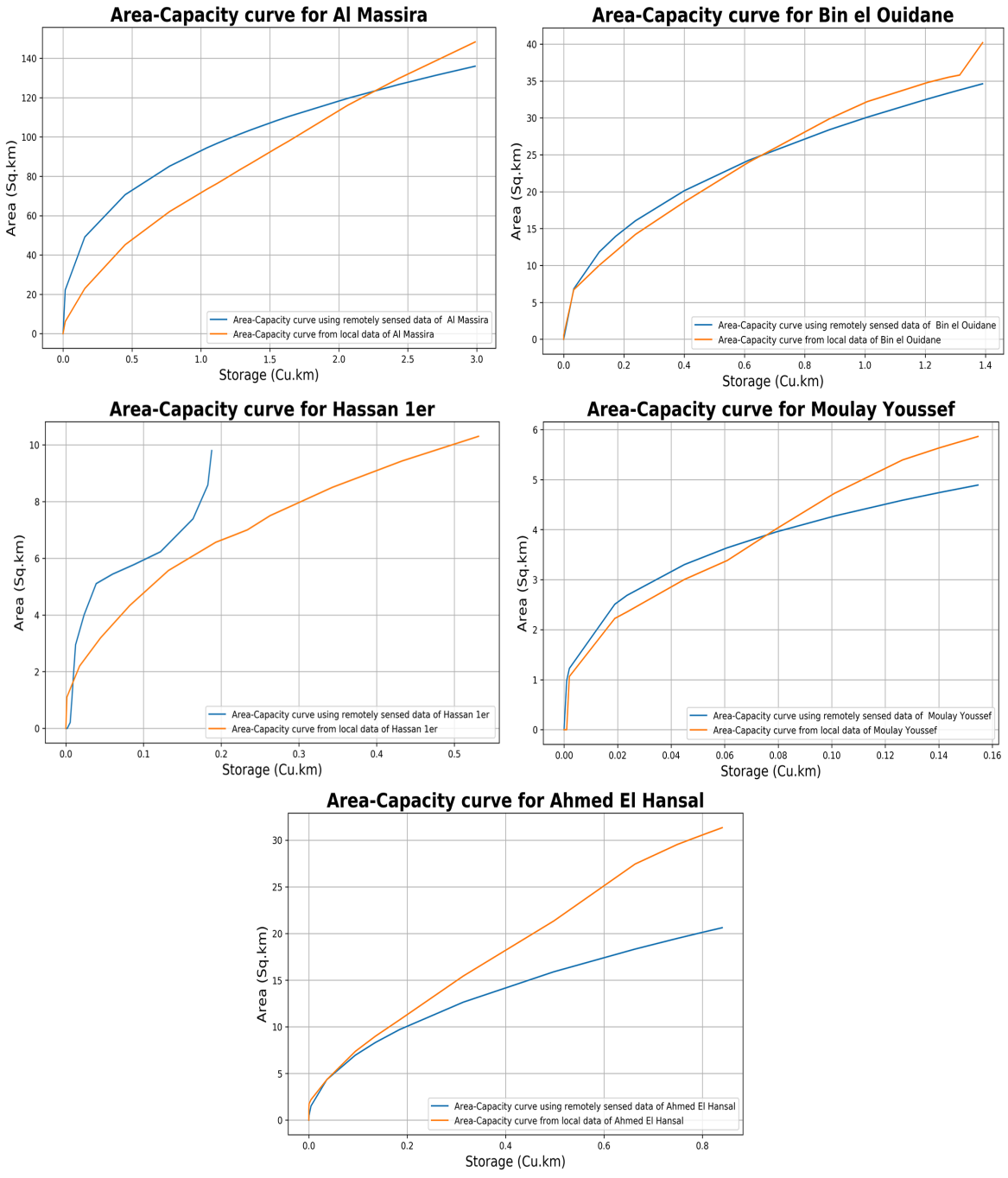

Figure 6.1: Local vs Derived area capacity curve for the five reservoirs in the OER basin

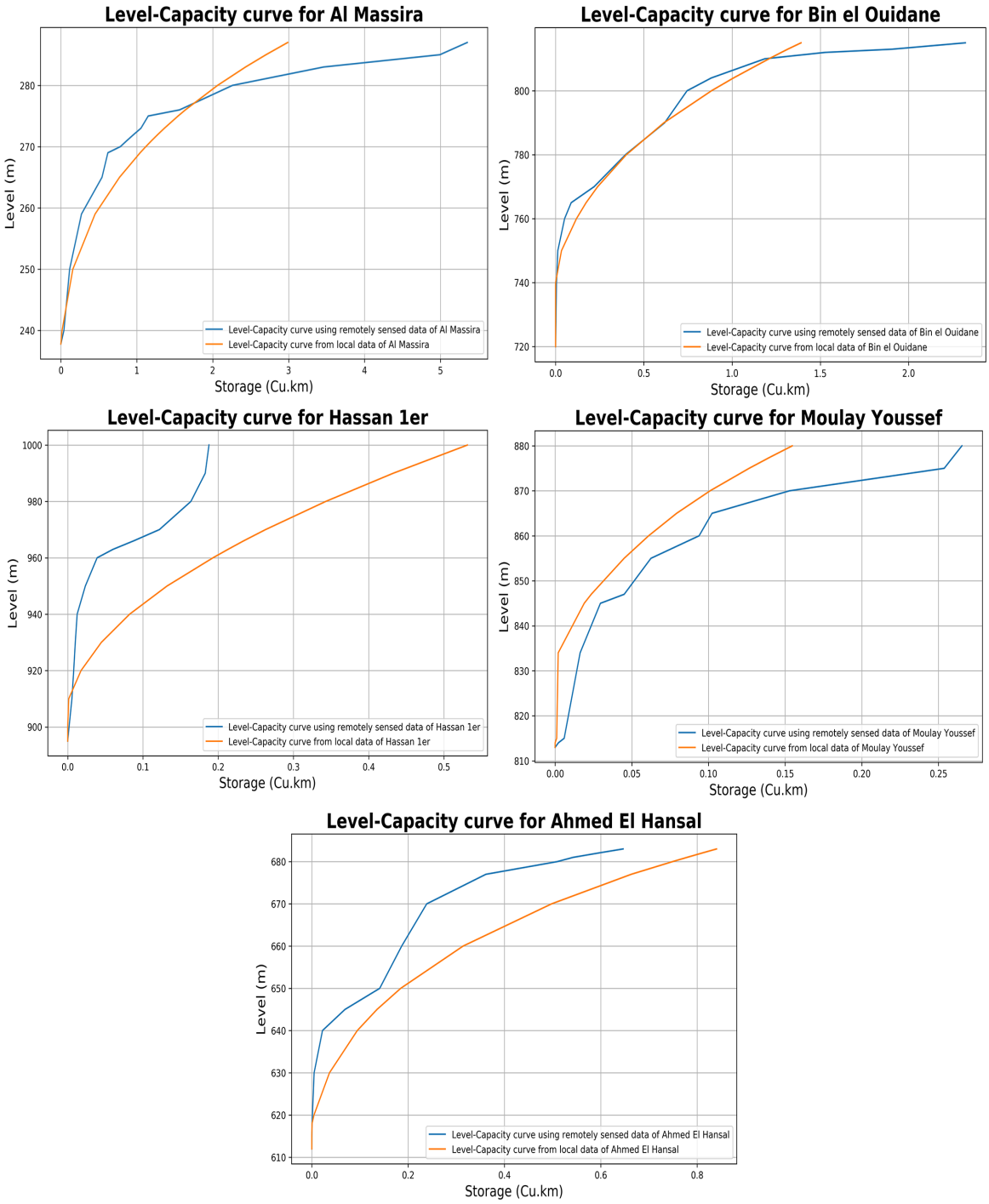

Figure 6.2: Local vs Derived level capacity curve for the five reservoirs in the OER basin

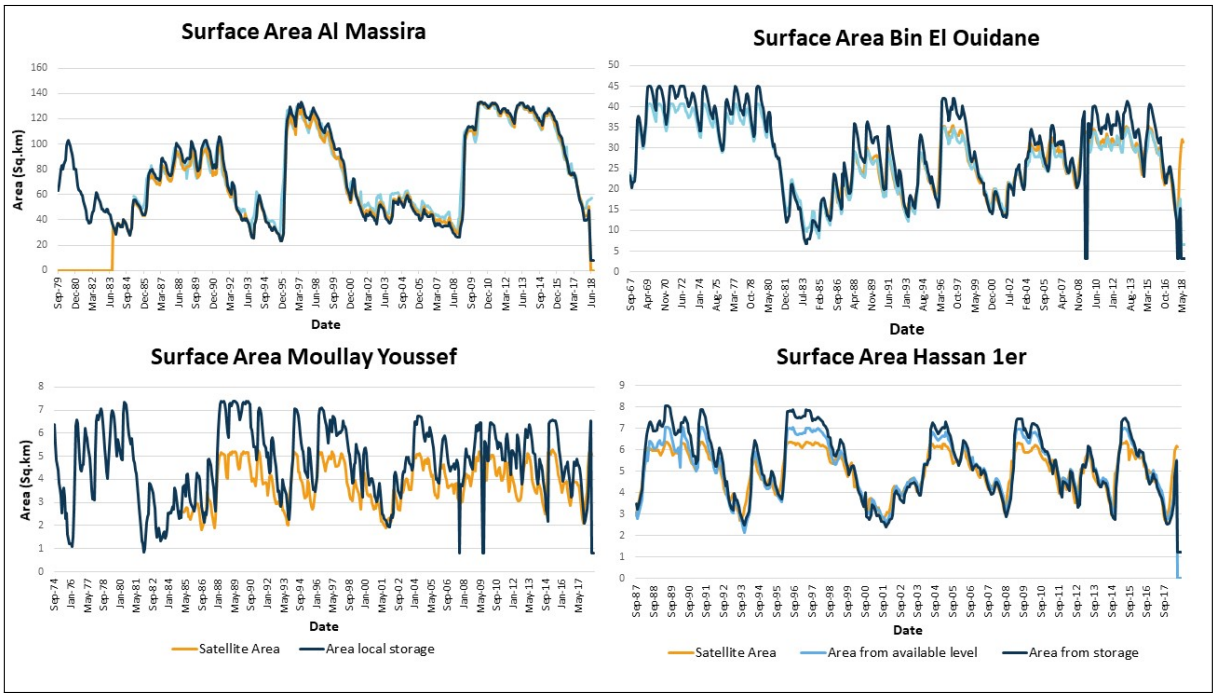

Figure 6.3: Surface area time series for Al Massira, Bin El Ouidane, Moullay Youssef and Hassan 1er reservoirs

Ouidane, Moullay Youssef, and Hassan 1er. Different lines show the surface area time series generated from different data sources. The orange line corresponds to remotely sensed time-series data, the light blue line corresponds to the area time series generated using the local level and local LAS curves. Finally, the dark blue line corresponds to the surface area time series generated using local storage and local LAS curves.

The area time series generated using the combination of local LAS curves and level data is quite close to the remotely sensed area for the Al Massira reservoir. Similarly, the surface area time series generated using level data for the Bin El Ouidane is quite close to the remotely sensed surface area time series. However, the area generated using storage data tends to overestimate the surface area of the reservoirs during wet periods compared to the remotely sensed reservoir surface area. For the Moullay Youssef and Hassan 1er reservoirs, there is a noticeable deviation of the area time series generated using level data and storage data furnished by the authorities compared to the remotely sensed time-series data. This suggests towards high rate of sedimentation along the sides of the reservoir as soil deposits at the sides of the reservoir can be detected by the satellite.

To assess the impact of the sedimentation on the storage of the reservoirs we try to analyze the storage time series plot generated using remotely sensed time-series data and local LAS curves. They are then compared to the local storage time series provided by the reservoir authorities.

Figure 6.4 shows the storage time series for the reservoirs. Similar to the area time series the orange line in the storage time series is for the storage generated using the remotely sensed reservoir surface area time series, and the dark blue line is the storage furnished by the authorities. The approximation of the storage furnished by the local authorities is quite close to the storage generated using remotely sensed time-series data of reservoir surface

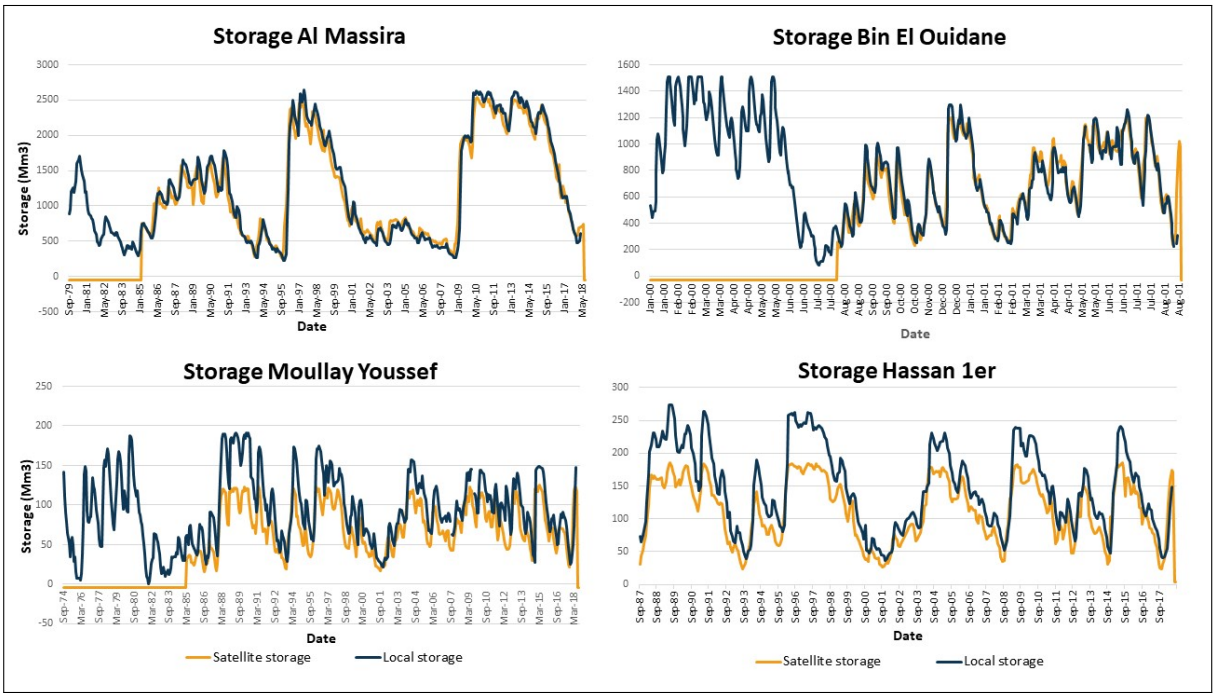

Figure 6.4: Storage time series for Al Massira, Bin El Ouidane, Moullay Youssef and Hassan 1er reservoirs

area for the Al Massira reservoir. As this approximation is really good throughout the plot we can infer that the reservoir is less prone to the effects of sedimentation and the LAS curve did not change much with time. This can be validated as table 6.2 shows that Al Massira has only 4.1% change with the percentage rate of change of 0.1%/year in storage due to sedimentation

For the Bin El Ouidane reservoir, the local storage furnished by the reservoir authorities is not quite close to what we get from the remotely sensed surface area time series and updated LAS curves. However, with time the approximation improves suggesting a change in shape due to sedimentation. Since the local LAS curves have been updated recently the storage approximation improves as we move from left to right in the plot. The Bin El Ouidane reservoir is smaller than the Al Massira reservoir, hence, a higher rate of sedimentation makes sense.

The storage of the Bin El Ouidane reservoir significantly decreases around the 1980s. This is due to the prevalent reservoir management policies in the basin. This shows a strong correlation between water supplies and volume stocked in the reservoir. The annual release program defined at the beginning of each hydrological year is determined by two factors: the statistically estimated water supply in the current year and the amount of water observed in the last year. Hence, the dry period of 1976-1995 reflects in the storage of the reservoir[8].

In a basin, the effects of sedimentation are not that pronounced in large reservoirs. For smaller reservoirs effects of sedimentation becomes more dominant. The storage time series plot for Moullay Youssef and Hassan 1er shows significant improvement in the approximation as we move from left to right, suggesting a change in the shape of the reservoir due to sedimentation. This happens because the LAS curves have been updated and are capable of approximating the storage well for the near past. This can be validated through a relatively inferior approximation of the storage time series during the initial years for the Moullay Youssef and Hassan 1er reservoirs as compared to the storage time series generated using remotely sensed sur-

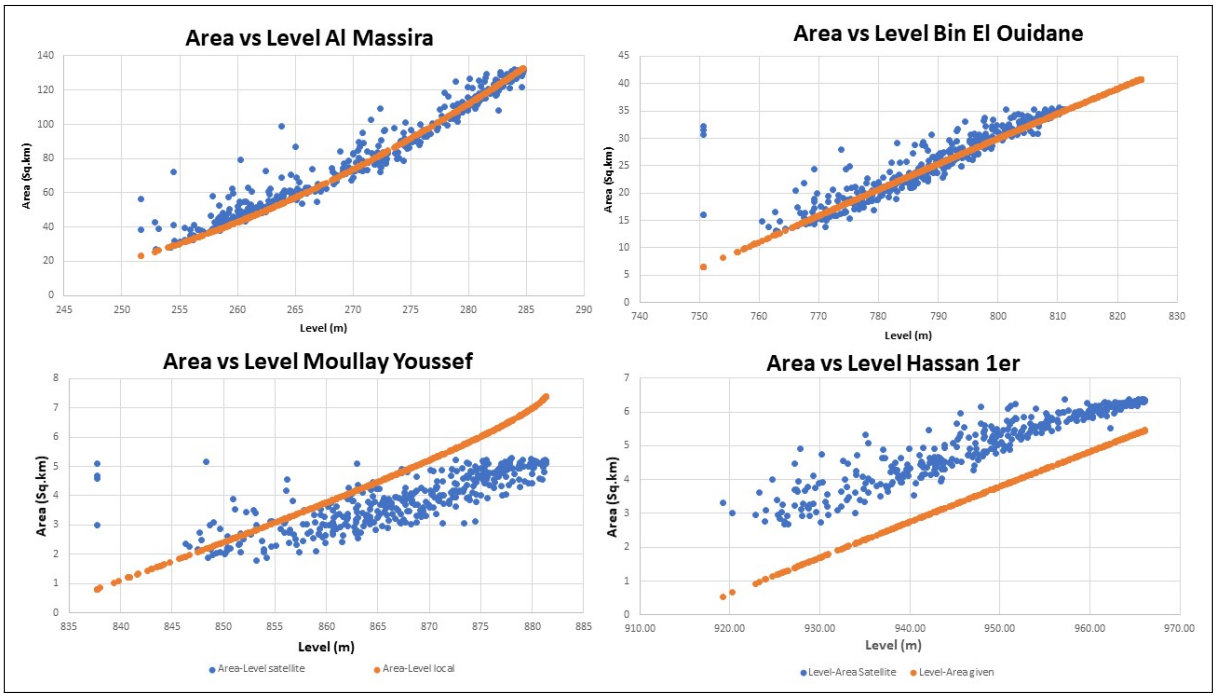

Figure 6.5: Area vs Level scatter plot for Al Massira, Bin El Ouidane, Moullay Youssef and Hassan 1er reservoir

face area time series and updated local LAS curves. This approximation, however, improves as we move from left to right in the plot suggesting that there was a change in the geometry of the reservoir and the updated LAS can capture the right shape.

Figure 6.5 shows the remotely sensed surface area against the local level time series. The scatter in the plots give us an idea of the degree of sedimentation in the reservoirs. Depending on the thickness of the scatter we can do a qualitative analysis of the sedimentation in each reservoir. The scatter plot for the Al Massira reservoir is not that spread, suggesting more or less the same area for a particular level in the reservoir. The plot however widens for the Bin El Ouidane reservoir, Moullay Youssef, and Hassan 1er reservoirs.

Reservoir	Max st (Mm^3)(Local)	Max area (Km^2) (Satellite)	Max st (Mm^3)(Satellite)	St change (Mm^3)	% Change	% Change/year
Al Massira	2644.9	132.287	2535.74	109.16	4.1	0.11
Bin El Ouidane	1507.486	35.62	1220.68	286.81	19.02	0.37
Moullay Youssef	191.5	5.28	125.46	66.04	34.38	0.78
Hassan 1er	273.2	6.38	186.20	86.99	31.84	1.03
Ahmed El Hansal	473	19.35	412.86	60.14	12.71	0.71

Table 6.2: Storage change due to sedimentation in different reservoirs

Table 6.2 shows the percentage changes as a result of sedimentation for the five reservoirs. The percentage change in the storage is high for smaller reservoirs like Moulay Youssef and Hassan 1er reservoirs with 34.38 and 31.84 percent change in the reservoir storage. For Al Massira this value goes down to 4.1%. Bin El Ouidane experiences a change in storage because of sedimentation of 19.02% while Ahmed El Hansal has a change of 12.71%. The Hassan 1er reservoir has a percentage change of 1.03%/year. Which is highest amongst five reservoirs in the basin.

6.3. Flow alteration

Figure 6.6 to 6.9 shows the flow alterations from different reservoirs as a result of the change in the respective LAS curves. The surface water flow through the system is important as it gives an idea of the overall water availability in the basin, and also plays an important role in determining the reservoir operations. Any alteration upstream of these dams shall reflect in the inflow to these reservoirs. Table 6.3 shows the alteration in average flow for an overall period from 1941 to 2015 as a result of changing the LAS curve in the reservoirs. The average outflow did not alter much for the overall period. There is a decline in the outflow from the Al Massira reservoir which went down to 38.40 m^3/s from 40.18 m^3/s. There is no change in the average outflow from the Bin El Ouidane reservoir. The other three reservoirs show minor changes. While Moullay Youssef shows a decline in outflow, the Hassan 1er, and Ahmed El Hansal shows an increase in the average outflow as a result of using remotely sensed LAS curves. These alterations are not significant and rest the case of using remotely sensed data to come up with the LAS curve in the absence of local LAS curves. However, these minor alterations become crucial when analyzing the extremes and can significantly alter our objectives. Which focuses on the worst and best 1 percentile across different water demands and energy generation.

Reservoir	Average Old (Cu.m/s)	Average new (Cu.m/s)
Al Massira Down	40.18	38.40
Bin El Ouidane Down	30.68	30.68
Moullay Youssef Down	8.20	8.12
Hassan 1er Down	7.34	7.63
Ahmed el Hansal Down	24.98	25.57

Table 6.3: Alteration in the surface water flow due to changed Level-Area-Storage relationship

We further delve into assessing the change in flow, This is done by assessing the mean flow and 90^{th} percentile flow bounds for the dry and wet seasons. The dry season in the OER basin lasts from May to October, the wet season starts in November and lasts till April.

6.3.1. Dry Seasons

Figure 6.6 and 6.7 shows the mean and 90^{th} percentile interval of the outflow from the reservoirs for the two LAS curves in dry seasons of the OER basin that starts from May and ends in October. For the Al Massira reservoir, the mean flow remains more or less the same for the remotely sensed LAS curve. The month of May observes a variation in the 90^{th} percentile interval. The lower bound of the 90^{th} decreases when we use the remotely sensed LAS curves for May. The upper 90^{th} limit also deteriorates for May. This increases the chances of a decrease in water availability in drier months for public water supply and irrigation for nodes having Al Massira reservoir as the source.

The Bin El Ouidane reservoir does not show any alteration in the outflow as a result of the change in the LAS curves. This can be validated by absolutely no change in the climatology plots for the dry seasons for the Bin El Ouidane reservoir shown in figure 6.6.

Table 6.3 shows that the overall change in the mean flow for the Moullay Youssef reservoir is

negligible. When we make a detailed analysis of the implications of changing the LAS curve on reservoir outflow for different months. We observe a slight decline in the average outflow for May and June, figure 6.6. The upper bounds for the 90^{th} percentile interval also decrease for June when we use the remotely sensed LAS curves. The lower bound of the 90^{th} percentile interval decreases for May when we use the remotely sensed LAS curves. Figure 6.7 shows that the mean flow for the dry season deteriorated for July and August in the Hassan 1er reservoir. While it increases for May with the remotely sensed LAS curve. The 90^{th} percentile lower bound also decreases for June and July. There is no change in the upper bounds of the 90^{th} percentile interval except for September which decreases for the remotely sensed LAS curves. This increases the chances of failure in meeting different water demands in dry months. Figure 6.7 shows the outflow from the Ahmed El Hansal reservoir. There is a significant change in the flow as a result of using remotely sensed LAS curves. There is an overall increase in the mean flow for the whole dry season. There is an upward shift in the 90^{th} percentile interval suggesting an increase in water outflow from the reservoir and hence, water availability downstream of the Ahmed El Hansal reservoir.

6.3.2. Wet Seasons

The wet season in the OER basin starts in November and continues until April. Though the optimization objective of this study aims at the worst-performing 1 percentile of water shortage at public water supply nodes and irrigation nodes. Water availability in wet seasons can influence the amount of energy being generated from each reservoir and improve or deteriorate the energy objective which is the sum of the top 1 percentile of the energy generated. Figure 6.8 shows the change in mean and 90^{th} percentile interval of the flow from the Al Massira reservoir. While there is no significant change in the average flow from the reservoir, the months of February, March, and April sees a decline in the mean flow from the reservoir when we use remotely sensed LAS curves. There is a deterioration in the upper bound of the 90^{th} percentile for the remotely sensed LAS curves. The lower bound of the 90^{th} percentile interval also decreases for April. As was the case for dry seasons, the Bin El Ouidane reservoir does not show any change in the flow for the wet months as well, figure 6.8.

Figure 6.8 shows that there is not much change in the outflow from the Moullay Youssef reservoir in the wet season. There is a slight increase in the upper 90^{th} percentile of the outflow for November and January, but there is a decrease in the upper 90^{th} percentile for February. There is a slight increase in the mean flow from the Moullay Youssef for December but that seems to be insignificant for the overall performance across the objectives owing to relatively small size and energy capacity of the reservoir (Table 7.1 when compared to the other reservoirs in the basin, also it serves only five of the forty-three public water supply and irrigation nodes. For Hassan 1er reservoir as well the alteration in the flow is quite minute, figure 6.9. The upper 90^{th} percentile increases for January, but there is a decline in this bound for December and February. Overall, the mean remains the same for the wet season as far as Hassan 1er reservoir is concerned.

Figure 6.9 shows the plot for the Ahmed El Hansal reservoir during wet seasons. February, March, and April observe an increase in the mean flow from the reservoir for the remotely sensed LAS curves. The upper 90^{th} percentile increases for February, March, and April. There is a decline in the lower 90^{th} percentile for January, while an increase in the lower 90^{th} percentile for February. This suggests an overall increase in the outflow from the Ahmed El Hansal reservoir for wet months.

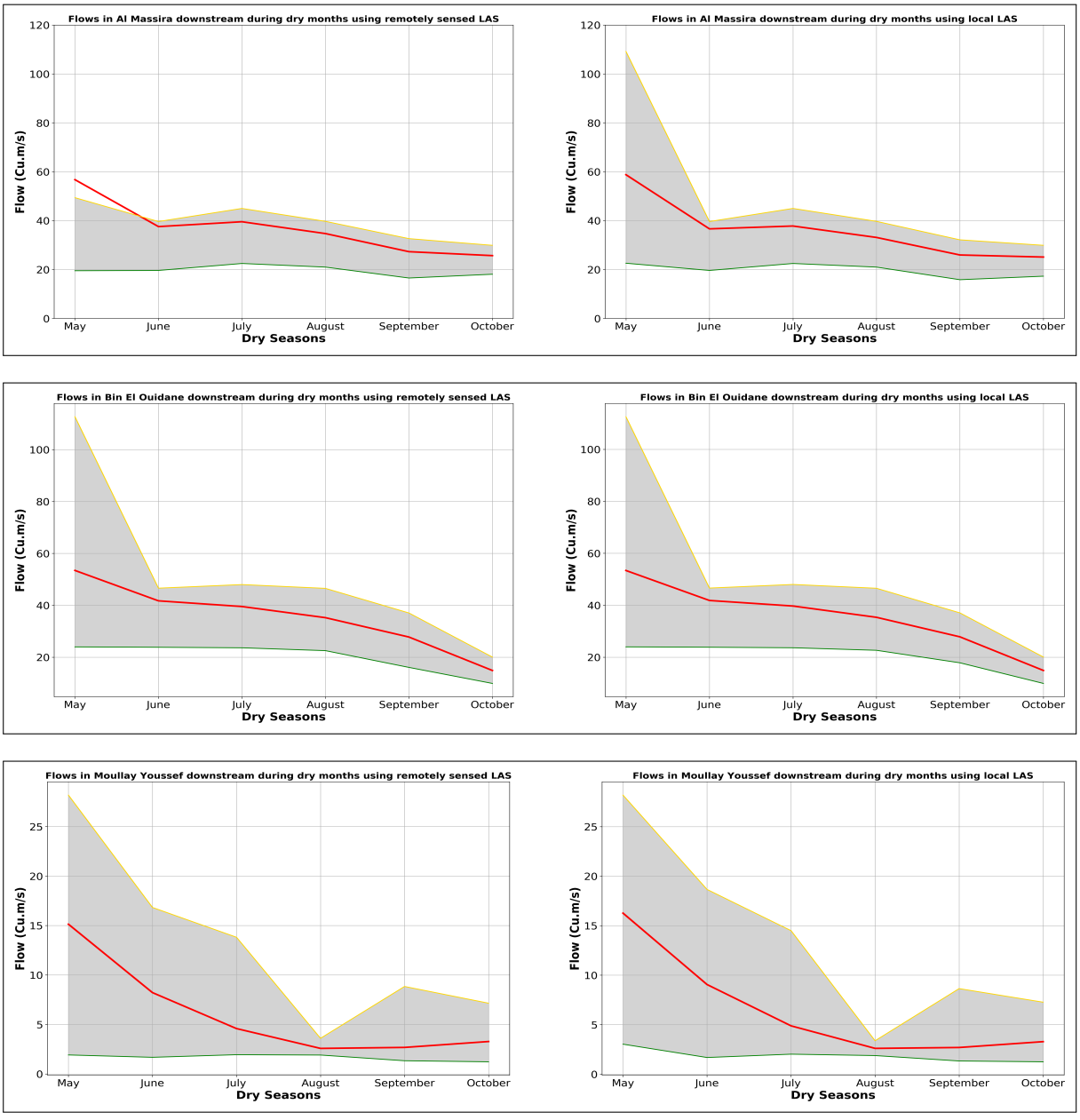

Figure 6.6: Climatology plot for dry seasons with mean and 90th percentile interval for outflow from Al Massira, Bin El Ouidane and Moullay Youssef reservoirs for remotely sensed and local LAS curve

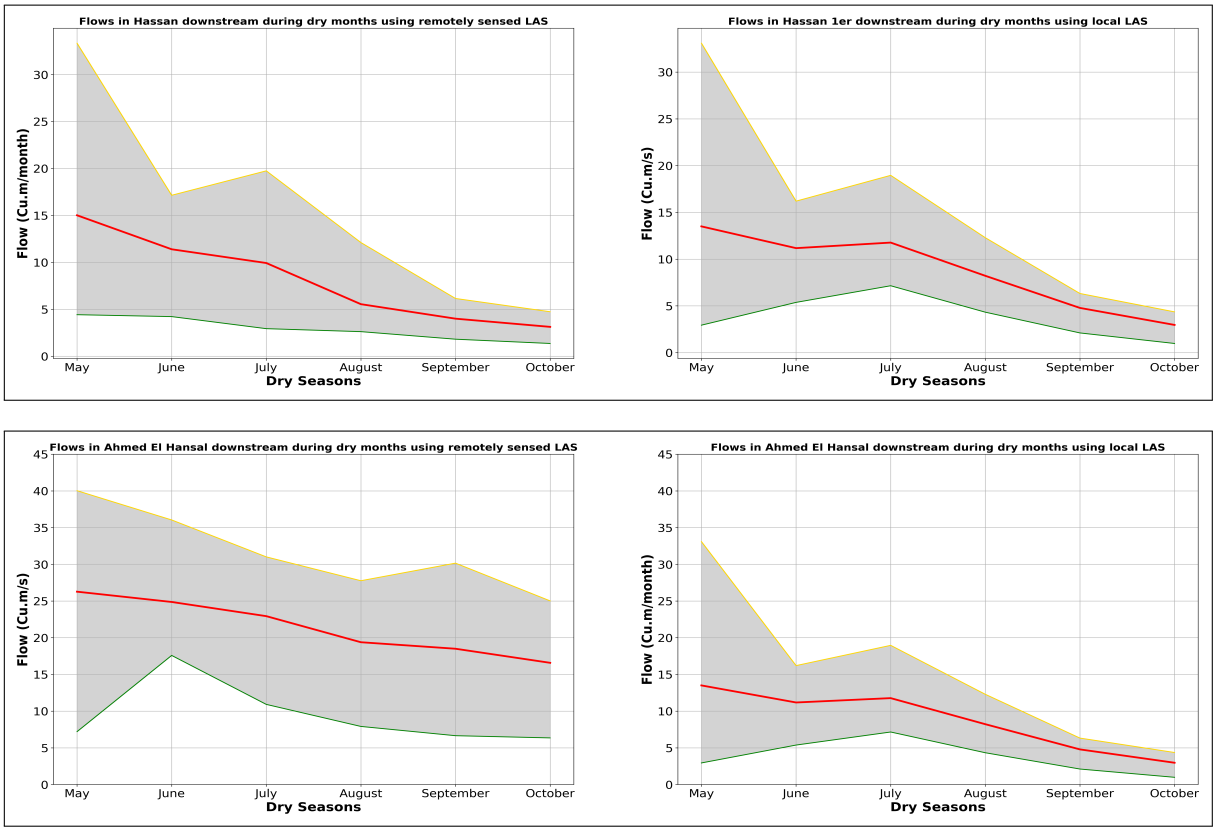

Figure 6.7: Climatology plot for dry seasons with mean and 90th percentile interval for outflow from Hassan 1er and Ahmed El Hansal reservoirs for remotely sensed and local LAS curve

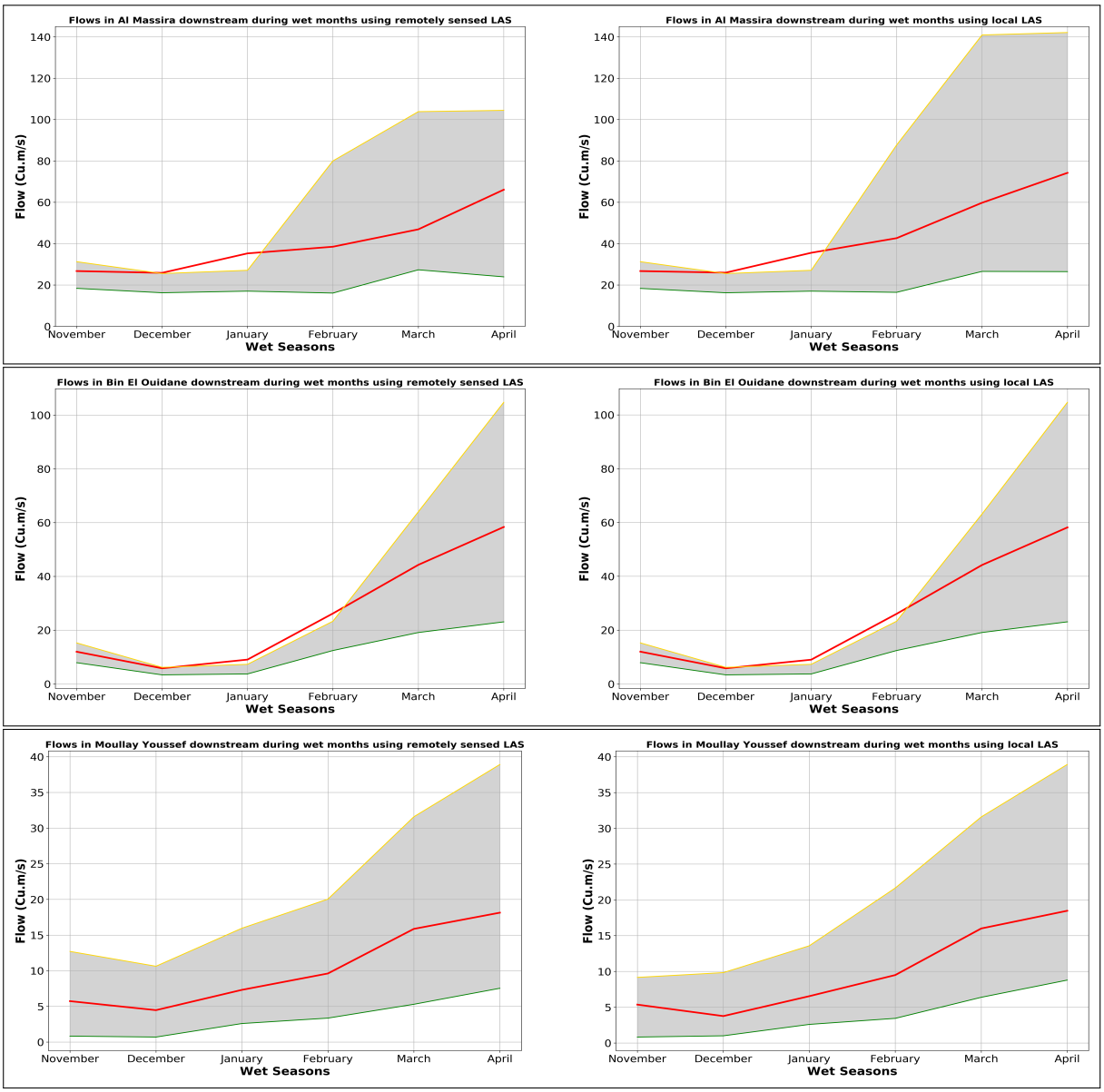

Figure 6.8: Climatology plot for wet seasons with mean and 90th percentile interval for outflow from Al Massira, Bin El Ouidane and Moullay Youssef reservoirs for remotely sensed and local LAS curve

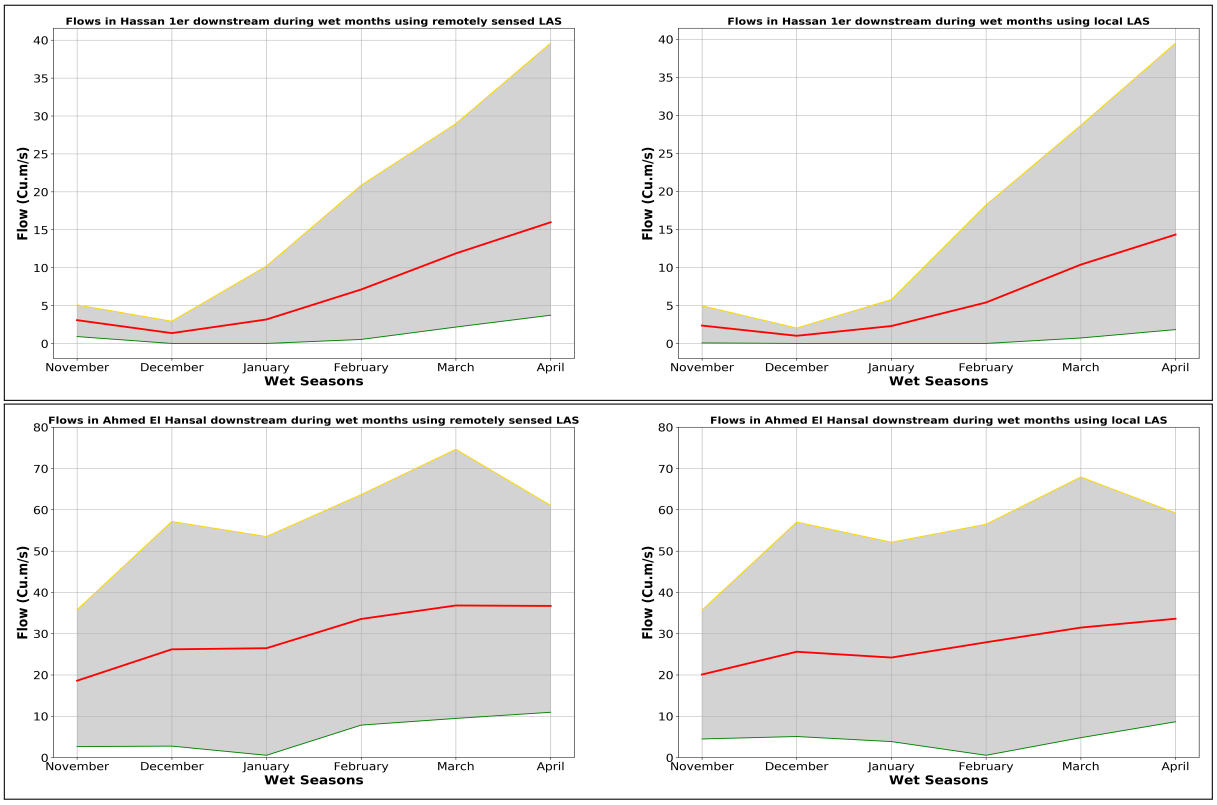

Figure 6.9: Climatology plot for wet seasons with mean and 90th percentile interval for outflow from Hassan 1er and Ahmed El Hansal reservoirs for remotely sensed and local LAS curve

6.4. Performance across objectives

Since the remotely sensed LAS curves were able to approximate the local LAS curves well, the next step shall be to use the two sets of curves to simulate the RIBASIM model to assess the change in performance across the three objectives. The two RIBASIM models were set up with different LAS curves:1) Local and 2) Remotely sensed. The RIBASIM model with the local LAS curve was executed first with three objectives: public water supply, energy generated, and variable irrigation demands. The EMA workbench was used with 250,000 nfe. Figure 7.2 shows that the algorithm converged for both epsilon progress and hypervolume convergence giving five optimum solutions for the local LAS curves. What is interesting to see that for the given set of local LAS curves, the solution converges to just five possible solutions. This indicates that the optimization algorithm is not able to find any other trade-offs other than these which serves the same level of utility. Table 6.4 shows the performance across objectives with the prevalent operating rules with local LAS and remotely sensed LAS curves this was done by running both the RIBASIM models once without optimization. Figure 6.10 shows that there is a significant improvement as far as the energy generation is concerned as a result of optimization with local LAS curves. The optimization results show that the minimum of the top 1 percentile of the sum of energy generation in the basin is 2591.64 GWh which can go up to 2596.71 GWh. While the energy generated without optimization with the prevalent operating rules and local LAS curve as shown in table 6.4 is 2432.99 GWh. The optimization improves performance across the other two objectives as well. The irrigation shortage under extreme conditions i.e. worst one percentile with prevalent operating rule curves is 550.60 m^3/s, This reduces to 405.19 m^3/s in the worst-case scenario and 402.08 m^3/s in the best-case scenario. The public water supply objective was already performing well, probably because of the prevalent water resources management policies in the basin that prioritize public water supply-demand over other water uses. Still, we observe an improvement in furnishing public water supply demands with the optimized operating rule curves.

Local Level-Area-Storage			
Runs	Public water supply shortage (m^3/s)	Energy generated (GWh)	Irrigation shortage (m^3/s)
Manual	0.79	2432.99	550.60
Remotely sensed Level-Area-Storage			
Runs	Public water supply shortage (m^3/s)	Energy generated (GWh)	Irrigation shortage (m^3/s)
Manual	1.85	2297.28	572.83

Table 6.4: Performance across objectives for manual and optimized runs

Table 6.4 shows that the use of remotely sensed LAS curves deteriorated the performance across all the objectives when used with existing operating rule curves. However, when we optimize the new LAS curve we get 290 solutions. Figures 6.11 shows that compared to the performance across the three objectives with existing operating rules and local LAS, optimization with remotely sensed LAS curves shows improvement across the energy objective and the variable irrigation objective. This can be seen from table 6.4 where the energy objective with prevalent operating rules and LAS curves is 2432.99 GWh which can improve from 2525.62 GWh to 2583.57 GWh when we employ the remotely sensed LAS curves for optimization. The performance for the public water supply objective however deteriorates from 8.69 m^3/s to 0.80 m^3/s. Shortage at the variable irrigation nodes decreases significantly with the variable irrigation objective under worst scenario going down to 371.19 m^3/s

Figure 6.13 shows the trade-offs between different objectives for the two optimizations with

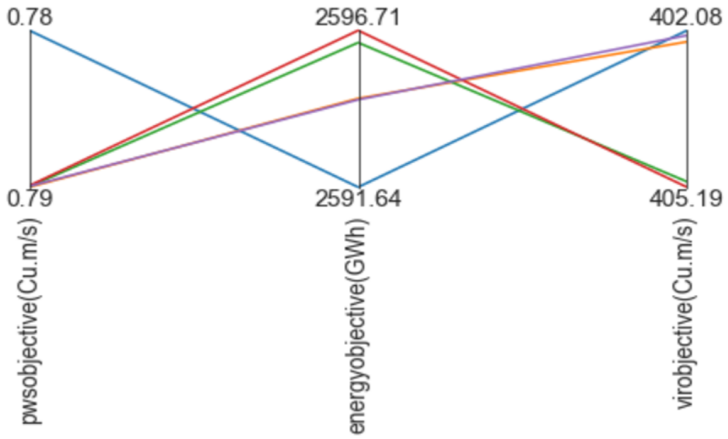

Figure 6.10: Performance across objectives for optimization with Local LAS curves

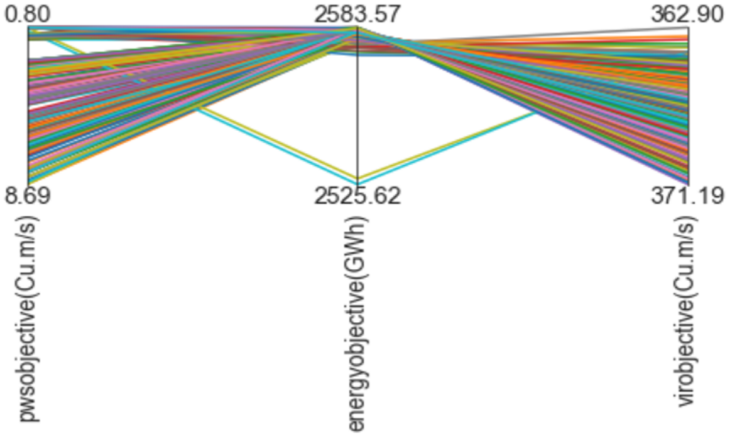

Figure 6.11: Performance across objectives for optimization with remotely sensed LAS curves

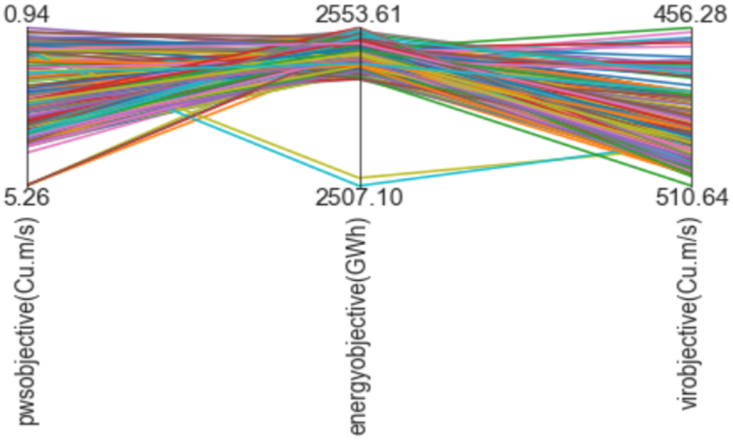

Figure 6.12: Performance across objectives of optimized operating rule curves using remotely sensed data with local LAS curves

local LAS curves and remotely sensed LAS curves. It also shows the performance of the system when we use the operating rules optimized using remotely sensed LAS curves with local LAS curves. The red dots correspond to the performance for the optimization with local LAS curves, the green dots are for the performance corresponding to optimization with

remotely sensed LAS curves and the blue dots show how will the system perform if we use operating rules optimized with remotely sensed LAS curves in a system with local LAS curves.

In all three plots, we see that the optimization with local LAS curves gives the best possible set of results except for the variable irrigation objective. As discussed the shortage at the irrigation nodes is least for optimization with remotely sensed LAS curves shown by green dots in figure 6.13. The performance deteriorates for the public water supply objective and energy objective for the optimization with remotely sensed LAS curves. To have remotely sensed time series data as an alternative to local data, the performance of the system should be at par or close to the performance we get when the model is optimized with local LAS curves. The performance deteriorates when we use the operating rules optimized with remotely sensed LAS curves in a system with local LAS curves. However, When compared to the performance across objectives for the existing rule curves and local LAS, the performance across energy objective and irrigation objective improves significantly. With the worst irrigation objective of 510.64 m^3/s which is still better than 550.60 m^3/s with the existing rule curves and local LAS. Table 6.4 shows that the energy generation with the existing rule curves is 2432.99 GWh which improves to 2507.10 GWh in the worst condition and 2553.61 GWh under the best scenario when we use operating rule curves optimized with remotely sensed LAS in a system with local LAS curves. As far as the public water supply shortage is concerned, it tends to deteriorate. Table 6.4 shows that the worst 1 percentile of the public water shortage under prevalent condition is 0.79 m^3/s. While the least shortage possible for the public water supply objective with the new set of operating rule curves and local LAS is 0.94 m^3/s

Figure 6.10,6.11,6.12, and 6.13 shows that using operating rule curves optimized with remotely

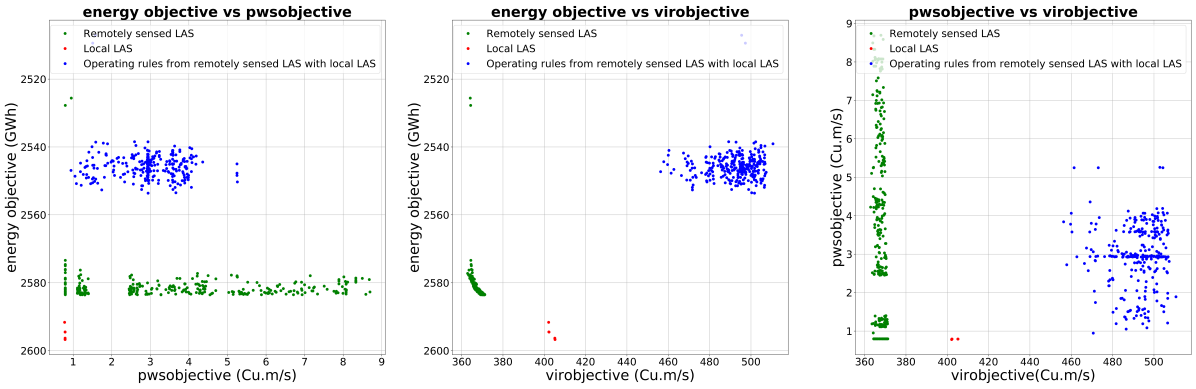

Figure 6.13: Trade offs between different objectives with local LAS curves, remotely sensed LAS curves and the performance with operating rules optimised with remotely sensed LAS curves in a model with local LAS curves

sensed LAS curves in a system with local LAS curve is bound to decrease the performance across all the objectives. Despite that, it is still a good option rather than sticking to the existing un-optimized set of operating rule curves. Since the public water supply-demand is one of the priorities in the basin everything finally trickles down to the discretion of the relevant stakeholders. As a policymaker, they have to decide whether they can afford this deterioration in meeting public water supply under extreme conditions while significantly increasing the energy generation and irrigation water supply in those months.

6.5. Operating rule curves

To assess the performance of the system across different objectives we need to assess the change in the operating rule curves before and after optimization. It is also essential to carry

out a detailed analysis of the optimized operating rule curves generated with different sets of LAS curves.

Optimization with local Level-Area-Storage curves				
Reservoir	Deviation flood (m)	Deviation target (m)	Deviation hedge (m)	Depth (m)
Al Massira	0.08	2.38	28.33	49
Bin El Ouidane	0.62	3.60	23.05	95
Hassan 1er	2.34	6.13	17.71	105
Moullay Youssef	1.19	6.30	43.10	67
Ahmed El Hansal	0.15	8.82	13.09	71
Optimization with remotely sensed Level-Area-Storage curves				
Reservoir	Deviation flood (m)	Deviation target (m)	Deviation hedge (m)	Depth (m)
Al Massira	0.07	0.52	35.83	49
Bin El Ouidane	0.59	2.5	19.08	95
Hassan 1er	0.64	14.07	68.13	105
Moullay Youssef	0.43	6.09	38.49	67
Ahmed El Hansal	1.47	24.21	59.24	71

Table 6.5: Variability in the rule curves shown by difference in the maximum and minimum levels in a year.

6.5.1. Flood rule curves

It shows the maximum possible water that a reservoir can store so that there will be space available to accommodate the coming floods. In figure 6.16 the red lines show the optimized flood rule curves with remotely sensed LAS curves, the black lines are for the optimized rules with local LAS curves while the green line shows the existing flood rule curves in the reservoir. For four of the five reservoirs, the flood rule curves being used now are a straight line while the Ahmed El Hansal reservoir has a somewhat sinusoidal flood rule curve. Figure 6.16 shows that for the Al Massira, Bin El Ouidane, Hassan 1er, and Moullay Youssef reservoir we observe that the optimization using local LAS gives flood rule curves that are quite close to what is existing in the basin. For most months they have the same value as the existing set of rule curves. There are dips in the flood rule curve level for the dry months from May to August in Al Massira, Bin El Ouidane, Hassan 1er, and Moullay Youssef reservoirs to make space for future incoming high flows that can inundate the basin. Table 6.5 shows the maximum dips in different operating rule curves for the five reservoirs when optimized with local and remotely sensed LAS curves. For flood rule curves, these dips are really small as compared to the depth of the reservoirs which can be seen in table. Though the change in level is not that significant it is still vital to accommodate an increase in inflows.

The optimized flood rule curve with the new set of remotely sensed LAS curves also have dips in the flood rule curves for December and January for Al Massira and Bin El Ouidane reservoir. The Hassan 1er and Moullay Youssef don't show any deviation from the existing rules for most of the months, there are dips in the flood rule curves for the months of May and July for Hassan 1er reservoir and May, June, July, and September for the Moullay Youssef reservoir. The optimized flood rule curves with remotely sensed LAS are characterized by regular dips. Table 6.5 shows these changes or dips are comparable for the optimized rule curves we get with local LAS or remotely sensed LAS curves when it comes to Al Massira and Bin El Ouidane reservoirs. For Hassan 1er and Moullay Youssef reservoir, the dips in the operating rule curves with the local LAS curves are almost three times to what we observe

with remotely sensed LAS curves.

For the Ahmed El Hansal reservoir, the existing flood rule curve is quite different from what

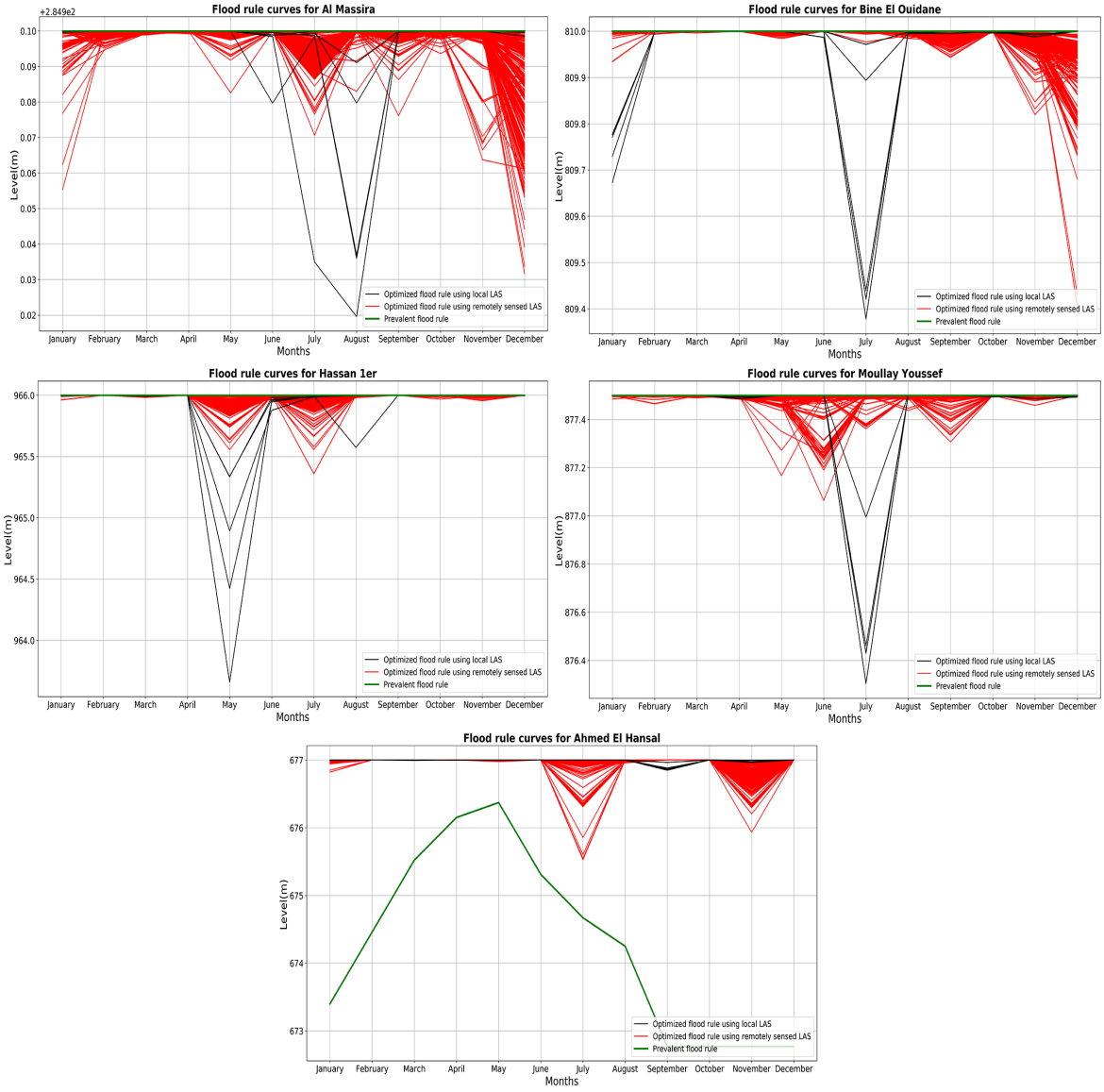

Figure 6.14: Flood rule curves

we have from the optimized rule curves (figure 6.16). The existing rule curve suggests much more space for future floods than necessary. Comparing the optimized flood rule curves us-

ing local LAS and the optimized flood rule curves using remotely sensed LAS shows that the flood rule curve shall be a straight line with regular dips depending on the incoming flow into the reservoir. Here, unlike other reservoirs flood rule curves optimized with remotely sensed LAS curves show greater deviation or dips as compared to the flood rule curves we get from local LAS curves.

6.6. Target rule curves

The target rule curves indicate the target storage for optimal hydropower generation under normal conditions. Similar to the flood rule curves the existing set of target rule curves are straight lines. For Al Massira, Bin El Ouidane, Hassan 1er, and Moullay Youssef reservoir. The optimized target rule curves are quite close to the existing rules. The deviations or dips in the optimized set of target rule curves are more prominent for all the five reservoirs as compared to the flood rule curves in those reservoirs, this can be seen in table 6.5. The dips in the target rule curves are slightly random. The optimized target rule curves with local LAS curves suggest a lesser level during July for the Al Massira reservoir. In the Bin El Ouidane reservoir there are dips in January, February, May, July, and September. The abrupt changes in level shall have implications downstream of the Bin El Ouidane reservoir. We observe similar deviations from existing target rule curves when we use remotely sensed LAS curves for optimizations.

For the Hassan 1er reservoir, the optimized target rule curves for local LAS curves are different from the remotely sensed LAS curves. The dips are quite significant for the target rule curves corresponding to the remotely sensed LAS while the dips are much more attenuated for target rules corresponding to the local LAS curves. For the latter part of the year, the target rule curves that we get from the local LAS are quite close to the existing target rule curves in the basin, while there are smooth dips every alternate month for the optimized target rule curves that we get from remotely sensed LAS curves. The curves for the Moullay Youssef reservoir are quite different when we use remotely sensed LAS curves instead of the local LAS curves for optimizations. Though there are abrupt dips in both cases and these dips are not in phase with each other. In the Ahmed El Hansal reservoir, we see that the optimized target rule curves corresponding to both local LAS and remotely sensed LAS are different from the existing rule curves. The existing curve suggests that the rule curve should be lower than what we get from the optimization results. This indicates sub-optimal utilization of water resources for the hydropower generation from the Ahmed El Hansal reservoir.

6.7. Firm rule curves

The firm storage curve indicates the level that should be maintained in the reservoir to make sure that the firm energy demands are met during critical dry conditions. The existing firm rule curves in most of the reservoirs are lower than what we get from the optimization of the RIB-ASIM system with local LAS and remotely sensed LAS curves for most of the months. These curves are random, unlike flood rule and target rule curves. Table 6.5 shows high intra-annual variations in the firm rule levels. The optimized firm rule curves that we get from local LAS and remotely sensed LAS are relatively similar to each other for the Al Massira reservoir. For the Bin El Ouidane reservoir, the firm rule curves are quite incoherent and show no similarity. These curves are always above the prevalent firm rule curves for the Bin El Ouidane reservoir and give more room to minimize shortage during dry conditions. For Al Massira, the firm rule curves are lower than the existing firm rules for the month of July when we use the remotely sensed LAS for optimization. When the local LAS curve is used for optimization the firm rule curve is lower than the existing firm rule curve for the month of August.

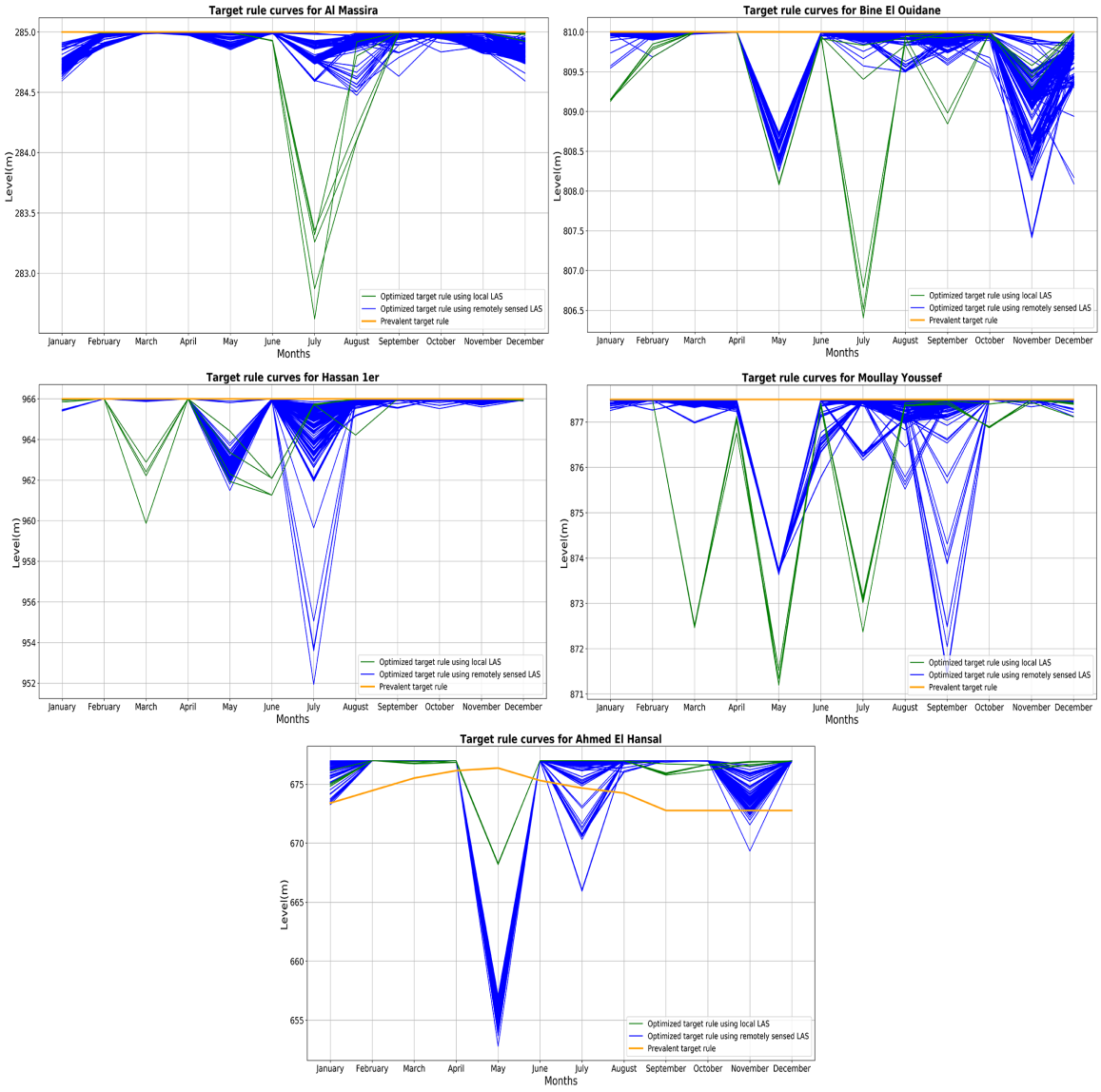

Figure 6.15: Target rule curves

The optimized rule curves for the Hassan 1er reservoir is more than the existing rule curves for the most part of the year. However, we see that every now and then, the optimized firm rule curves go below the existing firm rule curves for both remotely sensed and local LAS curves. This happens in the month of March, May, and June for the curves optimized with local LAS

and for July, August, September, and October for the firm rule curves optimized using remotely sensed LAS curves. A detailed analysis of the firm rule curves of the Moullay Youssef reservoir shows that the local LAS and remotely sensed LAS curves are incoherent and are mostly below the existing firm rule in the reservoir. For most of the dry seasons (March-September), these curves are below the existing firm storage curve.

Like all the other reservoirs the firm rule curves that are existing in the Ahmed El Hansal reservoir are lower than what we get from optimizations. Despite periodic dips in the rule curves, the firm rule curve optimized with local LAS curves never goes below the existing firm rule. Meanwhile, firm rule curves from the remotely sensed LAS tend to breach the existing firm rule for the months of May, June, and July, and in some cases, November.

Overall it seems that the optimization yields somewhat similar results for both local LAS and remotely sensed LAS. The existing firm rule curves are lower than most of the optimized firm rules for Al Massira, Bin El Ouidane, Hassan 1er, and Ahmed El Hansal reservoir. However, these firm rule curves go below the existing firm rule curve every now and then suggesting that there is more room for using the reservoir to address other water demands under harsh conditions. A detailed analysis of the RIBASIM model revealed that currently, the firm energy demand in all the five reservoirs is zero. This makes it an unconstrained problem and thus making the job of water resource managers in the basin easier.

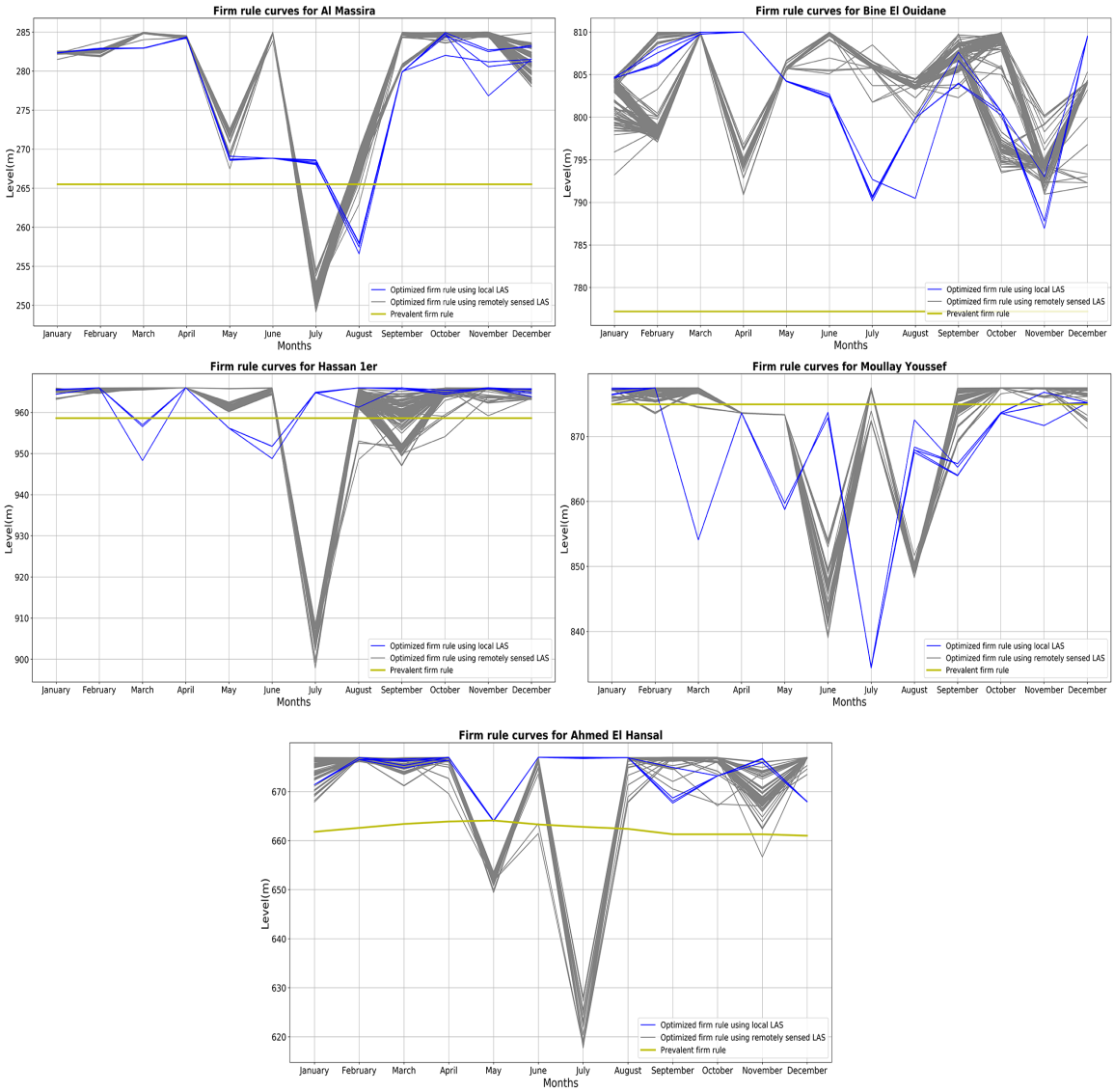

Figure 6.16: Firm rule curves

7

Discussions

7.1. Level-Area-Storage curve

The LAS curves were derived using the formula by Kaveh et al [33]. Here, the approximation of the shape factor/reservoir coefficient depends on two factors: a)Data of maximum storage, level, and area, b)Size of the reservoir. Hence, it is very vital to have reliable and accurate data sources for approximating the capacity of a reservoir at a particular level well enough to serve as an alternative to the local LAS curves. Similarly, for large reservoirs, the estimation of the LAS curves are better than the smaller reservoirs [29]. For the same source of data, the relatively larger reservoirs like Al Massira, Bin El Ouidane are approximated better than the Moullay Youssef reservoir and the relative rmse value of Ahmed El Hansal was lower than that of Hassan 1er. The lower relative rmse value of Moullay Youssef as compared to Hassan 1er in spite of being smaller of the two can be because of different sources of data. The average depth that we get from the GRanD database for the Moullay Youssef reservoir is 54.7 m which is quite close to 67 m, the actual maximum depth of the reservoir. For the Hassan 1er reservoir, we calculated the depth by subtracting the reservoir level at that pixel in the google earth pro software from the full reservoir level (FRL) of the Hassan 1er reservoir it was then used to calculate the shape factor. The depth that we got from there is equal to 120m which is not that close to the actual maximum depth of 105m as it is for the Moullay Youssef reservoir and also overestimates the maximum depth of the Hassan 1er reservoir. These discrepancies play an important role in estimating the LAS curves and shall be kept in mind when using such empirical formulas to generate LAS curves.

The formula suggested by Kaveh et al [33] performs better with larger reservoirs as there are more surface area and volume for approximation and finally coming up with relatively accurate values for the shape factor. The Al Massira, Bin El Ouidane, and Ahmed El Hansal reservoirs are large in size and hence, the formula came up with relatively accurate LAS curves when compared to Moullay Youssef and Hassan 1er reservoirs which are relatively smaller than the other three reservoirs in the basin.

7.2. Local LAS curve and sedimentation

The approximation of the reservoir surface area and storage by the area generated using local data and the latest LAS curves vary for each reservoir. The Al Massira being the largest of the five reservoirs is least affected by sedimentation. The close approximation of the surface area and storage throughout the operating period of the Al Massira using the updated LAS curves suggests that there is no significant change in the shape of the reservoir and the updated

local LAS curves did not change much from the original LAS curves created at the start of the reservoir operation. For the Bin El Ouidane reservoir, we have similar results, however, the approximation of the surface area and the storage improves as we move from left to right in the time series. This suggests that the latest LAS curve has changed slightly from the original LAS curve. Table 6.2 shows a percentage change of 19.02% for the Bin El Ouidane reservoir with a percentage rate of change of 0.37%/year. The change in storage due to sedimentation is quite significant for the Moullay Youssef and Hassan 1er reservoir. This is quite evident from their surface area and storage time series plots, figures 6.3 and 6.4. The combination of the updated local LAS and level data fails to approximate the initial storage and area for both the reservoirs well enough. The approximation at the end of the time series is better owing to the fact that the local LAS curve has been updated recently. The Ahmed El Hansal reservoir is very much prone to sedimentation. The lack of local data did not allow us to delve deeper into the surface area time series and storage time series for the Ahmed El Hansal reservoir. However, the updated local LAS curve in combination with the maximum surface area detected by remote sensing was used to come up with the percentage change in storage owing to sedimentation, which is found to be equal to 12.71% and percentage rate of change equal to 0.71%/year. The larger reservoirs are therefore less prone to effects of sedimentation, the high rate of change in the Ahmed El Hansal reservoir can be due to the fact that it is located in hilly regions with rough terrain and high velocity of incoming water capable of causing more erosion in its course, it also depends on soil texture of the region.

7.3. Flow Alteration

The LAS curve thus plays an important role in determining the water release from the reservoirs. When we use remotely sensed LAS curves we observe a decline in the upper bound of 90^{th} percentile interval for the month of May in the case of the Al Massira reservoir, this suggests that there is an attenuation in the extremes for the month of May. The level-capacity curve created using remotely sensed data for the Al Massira reservoir underestimates the level for particular storage during dry seasons, Hence, underestimation of a level decreases the release from the reservoir to ensure that the state of the reservoir is at the target rule curve. During wet seasons, there is also a decrease in the extremes that can be seen from the lowering of the 90^{th} percentile bound for the month of February, March, and April. This depends a lot on the storage in the reservoir. There can be no moment when the storage in the reservoir goes below the point as shown in figure 6.2 where the level-capacity curve starts overestimating the level in the reservoir. For the Bin El Ouidane reservoir, we observe no change in the flow alteration. This can be due to unchanged inflow to the reservoir and a pretty good approximation of the level-capacity curve. Figure 6.2 shows that in the case of the Bin El Ouidane reservoir, for some values of storage the remotely sensed level-capacity curve estimates the same level as estimated by the local LAS curves. The decrease in the extremes for the Moulay Youssef reservoir for the month of June and July makes sense as the level-capacity curve constantly underestimates the level for the same storage this means that there should be less release from the Moullay Youssef reservoir. This suggests that depending on the state of the reservoir, the release from the reservoir might be curtailed to ensure that the reservoir is at the target rule curve. For the Hassan 1er reservoir, a slight increase in the extreme for July, and a decline in the mean for July, August, and September has to do with the storage in the reservoir and demand from the reservoir. The operations of the reservoirs in the system are interdependent i.e. they also depend on the releases from other reservoirs in the network. Since, there is an increase in the outflow from the Ahmed El Hansal reservoir due to overestimation of level for particular storage the outflow from the Hassan 1er, Moullay Youssef and Bin El Ouidane reservoir can be affected. The level-capacity curve for

the Ahmed El Hansal reservoir constantly overestimates the level. Thus, there is an increase in the outflow from the Ahmed El Hansal reservoir for both wet and dry seasons.

7.4. Performance across objectives

For the manual run, the performance corresponding to the local LAS curves is better when compared to the performance with remotely sensed LAS curves. In section 6.3 we saw that the outflow from the Al Massira, Moullay Youssef, and Hassan 1er reservoir decreases for the dry months when we use the remotely sensed time-series data as a source of LAS curves. Thus, justifying the increase in water shortage at the public water supply and variable irrigation nodes. The Ahmed El Hansal shows an increase in the reservoir outflow in the dry seasons, However, it serves as a source for only seven of the twenty-two variable irrigation nodes, where it is not a primary source and therefore, serves water demand only when there is a shortage of water from other sources. Similarly, for public water supply nodes, the Ahmed El Hansal reservoir furnishes water to just two of the twenty-one public water supply nodes. The overall effect of Ahmed El Hansal on the public water and variable irrigation water supplies is not that significant. This further gets subdued by the decrease in the outflow from the Al Massira reservoir which is the most important reservoir in the basin furnishing water to twelve demand nodes.

Reservoir	Installed Capacity (MW)
Al Massira	128
Bin El Ouidane	135
Moullay Youssef	24
Hassan 1er	67.2
Ahmed El Hansal	92

Table 7.1: Hydropower capacity for each reservoirs[1]

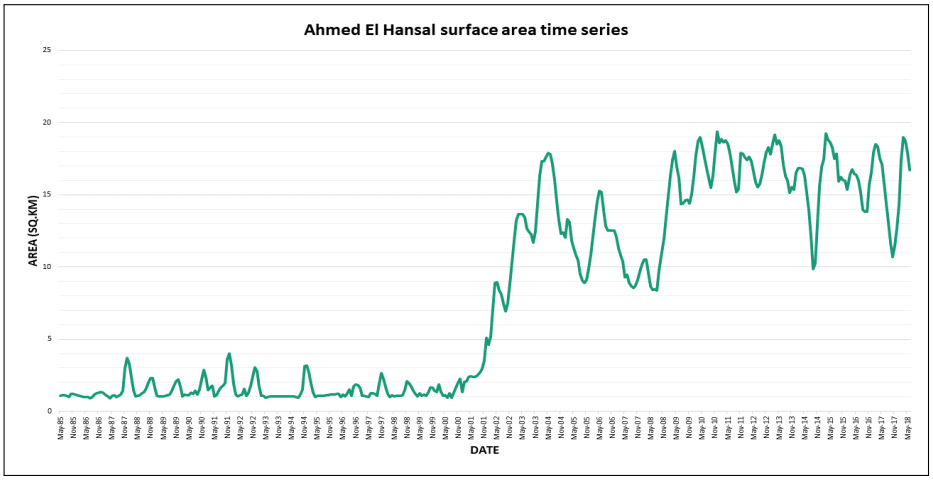

Figure 7.1: Remotely sensed surface area time series for Ahmed El Hansal reservoir

For the energy objective, there is a decline in the top 1 percentile of the energy generated when we use the remotely sensed LAS curves. This makes sense as the Al Massira, and Moullay Youssef witnesses decline in the upper 90^{th} percentile of the outflow from the reservoirs during the wet season. Al Massira being one of the major reservoirs in the basin influences the

overall energy generated from the reservoir system. Besides, figure 6.9 shows there is not much increase in the extremes from the Ahmed El Hansal and Hassan 1er reservoir that can compensate for the decreased outflow from the Al Massira reservoir. Table 7.1 shows the installed capacity for the five reservoirs. The Bin El Ouidane has the highest capacity followed by Al Massira, Ahmed El Hansal, Moullay Youssef, and Hassan 1er. Besides having low capacity compared to the Bin El Ouidane and Al Massira reservoir, the Ahmed El Hansal reservoir has been constructed quite recently in the year 2000. This also justifies the reduction in the performance of the energy objective shown in table 6.4 despite the increase in the outflow from the Ahmed El Hansal reservoir. Figure 7.1 is the remotely sensed time series of reservoir surface areas for the Ahmed El Hansal reservoir. There is a sudden rise in the surface area in the year 2000 suggesting the construction of the reservoir.

Figure 6.13 shows the trade-offs between different objectives. The performance is bound to be inferior when compared to the performance of the optimization results using the local LAS curve. The optimization algorithm comes up with the best possible set of results for a particular scenario. So it is unlikely that the operating rule curves using one set of LAS curves will improve the performance of the basin when we use it with the other set of LAS curves.

One thing peculiar about the optimization runs is that we got just five solutions for the optimum operating rule curve using the local LAS curve, while we get 290 solutions for the new set of LAS curves generated using remotely sensed data. This discrepancy can be due to the intrinsic randomness of the algorithm. Ward et al [56] shows that with increasing decision variables different optimization algorithms can have a different level of performance and ϵ-NSGA-II might not be the best option for optimization in cases with a high number of decision variables.

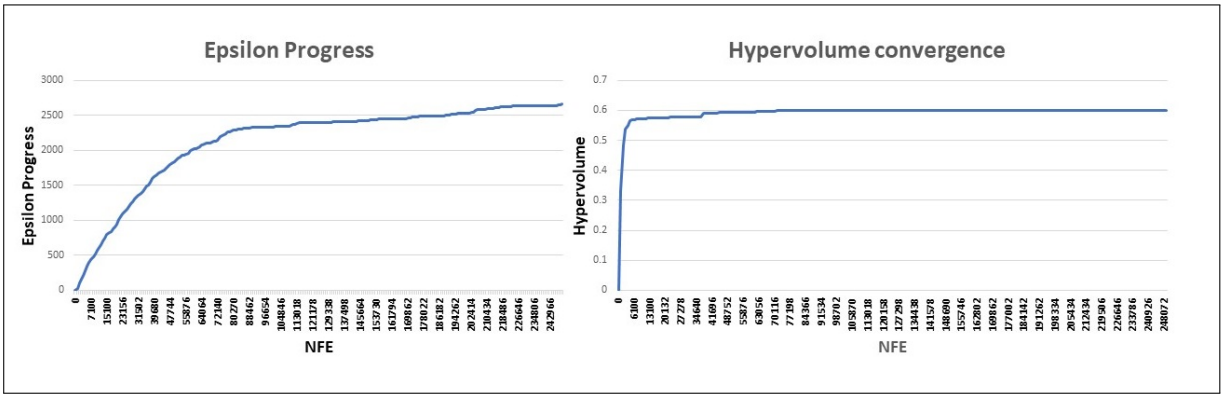

Figure 7.2: Convergence for optimization using local LAS curves

Figures 7.2 and 7.3 shows the epsilon progress and hypervolume convergence for the two optimizations using different sources of data. While, the hypervolume converges for both the runs, the epsilon progress does not converge in the optimization for the model with the remotely sensed LAS curves. This means that the algorithm can find the approximate best possible set of results for both the runs however, for the second run with remotely sensed LAS curves further runs are required to finally converge to a constant set of optimization results.

The results that we have are sufficient to give us an idea of what remotely sensed time-series data brings to the table and how it can prove to be an asset and an efficient source of data in bridging data gaps in the field of water systems science.

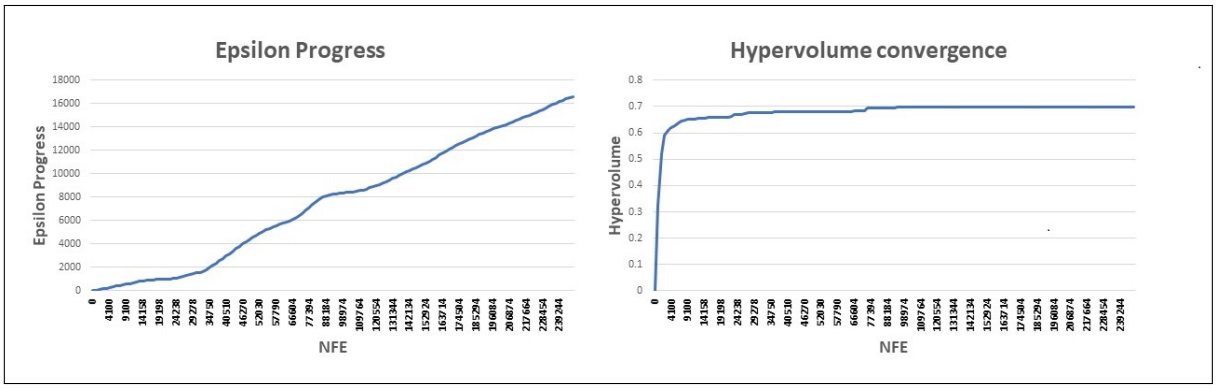

Figure 7.3: Convergence for optimization using remotely sensed LAS curves

7.5. Operating rule curves

The flood rule curves existing for the Al Massira, Bin El Ouidane, Hassan 1er, and Moullay Youssef reservoirs are a straight line. The OER basin is more prone to droughts than floods. Therefore, having a flood rule curve which is a straight line serves the purpose of protecting the basin from potential floods. The existing flood rule curves though suggest that the reservoir doesn't take into account the intra-annual variability of the inflow to the reservoir. The regular dips though small in the optimized flood rule curves suggest that there might be a regular need for the reservoirs to make extra space for increasing inflow to the basin. The flood rule curves corresponding to local LAS curves dip in the month of either May, June, July, or August leaving extra room for the wet months and gradually increasing inflow to the reservoir. Figure 7.4 and 7.5 show that May to November is marked by low inflow to the reservoirs, thereafter followed by rise in the incoming flows. This shall be the reason for the dips in the flood rule curves in the reservoirs to accommodate future high flows. The existing flood rule curves tend to ignore these variations in the incoming flows.

The operating rule curves that we get from the optimization of RIBASIM models with remotely

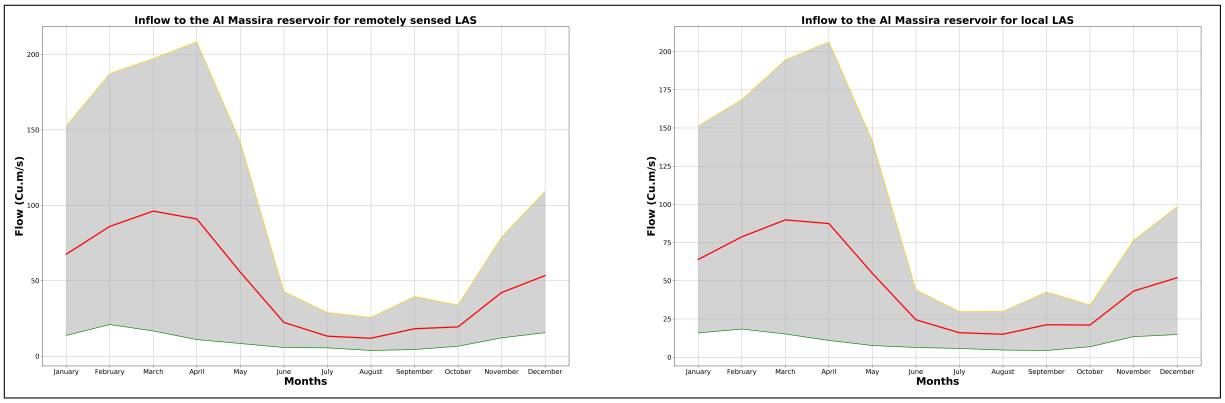

Figure 7.4: Inflow to the Al Massira reservoir with the two set of LAS curves

sensed LAS are slightly incoherent to what we get from the local LAS curves. The dips in the flood rule curves for the Al Massira reservoir when we use the remotely sensed LAS curves are mostly concentrated in the later parts of the year. This makes sense as we observe from figure 7.4 the highest inflow to the Al Massira reservoir happens in March and the reservoir needs to make room for the increased inflow accordingly. With the local LAS curves, the dips are much significant for the dry months of July and August which is enough to accommodate

a constant rise in inflow in the following months. We get similar trends in the flood rule curves of the Bin El Ouidane reservoir, the inflow to the Bin El Ouidane reservoir also peaks in March and starts rising from October. Besides, Al Massira and Bin El Ouidane are similar in size and installed energy capacity. Therefore, it makes sense if they have somewhat similar trends as far as the flood rule curves are concerned. The magnitude and time of these deviations in the rule curves depend a lot on the storage of the reservoir. Therefore, more analysis shall be done on the changes in the storage of the reservoir with time. Storage with LAS curves shall then be used to get the level in each of the reservoirs to have a detailed analysis of the variations in these rule curves.

The flood rule curves that we get corresponding to the two sets of LAS curves show simi-

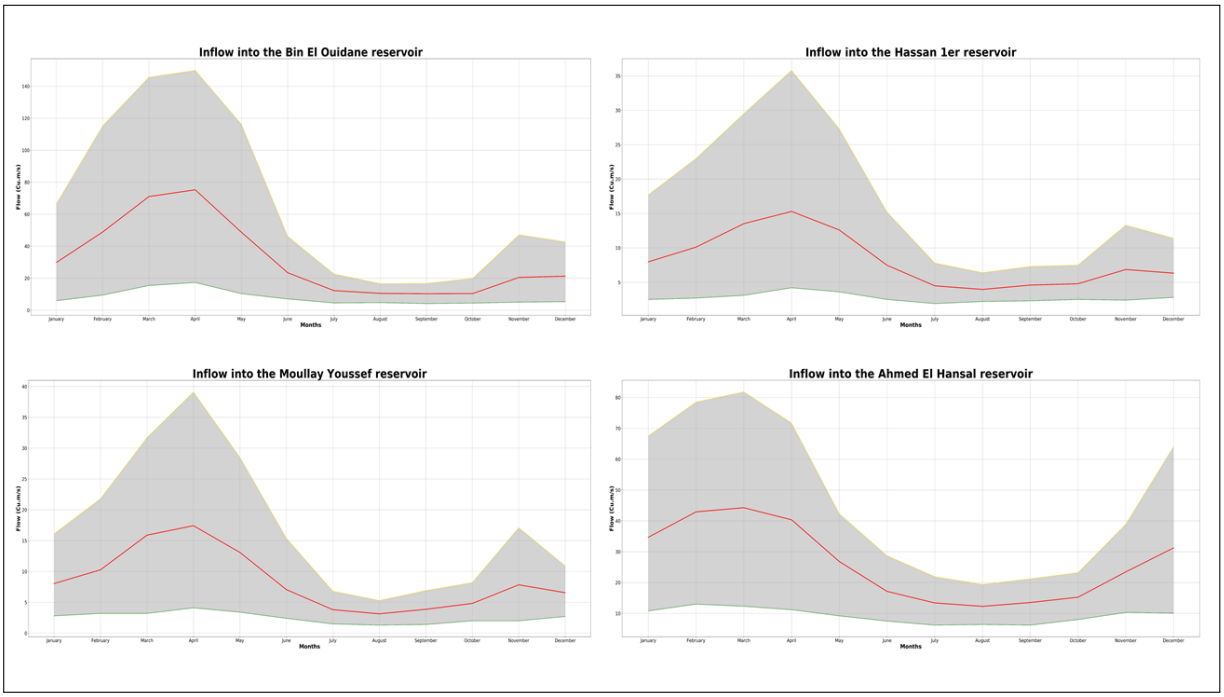

Figure 7.5: Inflow to Bin El Ouidane, Hassan 1er, Moullay Youssef and Ahmed El Hansal reservoirs

lar trends for the Hassan 1er and Moullay Youssef reservoirs. The dips in the flood rule curves for May, June, or July can be very much a reason for incoming high flows in these reservoirs as well.

The flood rule curves for the Ahmed El Hansal reservoirs are quite different from the existing flood rule curve in the basin. However, the rule curves that we get from the two optimizations are quite similar and more or less a straight line. The dips in the flood rule curve in the latter half of the year can be due to the forthcoming increase in the inflow to the reservoir which starts increasing in November and reaches its maximum in March. There is relatively less dip in the flood rule curves optimized with local LAS curves compared to the dips with remotely sensed LAS curves and are limited only to September.

Figure 7.5 shows that there is no change in the inflow for the Bin El Ouidane, Hassan 1er, Moullay Youssef, and Ahmed El Hansal reservoir with the change of the LAS curves as they are the upstream reservoirs in the basin. Therefore, the change in operating rules in these reservoirs are more influenced by downstream demands and response of the Al Massira reser-

voir. This can be one of the reasons why in figure 6.16 we observe the difference between the flood rule curves from remotely sensed LAS and local LAS are more pronounced in the Al Massira reservoirs than the other reservoirs as the flood rule curve majorly depends on the incoming flow to the reservoir which changed only for the Al Massira reservoir.

The Target rule curves are optimized in a way that it serves the energy demand of the basin. In section 6.4 we saw that the target rule curves optimized with local LAS curves are capable of generating more energy than the target rule curves created with remotely sensed LAS curves. The dips in the target rule curves for the dry months suggest optimizing public water supply and irrigation water supply in these months. During wet months the target rule curves for the large reservoir with high hydro-power capacity tends to decline less from their normal optimum value. This is reasonable as we try to maximize the energy generation in the system and the higher the target rule curves during the wet season greater shall be the energy production in the basin. The Hassan 1er and Moullay Youssef reservoirs have target rule curves that show dips in wet months as well, but this does not influence the overall energy production in the basin as they have relatively less installed capacity (Table 7.1). Thus, optimization algorithms compensate for this dip in the target rule curves for the Hassan 1er and Moullay Youssef reservoirs by furnishing other public water supply and irrigation demands.

Similar to the Al Massira and Bin El Ouidane reservoir the target rule curves for the Ahmed El Hansal shows the greatest dip in the dry month of May. Ideally, it would have been better if the target rule curve would have dipped for the month of June or July rather than May since the inflow is least in these months, but factors like storage and demands from the Ahmed El Hansal reservoir also plays an important role in finalizing the operating rule curves for the reservoirs and hence, needs further research to infer untimely deviation of the target rule curve for the Ahmed El Hansal reservoir.

The firm energy rule curve for the five reservoirs are above the existing firm energy rule curve. This indicates that the reservoir authorities can take a much more conservative approach while also maximizing the utility of the water system in the basin. In Al Massira, Hassan 1er, Moullay Youssef, and Ahmed El Hansal reservoir there are some months when the firm rule curves from the optimization with local LAS and remotely sensed LAS goes below the existing firm rule curve. This shall be due to the fact that here we try to minimize public water shortage and irrigation shortage under extreme conditions, and the system can afford to have a lower firm energy curve as the firm energy demand from the five reservoirs is set to be zero. The Moullay Youssef reservoir serves water to six of the twenty-two variable irrigation nodes, during dry months the reservoir aims at maximizing the supply of irrigation water. This becomes easier as the firm energy demand for all the reservoirs in the basin is 0 GWh. Thus, the firm energy rule curves are totally dependent on the target rule curve, and there is no constraint for the operating rule curves when it comes to addressing the three objectives of the basin. The firm energy rule curve that we get from the optimizations can therefore be used to come up with a structured firm energy supply in the basin.

Figure 7.6 and 7.7 shows that there is a rise in peaks for the incoming and outgoing flow from the Al Massira reservoir when we use an optimized set of rule curves. This is due to the dips in the target rule curves thus improving the performance of the system in attenuating water shortages across public water supply and irrigation nodes. The flood risk in the Oum Er Rbia basin is from low to very low [24]. Therefore, these peaks won't be a problem for water managers and hydrologists in the region.

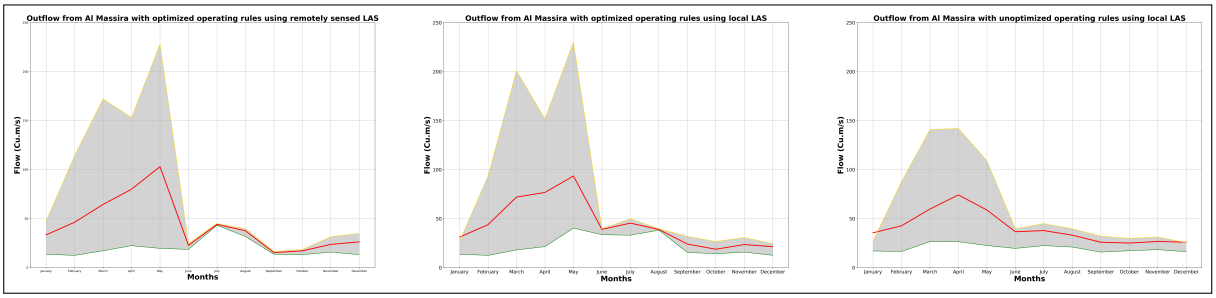

Figure 7.6: Outflow from Al Massira reservoir for operating rule curves optimized with remotely sensed LAS and local LAS curves, and prevalent rule curves

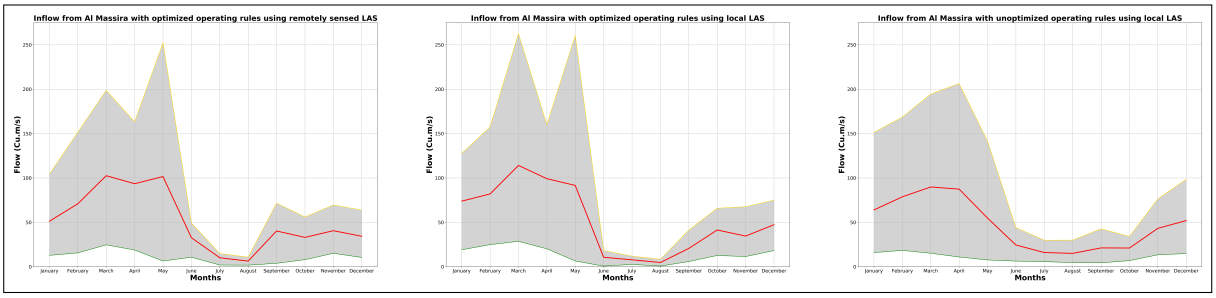

Figure 7.7: Inflow from Al Massira reservoir for operating rule curves optimized with remotely sensed LAS and local LAS curves, and prevalent rule curves

8

Conclusion

Donchyts [15] came up with an efficient technique for surface water detection. The outcome of his research was an accurate, robust, and dynamic dataset encapsulating temporal and spatial variability in surface water sources across the globe. This data was used to come up with LAS relationships in combination with other open-access data sources. The new set of LAS curves approximate the large reservoirs well and can be used for approximating the LAS curves in places where there are lack of accurate data [33]. The approximation of these curves are also dependent on other sources of data. This approximation can improve with the accurate source of maximum depth and storage. For this project, we retrieved those data from GRanD and Google Earth Pro. The approximation is good for large reservoirs. Thus, for large reservoirs pretty accurate LAS curves can be generated using precise local depth and storage data with remotely sensed time-series data of reservoir surface area.

This remotely sensed time-series data along with the use of an updated and accurate LAS curve can also help in assessing the rate of sedimentation in the reservoir. The relative sedimentation was found to be low in large reservoirs like Al Massira and Bin El Ouidane. There is a slight increase in the percentage change due to sedimentation for the Bin El Ouidane reservoir but it was low compared to smaller reservoirs like Moullay Youssef and Hassan 1er. The Moullay Youssef and Hassan 1er show the largest change in storage due to sedimentation (table 6.2). The Ahmed El Hansal being new has a low change in storage because of sedimentation but is prone to a high rate of sedimentation with a percentage rate of change in storage of 0.71%/year. The remotely sensed time-series data gives a fair idea of the rate of sedimentation in the reservoir and can help water managers avoid unnecessary bathymetry. When used with accurate sources of level, storage data to come up with LAS curves it can be used to update the rule curves from time to time without much hassle. Overall it gives a cheap and efficient alternative when carrying out tedious, and intensive bathymetry is not feasible.

The remotely sensed LAS curve does not alter the flow from the reservoirs much. While there is no significant alteration in the mean flow from the reservoirs in both wet and dry seasons. The 90^{th} percentile varied for the Al Massira, Moullay Youssef, Hassan 1er, and Ahmed El Hansal reservoirs. Since the three objectives in this thesis are focused on extremes these alterations affect the performance of the system across the three objectives. The Al Massira reservoir which is one of the largest reservoirs in the basin shows a decline in the lower and upper bounds of the 90^{th} percentile interval for May. While the decline in lower bound is capable of aggravating shortage in the basin, the decline in upper bound attenuates energy generation from the reservoir. Such, changes in 90^{th} were also observed in the Moullay Youssef. The

Ahmed El Hansal reservoir shows an increase in outflow for both wet and dry seasons but its effect on overall water availability for furnishing different water demands gets subdued by the decreased outflow from the Al Massira reservoir. The Al Massira being the most important reservoir in the basin with twelve demand nodes in the RIBASIM model dependent on it has the most pronounced effect on the overall performance of the basin. Hence, there is a deterioration in performance across the three objectives when the remotely sensed LAS curves are used with existing operating rules instead of the local LAS curves(Table 6.4).

Finally, the optimization results with the two LAS curves show that the local LAS curves if present is still the best option for optimizing water management decisions in the basin. In Morocco, the volume of water available per inhabitant per year is about 1000 m³/person/year[41]. 6% of this is used to meet domestic water demands this roughly translates to 164 litres/person-/day. As per the RIBASIM model, the average public water supply-demand including losses through the network is 241 litres/person/day. This leaves water managers in the basin with a buffer of 77 litres/person/day to address any shortage in public water supply demands. Figure 6.10 shows that the public water supply shortage varies between 0.78 to 0.79 m^3/s for optimization with local LAS curves. This roughly translates to a shortage of 1.8 to 1.9 litres/person/day. Which can still be accommodated in the water shortage buffer of 77 litres/person/day and minor policy changes in the basin can address that. The performance for the public water supply shortage deteriorates to 0.94 to 5.26 m^3/s as shown in figure 6.12, when we use the operating rule curves that have been optimized with remotely sensed LAS curves in a reservoir system with local LAS curves. This translates to a shortage of 2.3 to 12.6 litres/person/day. While the deterioration of 2.3 litres/person/day can still be addressed with such changes, the shortage of 12.6 litres/person/day can be a bit steep for the policymakers to address in water-scarce region of Morocco. Based on the priority of the different objectives in the basin policymakers can address this shortage by prioritizing public water supply-demand under extreme conditions at the cost of energy and irrigation water supply. However, the return period of such a situation to arise under the present climate scenario is around 74 years with a shortage of maximum 12.6 litres/person/day which is roughly 5% of the total public water demand per person per day. Hence, minor policy changes on the part of the policymakers and the stakeholders to address a shortage in public water supply-demand during dry months can enable the use of remotely sensed time-series data in coming up with water management decisions in the basin without significantly decreasing the utility of water and affecting the standard of living in the basin.

For all the three optimization runs the water shortage across the irrigation nodes are quite significant as the maximum demand in a month under extreme conditions is around 320,112,000 m^3 and the shortage of 402.08 to 405.19 m^3/s for the worst 1 percentile of the months translates to roughly between 130,273,920 and 131,281,560 m^3/month. This is almost 50% of the total monthly irrigation demand in the basin. Figures 6.12 and 6.13 shows that the situation further deteriorates when we use operating rules optimized with remotely sensed LAS curves in a system having local LAS curves. This strongly suggests for construction of new irrigation systems and water structures to tap into the incoming water during wet months. The change in reservoir operations in the basin cannot improve the situation much and shall not be looked as an option to improve the irrigation scenario in the basin. The reservoir operations should be more to address the shortages in public water supply node and in maximizing energy generation. Using the new set of operating rule curves optimized with remotely sensed LAS curves with local LAS curves also improves the amount of energy being generated from these reservoirs. Though it is not as much as the energy that shall be generated with the operating rule

curves optimized with local LAS curves in the absence, of such curves the authorities can rely on remotely sensed data to come up with operating rules to improve the energy generation from the reservoirs.

The existing set of operating rule curves are straight lines. They do not take into account the intra-annual variability of incoming flows and hence, do not exploit the full water potential in the basin. The optimized rule curves do take into account such variabilities and can improve the performance of the system across the three objectives. The firm energy demand in the basin is 0 GWh. This gives the reservoir authorities an unconstrained optimization problem. This is reflected in the firm energy rule curves where the optimized firm rule curves go below the existing firm rule curves in dry months for Al Massira, Hassan 1er, Moullay Youssef, and Ahmed El Hansal reservoir. The target rule curves and flood rule curves for both the optimized set of operating rule curves are close to the existing rule curves in the basin. Hence, the remotely sensed LAS curves can be a feasible alternative in absence of accurate and sufficient data.

The use of local LAS curves is capable of changing the extreme flows from the reservoir. It is viable for economically rich countries to address these changes in shortages by coming up with new policies, structures, or promoting lifestyle changes amongst the general population. In poorer countries with the vast majority of the population struggling to meet their basic water demands, completely relying on remotely accessible data is not advisable. Though economically burdening the government and policymakers should rely on local, accurate data to base their water management decisions on. However, in places where such data are not available the remotely sensed time series can prove to be an asset and a feasible alternative especially to formulate short-term policies and decisions.

9

Recommendations

The LAS curves constructed using the formula suggested by Kaveh et al[33] involved using other sources of data apart from remotely sensed time-series data of reservoir surface area. Hence, the quality of other data sources plays an important role in coming up with a better approximation of the LAS curves. For assessing the benefits of using remotely sensed data we should rather restrict ourselves in analyzing reservoir systems with large reservoirs and accurate data for maximum depth and storage.

To assess the change in storage due to sedimentation we took the maximum surface area of the reservoir from the remotely sensed reservoir surface area time series. This was based on the assumption that there should be at least one day when the reservoir is at its maximum capacity and hence, maximum surface area corresponds to the condition when the reservoir is full. This should be validated by comparing the date of the maximum surface area detected by the satellite to the level on that date. Ideally, it should be equal to the full reservoir level (FRL). Besides, the maximum surface area used should be for a recent past, which will be more representative of the changed shape of the reservoir.

The rate of sedimentation for the Hassan 1er and Ahmed El Hansal reservoir was found to be high, suggesting a high rate of erosion in hilly regions with steep topography. Apart from the topography, a detailed study of the soil structure and geology should be performed to have an accurate idea of the rate of sedimentation and its effect on the storage of the reservoir. However, the remotely sensed time-series data can give us an initial idea of the effects of sedimentation in the reservoir or any surface water body and can help in further studies.

The Bin El Ouidane reservoir did not show any change in the outflow from the reservoir despite changing the LAS curves. As discussed in section 6.3 this depends on the storage in the reservoir. The close approximation of the local level-capacity curve by the remotely sensed level-capacity curve can be a reason for the unaltered response of the reservoir. To further delve into the response of the reservoirs due to the new set of LAS curves the storage time series data shall be retrieved from the RIBASIM. This can give us a better idea of the operation of reservoirs in the basin.

The RIBASIM software takes as an input the percentage of distribution losses from the network. To have a better idea of the buffer available for water managers to accommodate any shortage in water supply, there is a need for further research to get an idea of the approximate loss of flows through the network and what can be done to minimize it this shall then be in-

cluded in the RIBASIM model. The RIBASIM model for the OER basin takes these distribution losses to be zero.

With the constant increase in population across the globe we need to know how sustainable these operating policies shall be in addressing future changes in demand and available water resources. In chapter 8 we saw that there is still a buffer for the policymakers in the OER basin to address public water shortage under extreme conditions. This shall not be the case with increasing urbanization and population growth. As per the research[2] water availability is predicted to decrease to 500 m^3/person/year by 2030. While, the demand is projected to continue growing, from 14.3 BCM in 2010 to 23.6 BCM in 2030 in Morocco. This makes it vulnerable to future changes in the climate and demography of the region. These changes shall be addressed and efforts shall be made to come up with future scenarios. Including such scenarios in optimization will give us a fair idea of how the remotely sensed LAS curves can address future water constraints and can also come up with robust decisions in the basin.

For the optimization we utilized epsilon-Non dominated Sorting Genetic Algorithm II(ϵ-NSGA-II). It has been observed that with a large number of decision variables, here monthly values of operating rule curves for the five reservoirs, this algorithm struggles[56]. The next step in this optimization is to use the Borg multi-objective evolutionary algorithm (MOEA) in one of its variants for optimizing the operating rule curves which tend to perform better than other algorithms.

The monthly values for the operating rule curves have been considered as different levers for the optimization problem. This makes them mutually exclusive and also increases the number of decision variables to be optimized by the algorithm. As we discussed earlier not all algorithms can perform well with high numbers of decision variables. As a decision-maker, we can opt for some sort of function that links the monthly values to each other and give as an output a curve. This will decrease the number of decision variables significantly, thus improving the performance of optimization algorithms. It also reduces the problem of randomness which leads to inefficient optimization that was encountered in this thesis.

Finally, there is a need of doing a hydro-economic analysis to get a better idea of the feasibility of using remotely sensed time-series data in optimizing water management decisions. This should be done to understand whether the economic cost of deterioration in the performance as a result of using remotely sensed time-series data is less than the economic burden local authorities have to bear to carry out regular bathymetry for different surface water bodies in the region. This shall also come in handy to quantify the loss in revenue by the deterioration of the amount of energy that could be generated with operating rules optimized with local LAS curves rather than remotely sensed LAS curves.

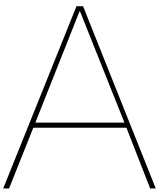

Appendix-A

Python Script to find the optimum set of operating rule curves with EMA workbench

New colors defined below

```
1
2  import glob
3  import os
4  import random
5  import shutil
6  import string
7
8  import numpy as np
9
10
11 import subprocess as subprocess
12
13 import struct as struct
14 import math as math
15
16 from datetime import datetime, timedelta
17
18 import time
19
20
21 from ema_workbench.em_framework.optimization import (HyperVolume,
22                                                       EpsilonProgress)
23 from ema_workbench import (RealParameter, ScalarOutcome,
24                            MultiprocessingEvaluator, ema_logging,
25                            SequentialEvaluator)
26 from ema_workbench.em_framework.model import AbstractModel, SingleReplication
27 from ema_workbench.util.ema_logging import method_logger, get_module_logger
28
29
30 _logger = get_module_logger(__name__)
31
32
33 class HisFile:
34     def __init__(self, fname):
35         self.fname = fname
36         self.sysnames = list()
37         self.segnames = list()
38         self.segnums = list()
```

```
        self.datetime = list()
        self.nstep=0

    def read(self):
        f = open(self.fname, 'rb')
        self.moname = f.read(160)
        year = int(self.moname[124:128])
        month = int(self.moname[129:131])
        day = int(self.moname[132:134])
        hour = int(self.moname[135:137])
        minute = int(self.moname[138:140])
        second = int(self.moname[141:143])
        self.startdate = datetime(year, month, day, hour, minute, second)
        self.scu = int(self.moname[150:158])
        #print(self.scu)
        self.nsys, = struct.unpack('i', f.read(4))
        self.nseg, = struct.unpack('i', f.read(4))
        #return self.nsys, self.nseg
        #print self.nsys, self.nseg
        for isys in range(self.nsys):
            self.sysnames.append(str.rstrip(str(f.read(20))))
            #print isys,self.sysnames[isys]
        #return self.sysnames
        for iseg in range(self.nseg):
            self.segnums.append(struct.unpack('i', f.read(4))[0])
            self.segnames.append(str.rstrip(str(f.read(20))))
        #return self.segnames, self.sysnames#print iseg,self.segnums[iseg],self.
segnames[iseg]
        size = os.path.getsize(self.fname)
        self.nstep += (size - 168 - 20 * self.nsys - 24 * self.nseg) / (4 * (self.
nsys * self.nseg + 1))
        #print self.nstep

        self.data = np.zeros((self.nsys, self.nseg, int(self.nstep)), 'f')
        for lstep in range(int(self.nstep)):
            fdays = struct.unpack('i', f.read(4))[0] * (self.scu / 86400.)
            iday = math.trunc(fdays)
            ihour = math.trunc((fdays - iday) * 24.)
            iminute = math.trunc((fdays - iday - ihour / 24.) * 60.)
            isecond = fdays * 86400 - 60 * math.trunc(fdays * 86400 / 60.)
            dt = self.startdate + timedelta(iday, ihour, iminute, isecond)
            self.datetime.append(dt)
            for iseg in range(self.nseg):
                for isys in range(self.nsys):
                    self.data[isys, iseg, lstep] = struct.unpack('f', f.read(4))
[0]
        f.close()


    def getseries(self, sysnam, segnam):
        isys = self.sysnames.index(sysnam)
        iseg = self.segnames.index(segnam)
        #print isys,iseg
        res = np.zeros(int(self.nstep))
        for lstep in range(int(self.nstep)):
            res[lstep] = self.data[isys, iseg, lstep]
        return res

    def gettimeseries(self, sysnam, segnam):
        isys = self.sysnames.index(sysnam)
        iseg = self.segnames.index(segnam)
```

```
97          #print isys,iseg
98          resdata = np.zeros(int(self.nstep))
99          resdate = list()
100         for lstep in range(int(self.nstep)):
101             resdate.append(self.datetime[lstep])
102             resdata[lstep] = self.data[isys, iseg, lstep]
103         return resdate, resdata#, self.nstep
104
105
106 def generate(a, maximum, k):
107     b = (maximum-a)*k+a
108     return b
109
110
111 def update_paths(files, string1, string2):
112     for file in files:
113
114         with open(file, 'rt') as f:
115             textin = f.readlines()
116             f.close()
117
118         textout = []
119         for line in textin:
120             line = line.replace(string1, string2)
121             textout.append(line)
122
123         with open(file,'wt') as f:
124             f.writelines(textout)
125             f.close()
126
127 class RibasimModel(SingleReplication, AbstractModel):
128
129
130     def __init__(self, name, original_dir=None):
131         super(RibasimModel, self).__init__(name)
132         assert original_dir != None
133
134         self.original_dir = original_dir
135         self.directory_setup = False
136
137
138     @method_logger(__name__)
139     def model_init(self, policy):
140         '''Method called to initialize the model.
141         Parameters
142         ----------
143         policy : dict
144                  policy to be run.
145         Note
146         ----
147         This method should always be implemented. Although in
148         simple cases, a simple pass can suffice.
149         '''
150         super(RibasimModel, self).model_init(policy)
151
152
153
154         if not self.directory_setup:
155             random_part = [random.choice(string.ascii_letters + string.digits)
156                            for _ in range(5)]
157             random_part = ''.join(random_part)
```

```
158
159             # TODO:: possible corner case if 2 processes generate same random
    string
160             # you might get a class
161             self.working_directory = os.path.join('C:', os.sep, random_part)
162             shutil.copytree(self.original_dir, self.working_directory)
163
164
165             folder = os.path.join(self.working_directory, 'OUMRBIA9.Rbn', 'CMTWORK
    ')
166             files = glob.glob(os.path.join(folder,'*.*'))
167             update_paths(files, '\Oer0T_1', self.working_directory[2:])
168
169             folder = os.path.join(self.working_directory, 'OUMRBIA9.Rbn', '3')
170             files = glob.glob(os.path.join(folder,'TIMESERI.*'))
171             update_paths(files, '\Oer0T_1', self.working_directory[2::])
172
173             #folder = os.path.join(self.working_directory, 'OUMRBIA9.Rbn', 'WORK')
174             #files = glob.glob(os.path.join(folder,'TIMESERI.*'))
175             #update_paths(files, '\OER0T', self.working_directory[2::])
176
177             files = [os.path.join(self.working_directory, 'Programs', 'RL_PSTPR.
    INI')] #Model_folder+'\\Programs\\RL_PSTPR.INI'
178             update_paths(files, 'C:\Oer0T_1', self.working_directory)
179
180             files = [os.path.join(self.working_directory, 'Programs', 'rib2his4.
    fnm')]
181             update_paths(files, 'C:\Oer0T_1', self.working_directory)
182             self.directory_setup = True
183
184     @method_logger(__name__)
185     def run_experiment(self, experiment):
186
187         model_output  = self.run_ribasimmodel(**experiment)
188
189         results = {}
190         for i, variable in enumerate(self.output_variables):
191             try:
192                 value = model_output[variable]
193             except KeyError:
194                 _logger.warning(variable + ' not found in model output')
195                 value = None
196             except TypeError:
197                 value = model_output[i]
198             results[variable] = value
199         return results
200
201
202     @method_logger(__name__)
203     def cleanup(self):
204         try:
205             shutil.rmtree(self.working_directory)
206         except OSError:
207             pass
208
209
210     @method_logger(__name__)
211     def run_ribasimmodel(self, c1,c2,c3,c4,c5,c6,c7,c8,c9,c10,c11,c12,
212                          fracb1,fracb2,fracb3,fracb4,fracb5,fracb6,fracb7,fracb8,
    fracb9,fracb10,fracb11,fracb12,
```

```
213                         fracc1,fracc2,fracc3,fracc4,fracc5,fracc6,fracc7,fracc8,
    fracc9,fracc10,fracc11,fracc12,
214                         f1,f2,f3,f4,f5,f6,f7,f8,f9,f10,f11,f12,
215                         frace1,frace2,frace3,frace4,frace5,frace6,frace7,frace8,
    frace9,frace10,frace11,frace12,
216                         fracf1,fracf2,fracf3,fracf4,fracf5,fracf6,fracf7,fracf8,
    fracf9,fracf10,fracf11,fracf12,
217                         i1,i2,i3,i4,i5,i6,i7,i8,i9,i10,i11,i12,
218                         frach1,frach2,frach3,frach4,frach5,frach6,frach7,frach8,
    frach9,frach10,frach11,frach12,
219                         fraci1,fraci2,fraci3,fraci4,fraci5,fraci6,fraci7,fraci8,
    fraci9,fraci10,fraci11,fraci12,
220                         l1,l2,l3,l4,l5,l6,l7,l8,l9,l10,l11,l12,
221                         frack1,frack2,frack3,frack4,frack5,frack6,frack7,frack8,
    frack9,frack10,frack11,frack12,
222                         fracl1,fracl2,fracl3,fracl4,fracl5,fracl6,fracl7,fracl8,
    fracl9,fracl10,fracl11,fracl12,
223                         o1,o2,o3,o4,o5,o6,o7,o8,o9,o10,o11,o12,
224                         fracn1,fracn2,fracn3,fracn4,fracn5,fracn6,fracn7,fracn8,
    fracn9,fracn10,fracn11,fracn12,
225                         fraco1,fraco2,fraco3,fraco4,fraco5,fraco6,fraco7,fraco8,
    fraco9,fraco10,fraco11,fraco12):
226 
227         _logger.info(self.working_directory)
228 
229         working_directory = self.working_directory
230         bin2prt = os.path.join(working_directory, 'Programs', 'Ribasim', 'System',
     'Bin2prt.exe')
231         simproc = os.path.join(working_directory, 'Programs', 'Ribasim', 'System',
     'Simproc.exe')
232         rib2his = os.path.join(working_directory, 'Programs', 'Ribasim', 'System',
     'Rib2His.exe' )
233         cwd = os.path.join(working_directory, 'OUMRBIA9.Rbn', 'CMTWORK')
234         #RL_PSTPR = os.path.join(working_directory, 'Programs', 'RL_PSTPR.INI')
235         hisfile1 =  os.path.join(working_directory, 'OUMRBIA9.Rbn', 'WORK', 'pws.
    his')
236         hisfile2 =  os.path.join(working_directory, 'OUMRBIA9.Rbn', 'WORK', '
    reservoi.his')
237         hisfile3 =  os.path.join(working_directory, 'OUMRBIA9.Rbn', 'WORK', 'vir.
    his')
238         hisfile4 =  os.path.join(working_directory, 'OUMRBIA9.Rbn', 'WORK', 'fir.
    his')
239         measures_file = os.path.join(working_directory, 'OUMRBIA9.Rbn', 'Actions',
     'Measures',
240                                      'R001-2015-RibasimRsvNodeOperRulesDataOER.mes
    ')
241         #c1objective=c1
242         part1min = 617.70
243         part2min = 741.55
244         part3min = 885.50
245         part4min = 815.50
246         part5min = 240.50
247 
248         part1max = 677.00
249         part2max = 810.00
250         part3max = 966.00
251         part4max = 877.50
252         part5max = 285.00
253 
254         i=1
```

```
255         b1 = generate(c1,part1max,fracb1);b2=generate(c2,part1max,fracb2);b3=
    generate(c3,part1max,fracb3);b4=generate(c4,part1max,fracb4);b5=generate(c5,
    part1max,fracb5);b6=generate(c6,part1max,fracb6);b7=generate(c7,part1max,fracb7
    );b8=generate(c8,part1max,fracb8);b9=generate(c9,part1max,fracb9);b10=generate(
    c10,part1max,fracb10);b11=generate(c11,part1max,fracb11);b12=generate(c12,
    part1max,fracb12)
256         a1 = generate(b1,part1max,fracc1);a2=generate(b2,part1max,fracc2);a3=
    generate(b3,part1max,fracc3);a4=generate(b4,part1max,fracc4);a5=generate(b5,
    part1max,fracc5);a6=generate(b6,part1max,fracc6);a7=generate(b7,part1max,fracc7
    );a8=generate(b8,part1max,fracc8);a9=generate(b9,part1max,fracc9);a10=generate(
    b10,part1max,fracc10);a11=generate(b11,part1max,fracc11);a12=generate(b12,
    part1max,fracc12)
257         e1 = generate(f1,part2max,frace1);e2=generate(f2,part2max,frace2);e3=
    generate(f3,part2max,frace3);e4=generate(f4,part2max,frace4);e5=generate(f5,
    part2max,frace5);e6=generate(f6,part2max,frace6);e7=generate(f7,part2max,frace7
    );e8=generate(f8,part2max,frace8);e9=generate(f9,part2max,frace9);e10=generate(
    f10,part2max,frace10);e11=generate(f11,part2max,frace11);e12=generate(f12,
    part2max,frace12)
258         d1 = generate(e1,part2max,fracf1);d2=generate(e2,part2max,fracf2);d3=
    generate(e3,part2max,fracf3);d4=generate(e4,part2max,fracf4);d5=generate(e5,
    part2max,fracf5);d6=generate(e6,part2max,fracf6);d7=generate(e7,part2max,fracf7
    );d8=generate(e8,part2max,fracf8);d9=generate(e9,part2max,fracf9);d10=generate(
    e10,part2max,fracf10);d11=generate(e11,part2max,fracf11);d12=generate(e12,
    part2max,fracf12)
259         h1 = generate(i1,part3max,frach1);h2=generate(i2,part3max,frach2);h3=
    generate(i3,part3max,frach3);h4=generate(i4,part3max,frach4);h5=generate(i5,
    part3max,frach5);h6=generate(i6,part3max,frach6);h7=generate(i7,part3max,frach7
    );h8=generate(i8,part3max,frach8);h9=generate(i9,part3max,frach9);h10=generate(
    i10,part3max,frach10);h11=generate(i11,part3max,frach11);h12=generate(i12,
    part3max,frach12)
260         g1 = generate(h1,part3max,fraci1);g2=generate(h2,part3max,fraci2);g3=
    generate(h3,part3max,fraci3);g4=generate(h4,part3max,fraci4);g5=generate(h5,
    part3max,fraci5);g6=generate(h6,part3max,fraci6);g7=generate(h7,part3max,fraci7
    );g8=generate(h8,part3max,fraci8);g9=generate(h9,part3max,fraci9);g10=generate(
    h10,part3max,fraci10);g11=generate(h11,part3max,fraci11);g12=generate(h12,
    part3max,fraci12)
261         k1 = generate(l1,part4max,frack1);k2=generate(l2,part4max,frack2);k3=
    generate(l3,part4max,frack3);k4=generate(l4,part4max,frack4);k5=generate(l5,
    part4max,frack5);k6=generate(l6,part4max,frack6);k7=generate(l7,part4max,frack7
    );k8=generate(l8,part4max,frack8);k9=generate(l9,part4max,frack9);k10=generate(
    l10,part4max,frack10);k11=generate(l11,part4max,frack11);k12=generate(l12,
    part4max,frack12)
262         j1 = generate(k1,part4max,fracl1);j2=generate(k2,part4max,fracl2);j3=
    generate(k3,part4max,fracl3);j4=generate(k4,part4max,fracl4);j5=generate(k5,
    part4max,fracl5);j6=generate(k6,part4max,fracl6);j7=generate(k7,part4max,fracl7
    );j8=generate(k8,part4max,fracl8);j9=generate(k9,part4max,fracl9);j10=generate(
    k10,part4max,fracl10);j11=generate(k11,part4max,fracl11);j12=generate(k12,
    part4max,fracl12)
263         n1 = generate(o1,part5max,fracn1);n2=generate(o2,part5max,fracn2);n3=
    generate(o3,part5max,fracn3);n4=generate(o4,part5max,fracn4);n5=generate(o5,
    part5max,fracn5);n6=generate(o6,part5max,fracn6);n7=generate(o7,part5max,fracn7
    );n8=generate(o8,part5max,fracn8);n9=generate(o9,part5max,fracn9);n10=generate(
    o10,part5max,fracn10);n11=generate(o11,part5max,fracn11);n12=generate(o12,
    part5max,fracn12)
264         m1 = generate(n1,part5max,fraco1);m2=generate(n2,part5max,fraco2);m3=
    generate(n3,part5max,fraco3);m4=generate(n4,part5max,fraco4);m5=generate(n5,
    part5max,fraco5);m6=generate(n6,part5max,fraco6);m7=generate(n7,part5max,fraco7
    );m8=generate(n8,part5max,fraco8);m9=generate(n9,part5max,fraco9);m10=generate(
    n10,part5max,fraco10);m11=generate(n11,part5max,fraco11);m12=generate(n12,
    part5max,fraco12)
265
```

```
266
267         with open(measures_file, 'rt') as f:
268             a = f.readlines()
269
270         t=0
271         for i in range(len(a)):
272             if (a[i]=='Node name=RSV_AHMEDELHANSALIDAM\n'):
273                 t=t+1
274                 a[i+2]='Flood control storage operation rule (t) (m)='+str(a1)+','
    +str(a2)+','+str(a3)+','+str(a4)+','+str(a5)+','+str(a6)+','+str(a7)+','+str(a8
    )+','+str(a9)+','+str(a10)+','+str(a11)+','+str(a12)+'\n'
275                 a[i+3]='Target storage operation rule (t) (m)='+ str(b1)+','+str(
    b2)+','+str(b3)+','+str(b4)+','+str(b5)+','+str(b6)+','+str(b7)+','+str(b8)+','
    +str(b9)+','+str(b10)+','+str(b11)+','+str(b12)+'\n'
276                 a[i+4]='Firm storage operation rule (t) (m)='+ str(c1)+','+str(c2)
    +','+str(c3)+','+str(c4)+','+str(c5)+','+str(c6)+','+str(c7)+','+str(c8)+','+
    str(c9)+','+str(c10)+','+str(c11)+','+str(c12)+'\n'
277             if (a[i]=='Node name=RSV_BINELOUIDANEDAM\n'):
278                 a[i+2]='Flood control storage operation rule (t) (m)='+str(d1)+','
    +str(d2)+','+str(d3)+','+str(d4)+','+str(d5)+','+str(d6)+','+str(d7)+','+str(d8
    )+','+str(d9)+','+str(d10)+','+str(d11)+','+str(d12)+'\n'
279                 a[i+3]='Target storage operation rule (t) (m)='+ str(e1)+','+str(
    e2)+','+str(e3)+','+str(e4)+','+str(e5)+','+str(e6)+','+str(e7)+','+str(e8)+','
    +str(e9)+','+str(e10)+','+str(e11)+','+str(e12)+'\n'
280                 a[i+4]='Firm storage operation rule (t) (m)='+ str(f1)+','+str(f2)
    +','+str(f3)+','+str(f4)+','+str(f5)+','+str(f6)+','+str(f7)+','+str(f8)+','+
    str(f9)+','+str(f10)+','+str(f11)+','+str(f12)+'\n'
281             if (a[i]=='Node name=RSV_HASSAN1ERDAM\n'):
282                 a[i+2]='Flood control storage operation rule (t) (m)='+str(g1)+','
    +str(g2)+','+str(g3)+','+str(g4)+','+str(g5)+','+str(g6)+','+str(g7)+','+str(g8
    )+','+str(g9)+','+str(g10)+','+str(g11)+','+str(g12)+'\n'
283                 a[i+3]='Target storage operation rule (t) (m)='+ str(h1)+','+str(
    h2)+','+str(h3)+','+str(h4)+','+str(h5)+','+str(h6)+','+str(h7)+','+str(h8)+','
    +str(h9)+','+str(h10)+','+str(h11)+','+str(h12)+'\n'
284                 a[i+4]='Firm storage operation rule (t) (m)='+ str(i1)+','+str(i2)
    +','+str(i3)+','+str(i4)+','+str(i5)+','+str(i6)+','+str(i7)+','+str(i8)+','+
    str(i9)+','+str(i10)+','+str(i11)+','+str(i12)+'\n'
285             if (a[i]=='Node name=RSV_MOULAYYOUSSEFDAM\n'):
286                 a[i+2]='Flood control storage operation rule (t) (m)='+str(j1)+','
    +str(j2)+','+str(j3)+','+str(j4)+','+str(j5)+','+str(j6)+','+str(j7)+','+str(j8
    )+','+str(j9)+','+str(j10)+','+str(j11)+','+str(j12)+'\n'
287                 a[i+3]='Target storage operation rule (t) (m)='+ str(k1)+','+str(
    k2)+','+str(k3)+','+str(k4)+','+str(k5)+','+str(k6)+','+str(k7)+','+str(k8)+','
    +str(k9)+','+str(k10)+','+str(k11)+','+str(k12)+'\n'
288                 a[i+4]='Firm storage operation rule (t) (m)='+ str(l1)+','+str(l2)
    +','+str(l3)+','+str(l4)+','+str(l5)+','+str(l6)+','+str(l7)+','+str(l8)+','+
    str(l9)+','+str(l10)+','+str(l11)+','+str(l12)+'\n'
289             if (a[i]=='Node name=RSV_ALMASSIRADAM\n'):
290                 a[i+2]='Flood control storage operation rule (t) (m)='+str(m1)+','
    +str(m2)+','+str(m3)+','+str(m4)+','+str(m5)+','+str(m6)+','+str(m7)+','+str(m8
    )+','+str(m9)+','+str(m10)+','+str(m11)+','+str(m12)+'\n'
291                 a[i+3]='Target storage operation rule (t) (m)='+ str(n1)+','+str(
    n2)+','+str(n3)+','+str(n4)+','+str(n5)+','+str(n6)+','+str(n7)+','+str(n8)+','
    +str(n9)+','+str(n10)+','+str(n11)+','+str(n12)+'\n'
292                 a[i+4]='Firm storage operation rule (t) (m)='+ str(o1)+','+str(o2)
    +','+str(o3)+','+str(o4)+','+str(o5)+','+str(o6)+','+str(o7)+','+str(o8)+','+
    str(o9)+','+str(o10)+','+str(o11)+','+str(o12)+'\n'
293
294         with open(measures_file, 'wt') as f:
295             f.seek(0)
296             f.writelines(a)
```

```
297
298
299
300
301
302         # run model
303         resrb = subprocess.call(f"{bin2prt} BIN2PRT.fnm", cwd=cwd) #Doubt
304         if resrb <0 and resrb> 0:
305             print('Error in RIBASIM:')
306             print(resrb)
307             exit()
308
309         resrb = subprocess.call(f"{simproc} simproc.fnm", cwd=cwd) #Doubt
310         if resrb <0 and resrb> 0:
311             print('Error in RIBASIM:')
312             print(resrb)
313             exit()
314
315         resrb = subprocess.call(f"{rib2his} rib2his4.fnm", cwd=cwd)#subprocess.
    call(f"{runlist}  {RL_PSTPR}") #subprocess.call(f"{rib2his} rib2his4.fnm", cwd=
    cwd)
316         if resrb <0 and resrb> 0:
317             print('Error in postprocessing RIBASIM')
318             print(resrb)
319             exit()
320
321         # extract the relevant results
322         reshis = HisFile(hisfile1)
323         reshis.read()
324         segnam = "b'Pws_Marrakech:P2(CR)'"
325         sysnam = "b'Shortage from networ'"
326         rdate,dataMarrakech = reshis.gettimeseries(sysnam, segnam)
327         segnam = "b'Pws_ElJadida:P5(DDao'"
328         rdate,dataEljadida = reshis.gettimeseries(sysnam, segnam)
329         segnam = "b'Pws_Azzemour(avalUsi'"
330         rdate,dataazzemour = reshis.gettimeseries(sysnam, segnam)
331         segnam =  "b'Pws_RuralDoukala(DIm'"
332         rdate,dataruraldoukal = reshis.gettimeseries(sysnam, segnam)
333         segnam = "b'Pws_Safi:P3(DBSImfou'"
334         rdate,datasafi = reshis.gettimeseries(sysnam, segnam)
335         segnam= "b'Pws_Casablanca1(DSSM'"
336         rdate,datacas=reshis.gettimeseries(sysnam,segnam)
337         segnam = "b'Pws_GWTaval_Kel\\xe2aDes'"
338         rdate,datagwtaval = reshis.gettimeseries(sysnam, segnam)
339         segnam = "b'Pws_MarrakechTransfe'"
340         rdate,datamarrakechtransfe = reshis.gettimeseries(sysnam, segnam)
341         segnam = "b'Pws_Casablanca2_Sett'"
342         rdate,datacasablanca = reshis.gettimeseries(sysnam, segnam)
343         segnam = "b'Pws_Ramnha_Benguerir'"
344         rdate,databenguerir = reshis.gettimeseries(sysnam, segnam)
345         segnam = "b'Pws_Bejaad-Khourib-O'"
346         rdate,databejaad = reshis.gettimeseries(sysnam, segnam)
347         segnam = "b'Pws_Azillal:P7+Kalaa'"
348         rdate,dataazillal = reshis.gettimeseries(sysnam, segnam)
349         segnam = "b'Pws_Khenifra:P0(AH) '"
350         rdate,datakhenifra = reshis.gettimeseries(sysnam, segnam)
351         segnam = "b'Pws_GW_BeniAmir     '"
352         rdate,databeniamir = reshis.gettimeseries(sysnam, segnam)
353         segnam = "b'Pws_GW_BeniMoussa   '"
354         rdate,databenimoussa = reshis.gettimeseries(sysnam, segnam)
355         segnam = "b'Pws_GW_Tadla(OCP)   '"
```

```
356         rdate,datagwtadla = reshis.gettimeseries(sysnam, segnam)
357         segnam =  "b'Pws_GWChaouiacotiere'"
358         rdate,datagwchaouiacotiere = reshis.gettimeseries(sysnam, segnam)
359         segnam =  "b'Pws_BeniMellal:P8(DA'"
360         rdate,databenimellal = reshis.gettimeseries(sysnam, segnam)
361         segnam = "b'Pws_GWBahira        '"
362         rdate,datagwbahira = reshis.gettimeseries(sysnam, segnam)
363         segnam = "b'Pws_GWDoukkalaSahel '"
364         rdate,datagwdoukkalasahel = reshis.gettimeseries(sysnam, segnam)
365         segnam = "b'Pws_GW_Dir          '"
366         rdate,datagwdir = reshis.gettimeseries(sysnam, segnam)
367
368         pws1=dataMarrakech
369
370         pws2=dataEljadida
371
372         pws3=dataazzemour
373         pws4=dataruraldoukal
374
375         pws21=datacas
376
377
378         pws6=datagwtaval
379
380         pws7=datamarrakechtransfe
381
382         pws8=datacasablanca
383
384         pws9=databenguerir
385
386
387         pws12=datakhenifra
388
389         pws13=databeniamir
390
391         pws14=databenimoussa
392
393         pws15=datagwtadla
394         pws16=datagwchaouiacotiere
395
396         pws17=databenimellal
397
398         pws18=datagwbahira
399
400         pws19=datagwdoukkalasahel
401
402
403          pwssum=pws1+pws2+pws3+pws4+pws5+pws6+pws7+pws8+pws9+pws10+pws11+pws12+
    pws13+pws14+pws15+pws16+pws17+pws18+pws19+pws20+pws21
404         pwssorted=sorted(pwssum)
405         pwsobjective=sum(pwssorted[880:-1])
406
407
408         reshis1 = HisFile(hisfile2)
409         reshis1.read()
410         segnam = "b'RSV_TAGZIRTDAM(P)    '"
411         sysnam = "b'Energy: Generated (G'"
412         rdate,datatagzirt = reshis1.gettimeseries(sysnam, segnam)
413         segnam = "b'RSV_HASSAN1ERDAM     '"
414         rdate,datahassan = reshis1.gettimeseries(sysnam, segnam)
415         segnam =  "b'RSV_TYOUGHZADAM(P)  '"
```

```
        rdate,datatyoughza = reshis1.gettimeseries(sysnam, segnam)
        segnam =  "b'RSV_MOULAYYOUSSEFDAM'"
        rdate,datamoulayyoussef = reshis1.gettimeseries(sysnam, segnam)
        segnam =   "b'RSV_ALMASSIRADAM    '"
        rdate,dataalmassira = reshis1.gettimeseries(sysnam, segnam)
        segnam = "b'RSV_BINELOUIDANEDAM '"
        rdate,databinelouidane = reshis1.gettimeseries(sysnam, segnam)
        segnam = "b'RSV_AHMEDELHANSALIDA'"
        rdate,dataahmedhansal = reshis1.gettimeseries(sysnam, segnam)
        segnam = "b'Rsv_SIDIDRISSDAM    '"
        rdate,datasididriss = reshis1.gettimeseries(sysnam, segnam)


        energy1=datatagzirt
        energy2=datahassan
        energy3=datatyoughza
        energy4=datamoulayyoussef
        energy5=dataalmassira
        energy6=databinelouidane
        energy7=dataahmedhansal
        energy8=datasididriss
        energytotal=(energy1+energy2+energy3+energy4+energy5+energy6+energy7+
    energy8)
        energysorted=sorted(energytotal)
        energyobjective=sum(energysorted[880:-1])

        reshis = HisFile(hisfile3)
        reshis.read()
        segnam="b'Vir_PMHTessaoutAval:'"
        sysnam="b'Shortage (m3/s)     '"
        rdate,dataPMHT = reshis.gettimeseries(sysnam, segnam)
        segnam="b'Vir_OeRavalMassira:I'"

        rdate,dataOeRaval = reshis.gettimeseries(sysnam, segnam)
        segnam="b'Vir_MoyenOeR:I4     '"

        rdate,dataMoyen = reshis.gettimeseries(sysnam, segnam)
        segnam= "b'Vir_Haouz:I7        '"

        rdate,dataHaouz= reshis.gettimeseries(sysnam, segnam)
        segnam= "b'Vir_GH-TessaoutAvald'"

        rdate,dataGHTessaout = reshis.gettimeseries(sysnam, segnam)
        segnam="b'Vir_PMH:AmontTadla:I'"
            '"
        rdate,dataPMHAmont= reshis.gettimeseries(sysnam, segnam)
        segnam="b'Vir_PMH:I11         '"

        rdate,dataPMHI11 = reshis.gettimeseries(sysnam, segnam)
        segnam= "b'Vir_GH_Haut_Doukkala'"

        rdate,dataGHHaut = reshis.gettimeseries(sysnam, segnam)
        segnam=  "b'Vir_GH_BeniAmir:I1  '"

        rdate,dataBeni = reshis.gettimeseries(sysnam, segnam)
        segnam=  "b'Vir_GHBeniMoussa:I5A'"

        rdate,dataMoussa = reshis.gettimeseries(sysnam, segnam)
        segnam= "b'Vir_GH-TessaoutAvaln'"

        rdate,dataGHTessain = reshis.gettimeseries(sysnam, segnam)
```

```
476         segnam=  "b'Vir_GH-TessaoutAmont'"
477
478         rdate,dataGHTessaamont = reshis.gettimeseries(sysnam, segnam)
479         segnam= "b'Vir_GH_BasDoukkala:I'"
480
481         rdate,dataGHBasDoukkala = reshis.gettimeseries(sysnam, segnam)
482         segnam= "b'Vir_Shtouka         '"
483
484         rdate,datashtouka = reshis.gettimeseries(sysnam, segnam)
485         segnam=  "b'Vir_IPAmontTadlaIp24'"
486        #
487         rdate,dataIp24 = reshis.gettimeseries(sysnam, segnam)
488         segnam=  "b'Vir_IPMoyenOeRIp4   '"
489
490         rdate,dataIp4moyen= reshis.gettimeseries(sysnam, segnam)
491         segnam=  'b"Vir_Droitd\'eauLakhda"'
492
493         rdate,dataeau = reshis.gettimeseries(sysnam, segnam)
494         segnam=  "b'Vir_IPLakhdaravalSid'"
495
496         rdate,dataiplakhdasid = reshis.gettimeseries(sysnam, segnam)
497         segnam=  "b'Vir_IPTadlaOeRIp3   '"
498
499         rdate,dataiptadlaoer = reshis.gettimeseries(sysnam, segnam)
500         segnam=  "b'Vir_PMH_TessaoutInte'"
501
502         rdate,datapmhtessa = reshis.gettimeseries(sysnam, segnam)
503         segnam=  "b'Vir_Dir:I2          '"
504
505         rdate,dataDir = reshis.gettimeseries(sysnam, segnam)
506         segnam=  "b'Vir_PMH:OERTadla:I3 '"
507
508         rdate,datapmhoertadla = reshis.gettimeseries(sysnam, segnam)
509         vir1=dataPMHT
510         vir2=dataOeRaval
511         vir3=dataMoyen
512         vir4=dataHaouz
513         vir5=dataGHTessaout
514         vir6=dataPMHAmont
515         vir7=dataPMHI11
516         vir8=dataGHHaut
517         vir9=dataBeni
518         vir10=dataMoussa
519         vir11=dataGHTessain
520         vir12=dataGHTessaamont
521         vir13=dataGHBasDoukkala
522         vir14=datashtouka
523         vir15=dataIp24
524         vir16=dataIp4moyen
525         vir17=dataeau
526         vir18=dataiplakhdasid
527         vir19=dataiptadlaoer
528         vir20=datapmhtessa
529         vir21=dataDir
530         vir22=datapmhoertadla
531         virsum=vir1+vir2+vir3+vir4+vir5+vir6+vir7+vir8+vir9+vir10+vir11+vir12+
    vir13+vir14+vir15+vir16+vir17+vir18+vir19+vir20+vir21+vir22
532         virobjective=sorted(virsum)
533         virobjective=sum(virobjective[880:-1])
534
535
```

```
536         return pwsobjective, energyobjective, virobjective
537
538
539
540 if __name__ == '__main__':
541
542     ema_logging.log_to_stderr(ema_logging.DEBUG)
543
544     #instantiate the model
545     basin_model = RibasimModel('ribasim', original_dir="C:\\Oer0T_2")
546
547     ahmed = np.array([['c1','c2','c3','c4','c5','c6','c7','c8','c9','c10','c11','
        c12'],
548                       ['fracb1','fracb2','fracb3','fracb4','fracb5','fracb6','
        fracb7','fracb8','fracb9','fracb10','fracb11','fracb12'],
549                       ['fracc1','fracc2','fracc3','fracc4','fracc5','fracc6','
        fracc7','fracc8','fracc9','fracc10','fracc11','fracc12']])
550     bine = np.array([['f1','f2','f3','f4','f5','f6','f7','f8','f9','f10','f11','
        f12'],
551                      ['frace1','frace2','frace3','frace4','frace5','frace6','
        frace7','frace8','frace9','frace10','frace11','frace12'],
552                      ['fracf1','fracf2','fracf3','fracf4','fracf5','fracf6','
        fracf7','fracf8','fracf9','fracf10','fracf11','fracf12']])
553     hassan = np.array([['i1','i2','i3','i4','i5','i6','i7','i8','i9','i10','i11','
        i12'],
554                        ['frach1','frach2','frach3','frach4','frach5','frach6','
        frach7','frach8','frach9','frach10','frach11','frach12'],
555                        ['fraci1','fraci2','fraci3','fraci4','fraci5','fraci6','
        fraci7','fraci8','fraci9','fraci10','fraci11','fraci12']])
556     moullay = np.array([['l1','l2','l3','l4','l5','l6','l7','l8','l9','l10','l11',
        'l12'],
557                         ['frack1','frack2','frack3','frack4','frack5','frack6','
        frack7','frack8','frack9','frack10','frack11','frack12'],
558                         ['fracl1','fracl2','fracl3','fracl4','fracl5','fracl6','
        fracl7','fracl8','fracl9','fracl10','fracl11','fracl12']])
559     almassira = np.array([['o1','o2','o3','o4','o5','o6','o7','o8','o9','o10','o11
        ','o12'],
560                           ['fracn1','fracn2','fracn3','fracn4','fracn5','fracn6','
        fracn7','fracn8','fracn9','fracn10','fracn11','fracn12'],
561                           ['fraco1','fraco2','fraco3','fraco4','fraco5','fraco6','
        fraco7','fraco8','fraco9','fraco10','fraco11','fraco12']])
562
563
564     part1min = 617.70
565     part1max = 677.00
566     diff1 = part1max-part1min
567
568     part2min = 741.55
569     part2max = 810.00
570     diff2 = part2max-part2min
571
572     part3min = 885.50
573     part3max = 966.00
574     diff3 = part3max-part3min
575
576     part4min = 815.50
577     part4max = 877.50
578     diff4=part4max-part4min
579
580     part5min = 240.50 #230.70
581     part5max = 285.00
```

```
582     diff5=part5max-part5min
583
584     dams = [ahmed,bine,hassan,moullay,almassira]
585     maximum = [part1max,part2max,part3max,part4max,part5max]
586     minimum = [part1min,part2min,part3min,part4min,part5min]
587     diff = [diff1,diff2,diff3,diff4,diff5]
588
589     l = []
590     for k, dam in enumerate(dams):
591         for j in range(12):
592             l.append(RealParameter(dam[0][j], minimum[k], maximum[k]))
593             l.append(RealParameter(dam[1][j], 0, 1))
594             l.append(RealParameter(dam[2][j], 0, 1))
595
596     basin_model.levers = l
597     basin_model.outcomes = [ScalarOutcome('pwsobjective', kind=ScalarOutcome.
    MINIMIZE,expected_range=(1,33.3)),
598                             ScalarOutcome('energyobjective', kind=ScalarOutcome.
    MAXIMIZE,expected_range=(641,3291)),
599                             ScalarOutcome('virobjective',kind=ScalarOutcome.
    MINIMIZE,expected_range=(315,1341))]
600                             #ScalarOutcome('firobjective', kind=ScalarOutcome.
    MINIMIZE),
601
602
603
604     convergence_metrics = [HyperVolume.from_outcomes(basin_model.outcomes),
    EpsilonProgress()]
605
606
607     with MultiprocessingEvaluator(basin_model,3) as evaluator:
608         #results, convergence=evaluator.optimize(nfe=1, searchover='levers',
609                                                 #epsilons=[0.1, 0.1, 0.1],
610                                                 convergence=convergence_metrics,
    reference=None)
```

Listing A.1: Python script to find the optimum set of operating rule curves using EMA workbench

Bibliography

[1] Global energy observatory (geo). URL http://globalenergyobservatory.org/.

[2] Water supply and sanitation needs model (wss), 2016 - africa infrastructure knowledge program portal. URL http://infrastructureafrica.opendataforafrica.org/WSSNM2016/water-supply-and-sanitation-needs-model-wss-2016?country=1000240-morocco.

[3] Morocco. URL https://www.hydropower.org/country-profiles/morocco.

[4] Assistance technique pour l'intégration et l'évaluation des risques climatiques (erc) dans la planification et le développement des ressources en eau au niveau du bassin de l'oum er□rbia, maroc consultant maîtrisan. 2016.

[5] Water infrastructure in morocco, Sep 2019. URL https://water.fanack.com/morocco/water-infrastructure-in-morocco/.

[6] Water and sanitation: Morocco, May 2019. URL https://www.usaid.gov/morocco/water-and-sanitation.

[7] Sirisha Adamala. An overview of big data applications in water resources engineering. *Machine Learning Research*, 2(1):10–18, 2017.

[8] A Ahbari, L Stour, and A Agoumi. The dam reservoir of bin el ouidane (azilal, morocco) face to climate change. *Int J Sci Eng Res*, 8(5):199–203, 2017.

[9] Steve Bankes. Exploratory modeling for policy analysis. *Operations research*, 41(3): 435–449, 1993.

[10] Ken Bowen. Sixty years of operational research. *European Journal of Operational Research*, 153(3):618–623, 2004.

[11] Blair T Bower, Maynard M Hufschmidt, and William W Reedy. Operating procedures: Their role in the design of water-resource systems by simulation analyses. *Design of water resource systems*, pages 443–458, 1962.

[12] Andrea Castelletti, Francesca Pianosi, and Rodolfo Soncini-Sessa. Water reservoir control under economic, social and environmental constraints. *Automatica*, 44(6):1595–1607, 2008.

[13] Edward J Clark. Impounding reservoirs. *Journal (American Water Works Association)*, 48(4):349–354, 1956.

[14] Urmila Diwekar. *Introduction to applied optimization*, volume 22. Springer Science & Business Media, 2008.

[15] Gennadii Donchyts, Fedor Baart, Hessel Winsemius, Noel Gorelick, Jaap Kwadijk, and Nick Van De Giesen. Earth's surface water change over the past 30 years. *Nature Climate Change*, 6(9):810–813, 2016.

[16] Andrew J Draper, Marion W Jenkins, Kenneth W Kirby, Jay R Lund, and Richard E Howitt. Economic-engineering optimization for california water management. *Journal of water resources planning and management*, 129(3):155–164, 2003.

[17] Zhour Echakraoui, Ahmed Boukdir, Olaide Aderoju, Abdelhamid Zitouni, António Guerner Dias, et al. The climate changes in the sub-basin of the oum er rbia central and the impact on the surface waters. In *E3S Web of Conferences*, volume 37, page 03003. EDP Sciences, 2018.

[18] Mounia El Azhari and Dalila Loudyi. Analysis of the water–energy nexus in central oum er-rbia sub-basin–morocco. *International Journal of River Basin Management*, 17(1): 13–24, 2019.

[19] Issa Elias, Nadhir Al-Ansari, and Sven Knutsson. Area-storage capacity curves for mosul dam, iraq using empirical and semi-empirical approaches. In *ICOLD Congress 2015: International Commission on Large Dams 15/06/2015-16/07/2015*, 2015.

[20] Jay Famiglietti. Op-ed: California has about one year of water left. will you ration now. *Los Angeles Times*, 2015.

[21] Andre R Ferreira and Ramesh SV Teegavarapu. Optimal and adaptive operation of a hydropower system with unit commitment and water quality constraints. *Water resources management*, 26(3):707–732, 2012.

[22] Gudina L Feyisa, Henrik Meilby, Rasmus Fensholt, and Simon R Proud. Automated water extraction index: A new technique for surface water mapping using landsat imagery. *Remote Sensing of Environment*, 140:23–35, 2014.

[23] Adrian Fisher, Neil Flood, and Tim Danaher. Comparing landsat water index methods for automated water classification in eastern australia. *Remote Sensing of Environment*, 175:167–182, 2016.

[24] GFDRR. River flood-morocco. URL `https://thinkhazard.org/en/report/169-morocco/FL`.

[25] Julien J Harou, Manuel Pulido-Velazquez, David E Rosenberg, Josué Medellín-Azuara, Jay R Lund, and Richard E Howitt. Hydro-economic models: Concepts, design, applications, and future prospects. *Journal of Hydrology*, 375(3-4):627–643, 2009.

[26] Markus Hrachowitz, HHG Savenije, G Blöschl, JJ McDonnell, M Sivapalan, JW Pomeroy, Berit Arheimer, Theresa Blume, MP Clark, U Ehret, et al. A decade of predictions in ungauged basins (pub)—a review. *Hydrological sciences journal*, 58(6):1198–1255, 2013.

[27] Maroc Ingenov. Abhoer 2012, . URL `http://www.abhoer.ma/index.cfm`.

[28] Maroc Ingenov. Abhoer 2013, . URL `http://www.abhoer.ma/index.cfm`.

[29] Issa E Issa, Nadhir Al-Ansari, Govand Sherwany, and Sven Knutsson. Evaluation and modification of some empirical and semi-empirical approaches for prediction of area-storage capacity curves in reservoirs of dams. *International Journal of Sediment Research*, 32(1):127–135, 2017.

[30] Sharon A Johnson, Jery R Stedinger, and Konstantin Staschus. Heuristic operating policies for reservoir system simulation. *Water Resources Research*, 27(5):673–685, 1991.

[31] Jack Kalpakian, Ahmed Legrouri, Fatima Ejekki, Khalid Doudou, Fouad Berrada, Abdelkrim Ouardaoui, and Driss Kettani. Obstacles facing the diffusion of drip irrigation technology in the middle atlas region of morocco. *International journal of environmental studies*, 71(1):63–75, 2014.

[32] Alexander Kaune, Micha Werner, Erasmo Rodríguez, Poolad Karimi, and Charlotte De Fraiture. A novel tool to assess available hydrological information and the occurrence of sub-optimal water allocation decisions in large irrigation districts. *Agricultural Water Management*, 191:229–238, 2017.

[33] K Kaveh, H Hosseinjanzadeh, and K Hosseini. A new equation for calculation of reservoir's area-capacity curves. *KSCE Journal of Civil Engineering*, 17(5):1149–1156, 2013.

[34] Maurice W Kirby and Rebecca Capey. The origins and diffusion of operational research in the uk. *Journal of the Operational Research Society*, 49(4):307–326, 1998.

[35] W.N.M Van Der Krogt. Ribasim version 7.00, technical reference manual. 2008.

[36] John W Labadie. Optimal operation of multireservoir systems: state-of-the-art review. *Journal of water resources planning and management*, 130(2):93–111, 2004.

[37] Bernhard Lehner, Catherine Reidy Liermann, Carmen Revenga, Charles Vörösmarty, Balazs Fekete, Philippe Crouzet, Petra Döll, Marcel Endejan, Karen Frenken, Jun Magome, et al. Global reservoir and dam (grand) database. *Technical Documentation, Version*, 1:1–14, 2011.

[38] J. R. Lopez, J. M. Winter, J. Elliott, A. C. Ruane, C. H. Porter, and G. Hoogenboom. Integrating growth stage deficit irrigation into a process based crop model. *Agric. Forest Meteorol.*, 243:84–92, 2017. doi: 10.1016/j.agrformet.2017.05.001.

[39] Daniel P Loucks, Jery R Stedinger, Douglas A Haith, et al. *Water resource systems planning and analysis.* Prentice-Hall., 1981.

[40] A Loukas and L Vasiliades. Streamflow simulation methods for ungauged and poorly gauged watersheds. *Natural Hazards and Earth System Sciences*, 14(7):1641, 2014.

[41] Laila Mandi and Naaila Ouazzani. Water and wastewater management in morocco: Biotechnologies application. *Sustainable Sanitation Practice*, 1(14):9–16, 2013.

[42] R Timothy Marler and Jasbir S Arora. Survey of multi-objective optimization methods for engineering. *Structural and multidisciplinary optimization*, 26(6):369–395, 2004.

[43] Stuart K McFeeters. The use of the normalized difference water index (ndwi) in the delineation of open water features. *International journal of remote sensing*, 17(7):1425–1432, 1996.

[44] Jahanshir Mohammadzadeh-Habili, Manouchehr Heidarpour, Sayed-Farhad Mousavi, and Amir H Haghiabi. Derivation of reservoir's area-capacity equations. *Journal of Hydrologic Engineering*, 14(9):1017–1023, 2009.

[45] Hamza Ouatiki, Abdelghani Boudhar, Aziz Ouhinou, Abdelkrim Arioua, Mohammed Hssaisoune, Hafsa Bouamri, and Tarik Benabdelouahab. Trend analysis of rainfall and drought over the oum er-rbia river basin in morocco during 1970–2010. *Arabian Journal of Geosciences*, 12(4):128, 2019.

[46] J-F Pekel, C Vancutsem, Lucy Bastin, M Clerici, Eric Vanbogaert, E Bartholomé, and Pierre Defourny. A near real-time water surface detection method based on hsv transformation of modis multi-spectral time series data. *Remote sensing of environment*, 140: 704–716, 2014.

[47] Julianne D Quinn, Patrick M Reed, Matteo Giuliani, and Andrea Castelletti. What is controlling our control rules? opening the black box of multireservoir operating policies using time-varying sensitivity analysis. *Water Resources Research*, 55(7):5962–5984, 2019.

[48] Joep F Schyns and Arjen Y Hoekstra. The added value of water footprint assessment for national water policy: a case study for morocco. *PLoS One*, 9(6):e99705, 2014.

[49] Justin Sheffield, Eric F Wood, Nathaniel Chaney, Kaiyu Guan, Sara Sadri, Xing Yuan, Luke Olang, Abou Amani, Abdou Ali, Siegfried Demuth, et al. A drought monitoring and forecasting system for sub-sahara african water resources and food security. *Bulletin of the American Meteorological Society*, 95(6):861–882, 2014.

[50] Yuan Si, Xiang Li, Dongqin Yin, Tiejian Li, Ximing Cai, Jiahua Wei, and Guangqian Wang. Revealing the water-energy-food nexus in the upper yellow river basin through multi-objective optimization for reservoir system. *Science of the Total Environment*, 682:1–18, 2019.

[51] Qiuhong Tang, Xuejun Zhang, Qingyun Duan, Shifeng Huang, Xing Yuan, Huijuan Cui, Zhe Li, and Xingcai Liu. Hydrological monitoring and seasonal forecasting: Progress and perspectives. *Journal of Geographical Sciences*, 26(7):904–920, 2016.

[52] William Thomas. *Rational action: The sciences of policy in Britain and America, 1940-1960*. MIT Press, 2015.

[53] WNM Van der Krogt and A Boccalon. River basin simulation model ribasim version 7.00. *User manual. Deltares report*, pages 1000408–002, 2013.

[54] Ted IE Veldkamp, Yoshihide Wada, Hans de Moel, Matti Kummu, Stephanie Eisner, Jeroen CJH Aerts, and Philip J Ward. Changing mechanism of global water scarcity events: Impacts of socioeconomic changes and inter-annual hydro-climatic variability. *Global Environmental Change*, 32:18–29, 2015.

[55] XiChun Wang and Zhiyu Sun. The design of water resources and hydropower cloud gis platform based on big data. In *International Conference on Geo-Informatics in Resource Management and Sustainable Ecosystem*, pages 313–322. Springer, 2013.

[56] Victoria L Ward, Riddhi Singh, Patrick M Reed, and Klaus Keller. Confronting tipping points: Can multi-objective evolutionary algorithms discover pollution control tradeoffs given environmental thresholds? *Environmental Modelling & Software*, 73:27–43, 2015.

[57] WMO.INT Webteam. Data management. URL `https://www.wmo.int/pages/prog/hwrp/datamanagement.php`.

[58] Hanqiu Xu. Modification of normalised difference water index (ndwi) to enhance open water features in remotely sensed imagery. *International Journal of Remote Sensing*, 27 (14):3025–3033, 2006. doi: 10.1080/01431160600589179. URL `https://doi.org/10.1080/01431160600589179`.

[59] Na Yang, Yadong Mei, and Chi Zhou. An optimal reservoir operation model based on ecological requirement and its effect on electricity generation. *Water resources management*, 26(14):4019–4028, 2012.

[60] William W-G Yeh. Reservoir management and operations models: A state-of-the-art review. *Water resources research*, 21(12):1797–1818, 1985.

[61] Xing Yuan, Joshua K Roundy, Eric F Wood, and Justin Sheffield. Seasonal forecasting of global hydrologic extremes: System development and evaluation over gewex basins. *Bulletin of the American Meteorological Society*, 96(11):1895–1912, 2015.

[62] Saloua Zhim, Abdelkader Larabi, and Hassane Brirhet. Analysis of precipitation time series and regional drought assessment based on the standardized precipitation index in the oum er-rbia basin (morocco). *Arabian Journal of Geosciences*, 12(16):507, 2019.